ASSESSING RECOMBINANT EXPRESSION OF UREASE ENZYME FROM *SPOROSARCINA UREAE* AS A CARBONATOGENIC METHOD FOR STRENGTH ENHANCEMENT OF LOOSE, SANDY SOILS

Justin Whitaker

Supervisor: Dr. Danielle Fortin

Co-supervisor: Dr. Sai Vanapalli

Thesis submitted to the

Faculty of Graduate and Postdoctoral Studies

in partial fulfillment of the requirements for the

M.Sc. degree in Earth Sciences,

University of Ottawa

Ottawa, Ontario, Canada

June 2016

TABLE OF CONTENTS

LIST OF FIGURES

LIST OF TABLES

RÉSUMÉ

Les sols qui ne rencontrent pas les normes d'ingénierie civile doivent êtres soumis à des améliorations géotechniques car les vibrations causées par les tremblements de terre ou par la surcharge sur des infrastructures en hauteur peuvent mener à la liquéfaction partielle ou totale des sols saturés en eau. Ceci peut donc entrainer des dommages importants aux structures construites sur ces sols. Certaines méthodes existent pour remédier à ce problème, mais elles demeurent couteuses et parfois toxiques car elles utilisent de l'acrylamide et des lignosulfates. La bio-précipitation *in situ* de calcite dans les sols représente une méthode alternative. Le tout se fait avec des bactéries qui démontrent une activité uréolytique. La présente étude s'est intéressée à l'activité uréolytique des souches *Escherichia coli, Sporosarcina ureae, Bacillus pasteurii, Lysinibacillus sphaericus, Bacillus subtilis et Bacillus megaterium.* Les résultats démontrent que l'urée est seulement dégradée par les souches *S. ureae* et *S. pasteurii*. L'incubation de S. ureae en présence de Ni^{2+} (0.1-1 ppm) et Fe^{2+} (1-10 ppm) a toutefois permis d'augmenter l'activité catalytique de la souche, ce qui démontre l'importance des éléments nutritifs lors de l'hydrolyse de l'urée. Afin de tester l'activité uréolytique des autres souches, nous avons introduit un système d'expression uréase dans la souche *E. coli* en substituant des amino-acides dans la structure primaire des protéines. Suite à cette modification, l'activité uréolytique de *E. coli* s'est améliorée et est devenue comparable à celle des souches *S. ureae* et *S. pasteurii.* L'injection de *S. ureae* et du mutant *E. coli* dans des sables non-consolidés a permis de cimenter de façon significative ($p < 0.05$) le matériel par rapport à des sables non inoculés, et ce après seulement 48 heures. Le transfert du système recombinant de *E coli* vers *S. ureae* est présentement en cours. Ces résultats prometteurs indiquent qu'il est possible de stimuler la précipitation *in situ* de calcite en utilisant des bactéries et de stabiliser les sols prônes à la liquéfaction.

ABSTRACT

Soils often do not satisfy functional requirements for civil engineering projects and as a result geotechnical improvements to soils are often made. Dynamic shaking during earthquakes or static overloading by overlying structures may still result in liquefaction in partially or fully water saturated soils. These have little bearing capacity for structures. Severe damages can result. Moreover, preventative soil grouting strategies are expensive, toxic, and permanent due to acrylamides, lignosulfonates, and otherwise harmful compounds present therein. Alternative methods of strength enhancement are advisable. Microbial induced calcite precipitation (MICP) was assessed in this investigation to consolidate loose, sandy soils. Ureolytic activty of *Escherichia coli, Sporosarcina ureae, Bacillus pasteurii, Lysinibacillus sphaericus, Bacillus subtilis and Bacillus megaterium* were assessed. Urea was readily degraded foremost by *S. ureae* and next by *S. pasteurii* with no significant ($p < 0.05$) activity in other strains. Incubation of *S. ureae* with 0.1 - 1ppm Ni^{2+} and 1-10ppm Fe^{2+} was shown to improve catalytic activity, suggesting their importance as a dietary source for urea hydrolysis. A urease expression system was established in *E. coli* and particular amino acid substitutions in protein primary structure made. Enhanced ureolytic activity was observed in these *E. coli* mutants, comparable to native S. ureae activity. Application of wild type *S. ureae* and recombinant *E. coli* for MICP in a model sand showed significant ($p < 0.05$) improvements compared to controls after 48 hours. Transfer of the recombinant system in *E. coli* to *S. ureae* is currently underway. These results provide valuable insight affirming that a practical system for the application of MICP may be feasible in the field for the strength enhancement of native and construction-laid loose, sandy soils.

ACKNOWLEDGEMENT

I would first like to express my sincerest gratitude to my two co-supervisors Dr. Sai Vanapalli and Dr. Danielle Fortin who have generously provided their advice, insight and, above all, enthusiasm throughout the entirety of this project from start to finish. The development, experimental progress and written thesis would not have been possible without their immense contributions. It is with great pleasure that I have so many others to thank (and there are so many) for their help with experiments, data analysis, writing or general support throughout the years: The labs of Dr. C. Boddy, Dr. A. Poulain, Dr. A. Pelling, Dr. T. Scaiano and Dr. S. Bennett, Mr. Jean Celestin and Mr. Philip Pelletier of the Geotechniacal and CAREG lab facilities of uOttawa, respectively as well as Dr. Matt Meier of Carleton University for vector donation and the detailed e-mails on bacterial expression, Dr. Aaron Hinzi for the insightful cloning protocols and strategies, George Mzarek for preparing thin sections, Paul Middlestead of the G.G. Hatch Stable isotope laboratory for isotopic interpretation, Dr.Erika Revesz for help with SEM and XRD analysis, Dr. Nimal De Silva for trace metal measurement and, of course, those members of the Fortin lab I have shared my time with as colleague and/or mentor including Tarek Najem, Sarina Cotroneo, Brandon Kahn, Graham Smyth, Maryam Kotait, Zacharie Cloutier, Linh Nguyen, Sheniz Jozef, Ryan Featherstone and Mélanie Robichaud. Last but certainly not least are my heartfelt thanks to my friends and family for their constant encouragement and support. The following funding agencies are also greatly appreciated and acknowledged: The National Scientific and Engineering Research Council (NSERC) and the University of Ottawa FGPS (Faculty of Graduate and Postdoctoral Studies).

PREFACE

The thesis is organized into manuscripts for publication. As such there may be some repetition among chapters of the Introduction section of this work.

CHAPTER 1

1.0 Calcium Carbonate

Carbonates, particularly in the form of calcium carbonate ($CaCO_3$) derived from calcium salts, are widespread among the terrestrial and aquatic environments of earth. Its ubiquity, geological and environmental significance is made apparent by its near 20% composition, by volume, in the Phanerozoic (0-547Ma) sedimentary layers of rock as carbonate material ($CaCO_3$) and Dolomite ($CaMg(CO_3)_2$).[1] A no less equivalent measure of its significance reports that 10^{23} grams of carbon dioxide (CO_2) is, or has been, bound by $CaCO_3$ material contributing to our atmosphere's rise to current levels of oxygen for the support of biological life. [1,2]

$CaCO_3$ exists in three crystalline morphologies: Calcite, Vaterite and Aragonite. The former most, Calcite is the most stable as reflected by its one order lower of magnitude thermodynamic solubility product ($K_{sp} = 3.31 \times 10^{-9}\ M^2$) compared to Vaterite ($K_{sp} = 1.22 \times 10^{-8}\ M^2$) and a more modest but lower value to Aragonite ($K_{sp} = 6.0 \times 10^{-9}\ M^2$). The precipitation reaction of $CaCO_3$ is summarized by the equilibrium described:

$$Ca^{2+} + CO_3^{2-} \leftrightarrow CaCO_3\ (s) \qquad (1)$$

Considering the above, it follows that $CaCO_3$ equilibrium and production can be made dependent on processes which produce carbonate anions. These typically involve a strong pH dependence[1,2,3] , as depicted by the equilibrium reactions:

$$CO_2 + H_2O \leftrightarrow H_2CO_3 \qquad (2)$$

$$H_2CO_3 + 2\ OH^- \leftrightarrow CO_3^- + 2\ H_2O \qquad (3)$$

Thus, an alkaline environment will produce more carbonate anions, favouring $CaCO_3$ precipitation.

There exists a collection of works on information regarding the general chemical and physical characteristics of $CaCO_3$, particularly calcite, which may be of interest to the avid

reader [4,5]. However, the abiogenic and biogenic factors of carbonate precipitation according to reactions (1-3) will be specifically addressed in this work and explored further below.

1.1 Carbonatogenesis

1.1.1 Abiotic Formation

Chemically induced $CaCO_3$ precipitation, driven primarily by thermodynamic processes without a major role played by biota have precipitated the mineral $CaCO_3$ through geological history. Contingent factors in addition to pH (previously mentioned) include the concentration of calcium ($[Ca^{2+}]$), the partial pressure of CO_2 (pCO_2) and temperature.

An example of abiotic, pH driven $CaCO_3$ precipitation is the weathering of silicates to carbonates, including $CaCO_3$. It is the main CO_2 sequesterization process, on geological time scales. It is reported that these process have helped lead to the value of some 13% of the earth's surface being accounted for by carbonates, which include $CaCO_3$ and its derivatives (e.g. Dolomite)[6] . Reactions related to silicate degradation to carbonates of calcium can be found in the review by Morse et al.[1] An example is provided below, for a calcium silicate[7].

$$CaSiO_3 + 2CO_2 + 3H2O \text{ <--> } Ca^{2+} + 2HCO{-}3 + H_4SiO_4 \text{ <--> } CaCO_3 + CO_2 + SiO_2 + 3H2O \quad (4)$$

Supersaturation of calcium in aqueous systems are considered in the literature to be one of, if not the most, critical player in $CaCO_3$ precipitation[8,9]. Typically, water systems such as seawater are supersaturated with calcium, promoting precipitation, particularly along the seabed floor where pressure and temperatures also promote precipitation[7]. They are fed by ground water, streams and mountainous ranges rich in calcium deposits such as sediment (silicate, clays etc). Ions normally present in seawater such as magnesium, phosphate and sulfate disrupt the precipitation of $CaCO_3$, by removing available carbonate or calcium ions in solution, making the salt more soluble. They may also disrupt effective crystal nucleation and growth. However, changes in the ionic environment will induce dissolution spontaneously if their concentrations changes, as described for magnesium[10]:

$$\text{I Action: } \downarrow Mg^{2+} + CO_3^{2-} \text{ <--> } MgCO_3 \text{ I Effect(a): } Mg^{2+} + \uparrow CO_3^{2-} \text{ <--> } \downarrow MgCO_3 \text{ I} \quad (5)$$

IEffect(b) : Ca^{2+} + ↑ CO_3^{2-} <--> $CaCO_3$ I Effect(c) ↓ Ca^{2+} + CO_3^{2-} <--> ↑ $CaCO_3$ I

Ground water under immense pressure from static loads of the earth above it will maintain partial pressures of CO_2 between 10-100 times that of atmospheric levels[7]. It will, therefore, be relatively acidified and dissolve excess $CaCO_3$ as it percolates through rock, fissures, aquifers, etc. This observation is especially concurrent around carbonate enriched deposits[7]. Changes in CO_2 levels as ground water rises and outgasses CO_2 in equilibrium with the atmosphere cause a dissolution of calcium as $CaCO_3$. Hard water of $CaCO_3$ (lime scale) in public tabs fed from deep water aquifers result from this thermodynamic process. The formations of stalactites and stalagmites of limestone caves are similarly driven in this fashion[11]. Partial CO_2 pressure is such an important indicator of $CaCO_3$ dissolution that it is extensively used as a proxy to indicate carbonate rich strata and the extent of precipitation of $CaCO_3$ from solution[12].

↑ Temp : ↑ CO_2 (g) <--> ↓ CO_2 (aq) + H2O <--> ↓ H_2CO_3 + ↑ $CaCO_3$ <--> ↓ $2HCO_3^-$ + ↓ Ca^{2+} (6)

Increases in temperature decrease $CaCO_3$ solubility in supersaturated solutions, typical of sea water, marine tanks and hot water heaters. The effects of dissolution can be understood with the effect of temperature on partial CO_2 pressure (equilibrium 6). All species decrease save for gaseous CO_2, favoured at higher temperatures and $CaCO_3$ becomes favoured as equilibrium moves right to left towards gaseous CO_2. This can also be illustrated numerically by the thermodynamic solubility product of carbonate ions as water is heated at room temperature (Ksp = $10^{-6.19}$ at 25^{o}C) and near boiling (Ksp = $10^{-6.44}$ at 80^{o}C). Hard substances and solids of $CaCO_3$ along pump impellers of heaters for Jacuzzis, pools and pipe lines of residential or industrial feeds are observed as a result of this temperature phenomenom[13].

Authors have explored these conditions and have found they each play chief roles in the thermodynamic (i.e. [Ca^{2+}]) and kinetic (pCO_2, pH, temperature) precipitation of $CaCO_3$ [14,15]. For example, the rate of CO_2 production and removal, encourages crystal $CaCO_3$ v. amorphous $CaCO_3$ precipitation when inputted slowly into a system [16]. With this in mind, the nucleation of crystalline $CaCO_3$, driven by the presence of CO_2, must be inevitably and significantly connected to the biota which utilize and produce it and will be the next topic for discussion.

1.1.2 Biotic Formation

Biominerals are produced by the natural activity of biota in marine or terrestrial environments. Among the variety possible it has been argued that carbonate production, particularly as $CaCO_3$, is the most important[17]. The production of $CaCO_3$ crystals as a result of biological systems is considered a complex process compared to its chemical dissolution[18] . Synthesis of $CaCO_3$ by biological activity can be subdivided into the autotrophic and heterotrophic organisms and further still to those that control or induce its mineralization[19,20].

1.1.2.1 Autotrophic Pathways

Three important classes of organisms produce carbonate by the utilization of gaseous or dissolved CO_2 during normal metabolic flux. The first are the oxygenic photosynthetic bacteria, including cyanobacteria. There are also the anoxygenic photosynthetic bacteria such as the green sulfur bacteria and purple phototrophic bacteria. Finally, non methylotropic archaebacteria produce carbonate during respiration of CO_2 in anoxic environments utilizing H_2 gas to produce CH_4 [21].

Cyanobacteria precipitate $CaCO_3$ on its S layer as a result of creating disequilibrium in the microenvironment at its cellular surface. As the bacteria utilize CO_2 it increases local pH and localized calcium ions at its S layer of its cell wall combine with carbonate. The cell surface is proposed to act as a nucleation site where it has been shown in the literature to induce mineral dissolution [21,22]. To protect itself against incrustation it will typically shed its S layer resulting in a aqueous surface of calciferous minerals[21]. As calcium is not utilized in respiration or other major cell function this is a type of passive precipitation[19]. The process may be detailed in the proposed mechanism[23]:

$$H_2O + 2HCO_3^- \text{ <--> } CH_2O + O_2 \ / \ OH^- + HCO_3^- + Ca^{2+} \text{ <--> } CaCO_3 + H_2O \quad (7)$$

Photosynthesis / Calcification

The action of cyanobacteria have partly contributed to the construction of the coral reefs over rocky sediments through $CaCO_3$ deposition overtime. [24] The production of calcareous

stromatolites in caves is not only controlled by thermodynamics but also biologically driven when the shedding and breakdown extra polysaccharide (EPS) layers from cyanobacteria (other heterotrophic bacteria) occur and form $CaCO_3$ deposits[24].

Nonsulfur purple bacteria, as part of the anoxygenic photosynthetic $CaCO_3$ precipitators can produce calcite in significant amounts[25]. They do so without water as the electron donor nor oxygen the electron acceptor, instead functioning with H_2 gas as a reducer to create carbonate microenvironments. This limits their ubiquity to anoxic areas of biomats and other extremes such as hypersaline lakes or soda bodies [25].

1.1.2.2 Heterotrophic Pathways

Multicellular and unicellular heterotrophs are widespread in their use of $CaCO_3$. Calciferous organisms such as crabs, mollusks and other marine organisms create hard shells of the mineral. Terrestrial mammals and aves utilize $CaCO_3$ for the shells of their eggs. Other multicellular eukaryotes, including humans, utilize $CaCO_3$ to create specialized structures such as skeletons, bone and teeth[26]. These applications of $CaCO_3$ represent biologically controlled precipitation (BCP) of $CaCO_3$ where the organism is directly involved in its production to a high degree[19]. For example, they utilize calcium pumps across cellular membranes to induce precipitation and form structures for environmental advantages such as protection[26].

Similar to autotrophic cyanobacteria, unicellular heterotrophs of eukarya but also prokarya typically undergo biologically induced precipitation (BIP) of $CaCO_3$ where the mineral's production is an indirect result of metabolic activity. For example, the aerobic, as well as anaerobic respiration of carbon compounds, producing CO_2 has been shown to produce $CaCO_3$ in the literature, typically when in a well buffered, alkaline environment with excess calcium ions [26,27,28].

With focus on prokarya there are a diversity that precipitate $CaCO_3$ and which fall into two main categories: nitrogen and sulfur cycle producers. General oxidation of calcium sources, such as calcium acetate, are possible as well. The microbially induced precipitation reaction is

driven by electron acceptors ranging from oxygen, nitrate/nitrite, sulphite, sulfur and manganese/iron[29].

The sulfur cycle involves the reduction of sulfur to hydrogen sulfide (H_2S) producing $CaCO_3$. Nitrogen cycle bacteria utilize nitrogen during ammonification of amino acids, reduction of nitrate and/or urea breakdown to produce solid precipitate. The reactions producing mineralization are highlighted[29]:

1. $CO(NH_3)_2 + CaCl_2 + H_2O <--> NH_4Cl + CaCO_3$ (Urea Hydrolysis / Ammonification)
2. $Ca(NO_3)_2 + CHO <--> N_2 + CO_2 + CaCO_3$ (Nitrate Reduction)
3. $CaSO_4 + CHO <--> CO_2 + H_2O + CaCO_3 + H_2S$ (Sulfate Reduction)
4. $Ca^{2+} + CHO + O_2 <--> CO_2 + H_2O + CaCO_3$ (Aerobic Oxidation) (8)

With special mention to reaction 4, as cited previously, the literature has shown that general production of CO_2 can induce some level of $CaCO_3$ production while in buffered environments with alkaline pH levels[30]. An example is the oxidation of glucose by yeasts producing CO_2 and $CaCO_3$ when combined with Ca^{2+} in the growth medium. However, the rate of production as crystal aggregates has been shown to be hindered compared to reaction 1 - 3[29]. Further still, while capable of producing $CaCO_3$, reactions 2 and 3 are limited to oxygen poor or anoxic environments due to the requirement for oxygen not to interfere as an electron acceptor during respiration[31]. Urea degradation or ammonification of amino acids during organic matter decay can produce $CaCO_3$ in aerobic conditions and at high amounts of up to 1200mM / hour given proper solution conditions of alkalinity and ionic makeup[32]. Particular importance will be given to these $CaCO_3$ producing, urea decomposing organisms.

Ureolytic organisms are able to breakdown peptide bonds to form CO_2 and NH_3/NH_4. They play an important part in the ammonification of soils as part of terrestrial ecology. The conversion of organic matter back into usable forms of ammonia (NH_3) are part of the nitrogen cycle for the maintenance of plant, fungi and soil flora[33]. The simplest and most common ammonification reaction is with urea ($CO(NH_4)_2$). The ammonia can then be converted to

nitrate, nitrite, etc. It can also be used by the bacteria themselves as a nitrogen source in peptide synthesis or energy production[33]. A schematic is detailed on the process of ammonification:

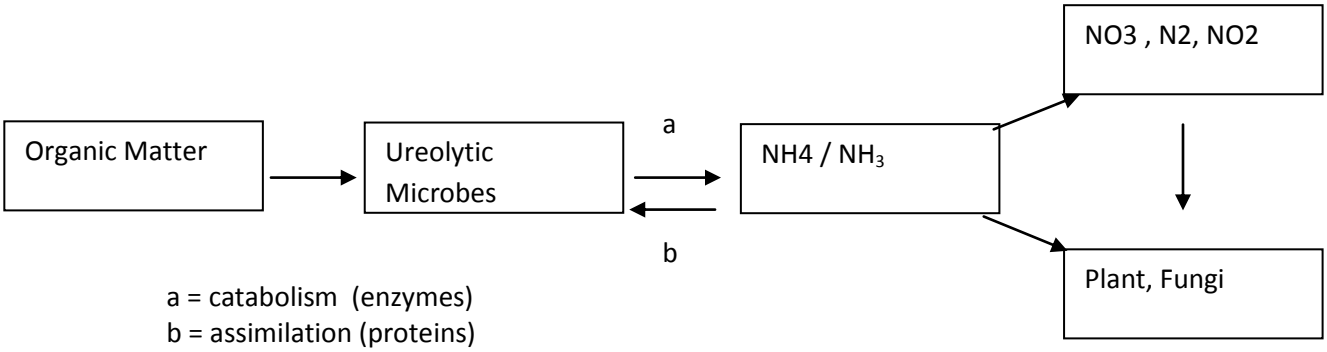

Figure 1.1: Nitrogen Cycle involving Ureolytic Organisms and their Role in Ammonification

Species of bacteria with a ureolytic function are also found as common vectors for infection in animals and humans. For example, the species *Helicobacter pylori* colonizes the highly acidic human gut, in part, due to a ureolytic function alkalizing its microenvironment[34]. Other infectious microrganisms such as *Proteus mirabilis* colonize the urinary and gastrointestinal tract as a result of ureolytic capability. They utilize urea breakdown in peptide and energy synthesis. Many strains of *Stapylococcus* also maintain infectious ability due to ureolysis. Kidney and gallstones have been recorded as resulting from the processes of their ureolysis which encourages mineralization of compounds such as $CaCO_3$ [34,35].

Less pathogenic organisms, termed GRAS (Generally Regarded As Safe), are involved with the immediate fertilization of soils via ammonification. Some species include those of *Sporosarcina* and *Bacillus*. They are Gram positive, motile organisms with various levels of ureolytic capability[32,36]. The process by which these precipitate $CaCO_3$ is similar to calcareous cyanobacteria; nucleation at the cell surface is encouraged as ammonia is produced intracellularly and released extracellularly to produce carbonate which combines with Ca^{2+} to create $CaCO_3$. Unlike cyanobacteria, species of Sporosarcina and Bacillus such as *Bacillus*

pasteurii and *Sporosarcina ureae* do not contain an S-layer to prevent deposition along their cellular body. The process is summarized:

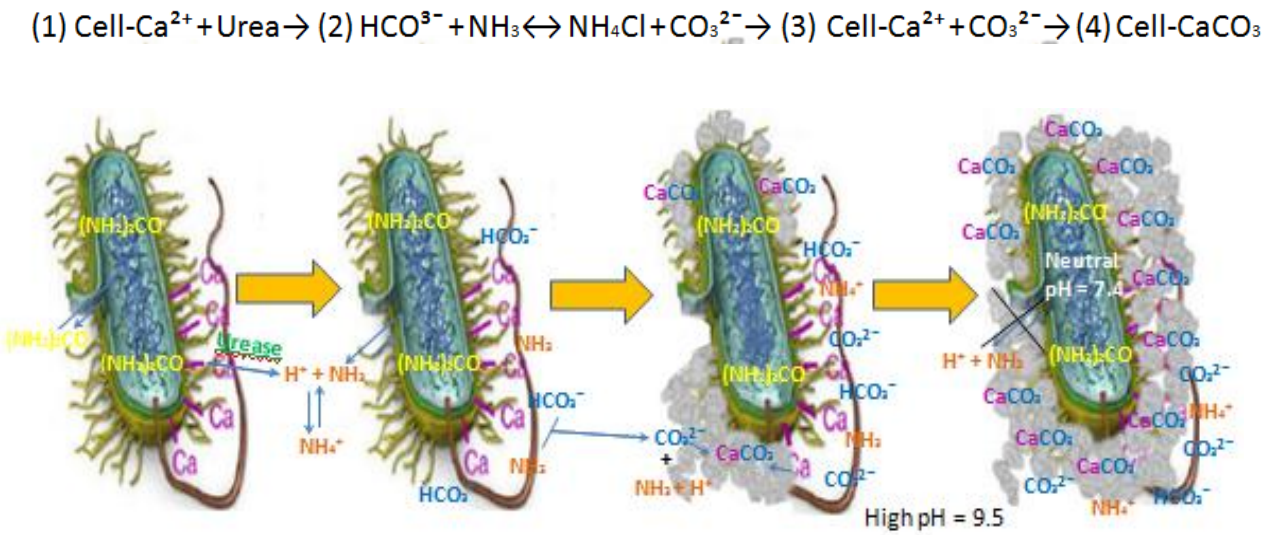

Figure 1.2: Proposed mechanism of bacteria-induced biocementation in sand grains over time (left to right).

The species of *Bacillus* and *Sporosarcina* have been studied extensively in the recent body of research as $CaCO_3$ producers[20,32,36]. Their room temperature growth, rigidity against alkaline conditions and aerobic growth conditions have been cited as an encouraging aspect for their selection and study of $CaCO_3$ dissolution. One application of their MICP capability is soil strength enhancement of loose, sandy soils to prevent settling and erosion caused by a phenomenon known as liquefaction[36,37] . A brief overview of geotechnique will be provided in its explanation.

1.2 Introduction to Geotechnique

Geotechnique is a branch of civil engineering concerned with the properties of earth materials, such as soils including strength, porosity, stability and level of compaction.

Unconsolidated soil is defined as being in a state of looseness, low density or, more technically, maintaining a high void ratio between soil grains[38]. The voids may be filled with air and or water in both terrestrial and marine considerations. In geology, the term overconsolidated, a state of over compaction and opposite to unconsolidated, is commonly applied to describe soils and clays which had previously endured the force of a glacier[38]. If the stress is reapplied on these soils they will compress without a significant change in volume, having already been made consolidated. However, a force applied to loose soils, termed unconsolidated will cause them to come together. If the voids of the soils are filled with water depending on the rate of the applied force and the ability to dissipate pore water pressure the stability of the soil may be compromised[38,39] .

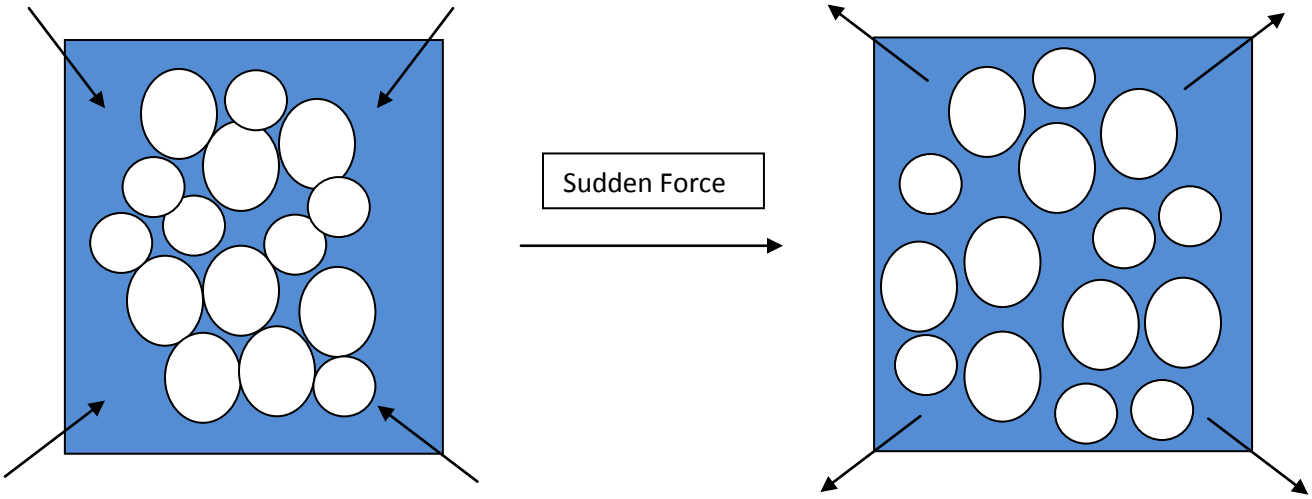

Figure 1.3: Liquefaction of Soil Grain Network. Dynamic forces (e.g. Earthquake, Blasting, etc) Increase Pore Pressure, Spreading Grains apart as Water Squeezes Between Soil Grains.

During an earthquake, soil bases undergo what is known as dynamic shaking. This can lead to a process known as liquefaction. It is a phenomenon in which loose unconsolidated soils lose strength and stiffness (i.e. effective stress or contact strength) as the pore water pressure begins to carry dynamic, sudden loads and hold soil particles apart. Bearing capacity is lost and top loads (i.e. buildings, structures, etc) sink. Well graded (i.e. rounded) and uniform sandy soils typical of marinas or other civil construction projects are particularly susceptible to this

process[39] . Events such as these have been well documented in the news and literature in Niigata (1964), Haiti (2010) and Christchurch (2011)[40].

Liquefied-induced events are detrimental and result in indescribable costs in building damages, losses of human life and massive changes in geographic stability. Some studies postulate that the earth is in the middle of a magnitude 8 or greater earthquake cycle, with the greatest event may yet to occur[41]. Current grouting techniques to help mitigate the potential damages work to induce a more permanent connection between sand granules. Resins, gels and polymers can be injected into the ground and connect soil particles into a solid network (Schematic 4). The group of NA Blesinka found carbamide resins and epoxy gels achieved a stabilized soil of 13MPa compressive strength from 0.8MPa [42]. However, while progress has been made to safeguard synthetic injections it has been reported that many remain costly, permanent and toxic[43].

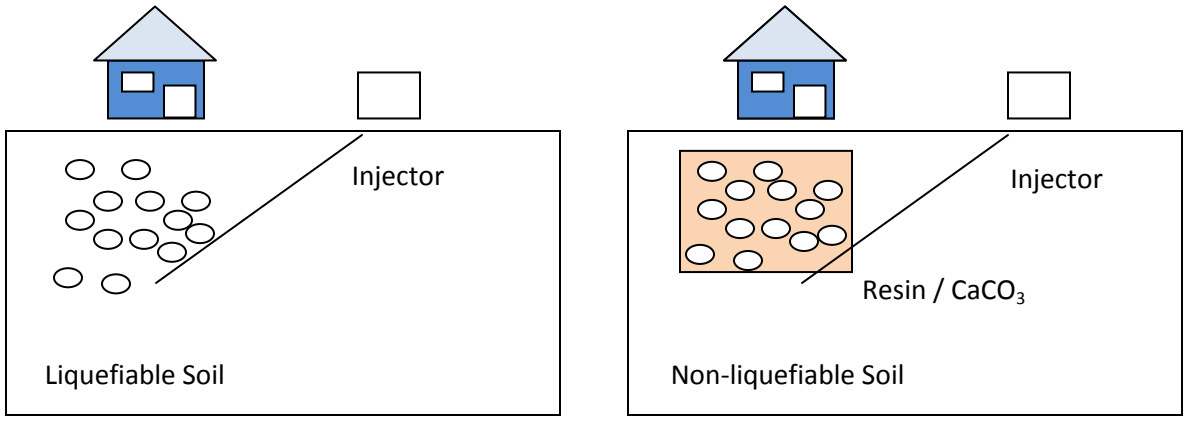

Figure 1.4: (a) Injection of Resin or $CaCO_3$ Mineralizing Bacteria to Bind Soil Particles Removing Liquefaction Capability by Increasing Soil Density and Network Strength

The biominerilzation of $CaCO_3$ has been suggested as an alternative to chemical grouts by several research groups[27,36,37,39]. Whiffin et al. claimed to achieve a comparable strengthening agent through $CaCO_3$ precipitation utilizing *Sporosarcina* and *Bacillus* species in soils with compressive strengths of up to 7Mpa achieved[27].

1.3 Biocarbonatogenic Soil Enhancement

The dissolution of $CaCO_3$ under biological influence has been termed, 'Microbially Induced Calcite Precipitation (MICP)' in the literature particularly, though not exclusively, when applied to the engineering parameters of soils. The process, as previously described, involves the normal, biochemical respiration of bacteria to induce a passive (as opposed to controlled) precipitation of $CaCO_3$ as calcite between soil grains (Schematic 5). The method has found application in diverse fields in civil engineering including improvement of concrete, soil and sand durability and strength and in some applications, sand plugging (i.e. oil deposits)[44,45,46,47].

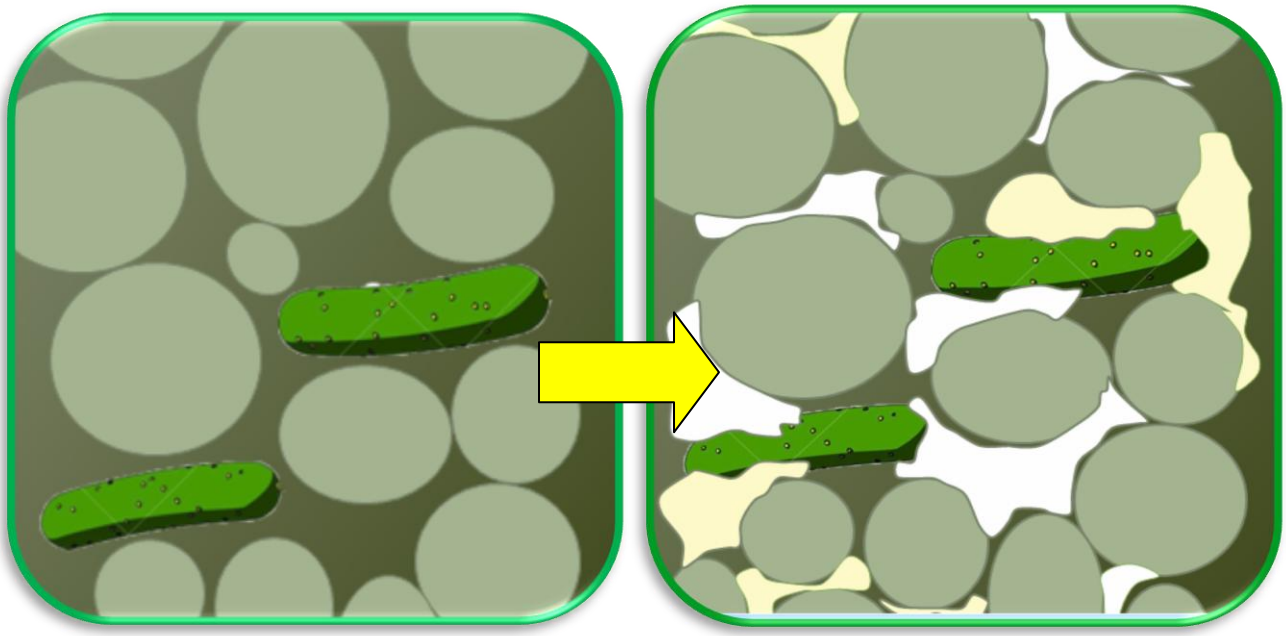

Figure 1.5: Precipitation of $CaCO_3$ (White) by MICP across Soil Particles (Grey) by Bacteria (Green) (e.g. Ureoyltic MIP)

Other fields have also had applied what has been termed by Whiffin et al. the, 'biotechnology'[27]. For example, the group of Ferris et al. utilized $CaCO_3$ precipitation by bacterial urea hydrolysis as a method of entrapment for heavy metals allowing for partitioning and straightforward clean-up of contaminants of aquifers such as Strontium (Sr)[48]. The same group also utilized bacterial ureolysis to plug sands to help improve oil recovery in the sands of Western Canada[49]. Another novel application has visualized MICP as a method to prevent the

encroachment of sands on desert communities by providing a superficial hardening, and thus erosion resistant coating, of the earth around the periphery of the city[50].

Certain disadvantages are innate to MICP and have been summarized by Van Passen et al. to include the pH, temperature, rate of $CaCO_3$ production and soil profile. Environments supporting acidic pH ranges will naturally degrade any MICP overtime, preventing a long-term soil enhancement. A complete loss of strength resulted from soils treated with an acid rain model by Van Passen et al[51]. Including a synthetic buffer such as Tris Base has been suggested to reduce these affects[52]. Effective conductivity of injected bacteria through soil, based on grain size and profile has been a detriment to consistent deposition of $CaCO_3$ as experienced by Whiffen and Van Passen[27,51]. Temperatures between 15oC to 25oC are expected in soils and limit the selection of bacteria to those most active at these temperature[52] . Freeze-thaw cycles were found not to degrade the quality of strength achieved and reduced pore size actually increased sand strength relative to more coarse grain profiles that allow for larger pore sizes[53]. The rate of $CaCO_3$ is reported to be a crucial factor, requiring the most adept bacteria to induce a meaningful cementation[52]. This was addressed by some groups by genetic manipulation of highly capable organisms of MICP[54,55]. Only two such studies have been found in this work's literature review and the groups focused on optimization of the ureolytic pathway of MICP. The author's noted that genetic engineering may be a valuable tool for the future, field viable application of the biotechnology[54,55].

1.4 Genetic Optimization of Organisms

A genetic recombinant is an organism containing pieces of DNA in its genome, its collection of DNA as a species, that are not normally found in its genomic structure in nature. The general procedure of recombinant technology, referred to as, 'cloning' achieves a genetic recombinant and involves several steps. The essence of DNA cloning is to create many copies of a desired genetic sequence, known as a gene via repeated DNA replication cycles in a process known as PCR (Polymerase Chain Reaction). The amplified sequence is cut (i.e. digested) then linked (i.e. ligated) to a vector molecule or plasmid which can replicate (i.e. express) the sequence (i.e. gene) once inside (i.e. transformed in) a host cell (e.g. *Escherichia coli*). Confirming a gene in a

plasmid and its product, typically a protein, are done in part by gel analysis. The process can be repeated for any number of DNA sequences (Schematic 6). Subcloning describes the transfer of a gene to another vector and sometimes another organism entirely (e.g. Gram positive host) following a successful cloning protocol.

The ability to express genes in E. coli are well understood[56]. However, challenges with transferring a plasmid to Gram positive organisms such as *Bacillus* and *Sporosarcina* include vector viability (i.e. the ability to express) and plasmid efficiency (the ability to enter into the host). In order to achieve high efficiencies of Bacillus species the group of Turgeon et al. utilized electroporation (electroshocking of cells) combined with plasmids containing DNA sequences allowing for replication in both *E. coli* and *Bacilli*[57]. The technique of electroporation has been utilized to achieve a expression of urease in *Bacillus subtilis* for study of its biomolceular activity[58].

The DNA sequences housed in a plasmid can be changed to optimize the expression and activity of its product, a protein (e.g. urease). A process known as site directed mutagenesis selectively mutates (i.e. changes) DNA nucleotides to make a gene product more soluble, active or otherwise efficient. The group of changes are not always beneficial and trial and error must be applied when employing the technique, even with rationalized changes supported by software analysis[56].

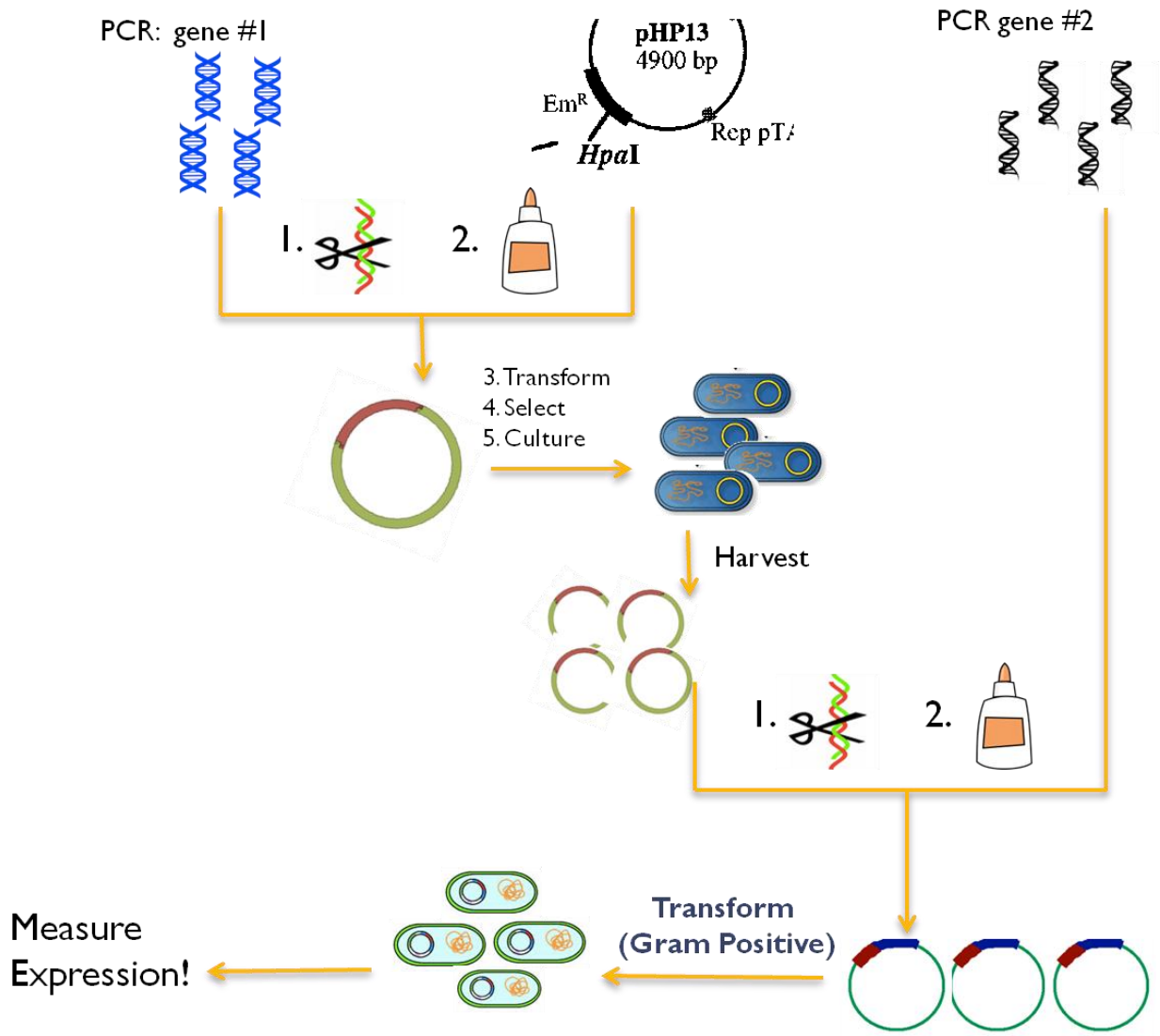

Figure 1.6: General Cloning and Subcloning Protocol for Creating Recombinant Organism of DNA Sequences .

1.5 Objectives and Research Goals

The goal of this research was to assess the ability of a recombinant system of urease expression to improve the ureolytic ability and, in turn, MICP efficiency of host Gram negative and Gram positive organisms. This, accompanied alongside selection of a superior candidate for the optimized recombinant system to be applied to for strength enhancement of soil. To address this goal the research was subdivided into two parts:

(1) Assess ureolytic capabilities of several Gram positive species based on exposure to, and degradation of, urea for selection of an optimal host strain of a recombinant urease system created concurrently, and assessed of its ability, to enhance urea hydrolysis in Gram negative *E coli.*

(2) Optimize the recombinant system, selected Gram positive growth conditions and urease protein structure for expression and activity of urease while establishing a final recombinant expression inside the selected Gram positive strain identified in part (1) of the investigation.

CHAPTER 2

ASSESSING UREOLYTIC ACTIVITY OF *BACILLUS* AND *SPOROSARCINA* WITH ESTABLISHMENT OF HOST EXPRESSION STRAIN AND INITIAL RECOMBINANT UREASE EXPRESSION SYSTEM

2.1 Introduction

In many regions of the world, the integrity of construction materials such as sand, stone and concrete is compromised due to the long term weathering action of physical, chemical and biological factors, which affects the mechanical properties of such materials[1, 2, 3]. For example, earthquakes and prolonged erosion lead to a phenomenon known as liquefaction, where pore water pressure increases in low-density soils, loose sediments, and saturated foundations; ultimately, this drastically reduces the strength of their bearing capacity and consequently damages structures on top of those soils[2, 4]. Settlement of roads and railways produces a need for continuous maintenance. Also, dikes, dunes and slopes become unstable[1]. Additionally, over time, weathering of soil causes progressive dissolution of mineral matrices and increased porosity, which further decreases the soils' mechanical features and renders desired land insufficient for use[1, 5]. In an effort to mitigate the susceptibility of construction materials to weathering effects, various geotechnical engineering procedures are used for ground improvement. Traditional methods include cement grouting[1], deep mixing of soil[1, 5], jet grouting[2], soil compaction[3], installation of fortifying mechanical structures, and chemical grouting (where sandstone is produced by filling sand voids with chemical grouts) [2,6,7]. However, in addition to being expensive, most of those methods require heavy machinery[1] and disturb urban infrastructure[1]. They are not always viable across different conditions, or are not suitable for treating large volumes of soil[1, 3]. Economic chemical grouts often require organic treatments, such as isocyanates or phenols, which have to be used in large quantities and are environmental pollutants that are usually at risk for toxic run offs [3, 6, 7]. Therefore, geotechnical engineering paradigms have recently started shifting from mechanical and chemical grouting methods to a more environmentally friendly sand consolidation technology known as bio-grouting[4, 8].

Bio-grouting is an *in situ* soil strengthening technique that involves microbial induced calcium carbonate ($CaCO_3$) precipitation[1, 3-8]. Biomediated $CaCO_3$ production, also known as carbonatogenesis (shown in Figure 1), is a biomineralization process whereby ureolytic bacteria use their urease enzyme to catalyze the hydrolysis of urea into ammonium and carbonate, and in the presence of a calcium rich environment, the latter ion precipitates as calcium carbonate minerals known as calcite [1, 3, 4, 6,7]. The bacteria serve as a nucleation sites for the crystals: the calcite crystals form cementing bridges between sand grains, which results in sand solidification and an improvement in the stiffness, as well as strength of sand, leading to a higher bearing capacity and resistance against liquefaction, erosion or shear forces[1, 2]. Bio grouting can also be used for the remediation of cracks in building materials[1], and for protection of dunes, river bends, and general sandy soil structures against erosion without disrupting hydraulics of treated soil[2]. Therefore, bio-grouting is emerging as a superior alternative to chemical and mechanical grouting for resistance against weathering factors[1, 8].

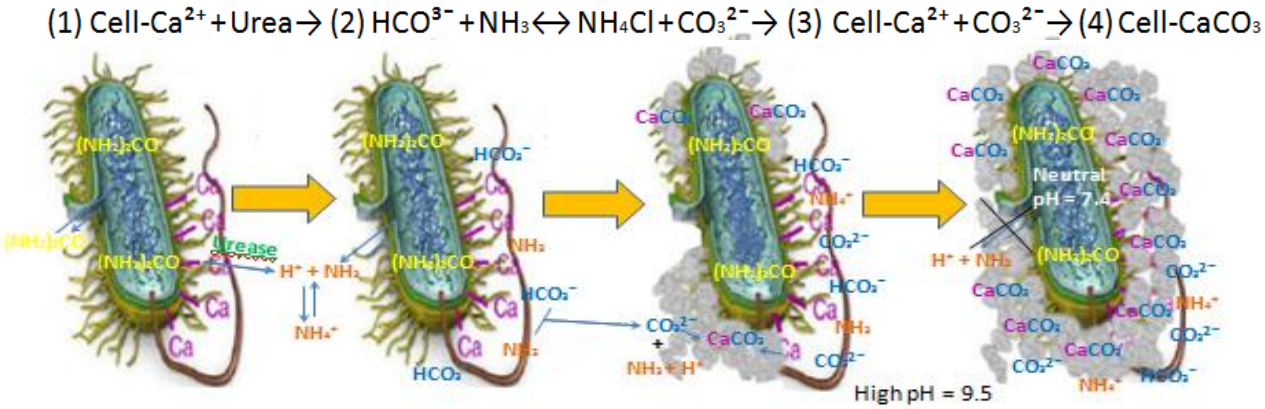

$$*S = (Ca^{2+}) \times (CO3^{2-})/K_{sp\text{-}max}* \leftrightarrow S > 1 = CaCO_{3(s)}$$

Figure 2.1: Mechanism of bacterial mediated bio-grout in sand grains with the general chemical reaction (left to right). A solubility product (S*) of over 1 for $CaCO_3$ leads to precipitation of crystals out of solution. (Figure obtained from unpublished results)

Microbially induced calcium carbonate precipitation (as calcite crystals) is a ubiquitous process observed in various natural environments such as soil, geological formations, freshwater biofilms, and saline lakes [9-11]. A common example is stalagmite and stalactites formation in limestone caves, mediated by bacterial carbonatogenesis[9]. Microbial processes,

such as cyanobacteria and coralline algae, induce calcite formation onto the surface of coral reef rocky sediments[9, 10], and secondary infections with *Helicobacter pylori,* a urease-possessing bacteria, cause calcium carbonate crystal aggregation in the kidney and gallbladder[11]. However, such systems are uncontrolled and temporary, and occur over extended periods of time[1, 9, 12]. Thus, geotechnical enhancement of reinforced body strengths necessitates the control of the amount of bacteria and reagents present in foundational volumes in order to regulate the amount of calcium carbonate produced[2, 4]. The goal is to achieve consolidation of porous sand by injecting ureolytic bacteria in it to allow the build up of sand binding calcite structures, with the direct use of bacterial cultures negating the need for the genomic extraction of the urease enzyme[1, 2].

A review of the available literature reveals that the main ureolytic bacterial strains used in previous biogrout and carbonatogenesis studies are *Sporosarcina pasteurii* (formerly known as *Bacillus pasteurii*), *Bacillus sphaericus, Bacillus subtilis* and *Bacillus megaterium*[4, 13-15]. All those strains possess the highly conserved urease metalloenzyme, which was first isolated from Jack Bean (*Canavalia ensiformis*) seeds and was the first enzyme to be crystallized, as well as the first protein shown to contain nickel[1, 16, 17]. The urease enzyme consists of the apoprotein UreABC and the accessory proteins UreD-G; they orchestrate the apoprotein activation by ensuring the insertion of nickel into the bimetallic nickel center in the UreABC active site - nickel is essential for the functional activity and structural integrity of urease[17]. Accessory proteins also promote protein conformational change and facilitate post-translational modifications fundamental to the activity of the protein[17, 18]. Metal supplements of other various transition metals (such as cobalt and iron) have been investigated for Jack Bean and *S. pasteurii,* with a potential of supplemental activity like nickel to urease [15, 18]. As previously explained, the activity of the urease enzyme is chiefly responsible for the production of carbonate for calcium carbonate precipitation. Therefore, the efficiency of the urease enzyme correlates to the amount of calcium carbonate produced. Thus, research into more efficient ureolytic bacterial strains may further cement the feasibility and applicability of biogrouting for a larger industrial scale.

A previous research effort conducted by the Fortin research group used a novel ureolytic, Gram-positive bacterium, i.e., *Sporosarcina ureae,* as a biomineralization model of $CaCO_3$[25]. This strain is less understood in the literature; yet it has shown a potential for a higher urease activity than the established ureolytic strains. Therefore, the first goal of this study is to characterize the activity of the urease enzyme in *S.ureae* for carbonatogenesis and compare it to the studied strainsof *Bacillus* and *Sporosarcina* to confirm its comparative efficiency. Furthermore, this study will optimize the urease activity by genetic modification: an expression vector will be used to insert aspects of the urease gene cluster into a Gram negative *E. coli* host. Thus, the second goal of this study is to verify the overexpression of urease and investigate if this will correlate to an increase in a higher rate urea hydrolysis and, by inference, carbonatogenesis ($CaCO_3$ / unit of time). Hence, this study has the potential of establishing a novel ureolytic strain and urease expresion system that may upgrade the feasibility of using biogrout as a geotechnical engineering strategy for strengthening and improving mechanical properties of sandy materials.

2.2 MATERIALS AND METHODS

2.2.1 Bacterial Strains, Plasmid, Media and Culture Conditions

Strains of *Sporosarcina ureae*, *Bacillus megaterium*, *Bacillus sphaericus* and *Bacillus subtilis* were obtained from the Bacillus Genetic Stock Centre (BGSC). Sporosarcina pasteurii was donated by the group of Strains were stored under standard laboratory conditions on agar plates composed of either yeast extract (Y.E.) agar (10 g/L yeast extract, 10 g/L TRIS, 5 g/L NaCl, 5 g/L NH_4Cl 16g/L agar, pH 8.0) or LB (10 g/L Trpytone, 5g/L yeast extract, 10g/L NaCL, pH 7.5) at 4°C. For culturing, all strains were grown in either LB media or ATCC 1832 medium with the following modifications: 5g/L NH_4Cl in place of $(NH_4)_2SO_4$ and no added glutamic acid, pH 7.5. S. pasteurii and S. ureae were incubated at 30^0C at 200-225 RPM overnight, while others were inoculated and incubated at 37^0C at 200-225 RMP overnight. Jack bean urease (Type III) was obtained for Sigma Aldrich.

The promoter-trap expression vector pAD123[19] was donated by the Biology Department of Carleton University (Ontario, Canada) in *Escherichia coli* strain DH5α (Life Technologies, Carlsbad, CA, USA). pUC57 in Dh5a was donated by the Boddy lab of uOttawa. pAD123 contains ampicillin and chloramphenicol resistance genes and pBR322/pTA1060 origin of replication for expression in *E.coli / Bacillus*[19]. pUC57 plasmid containing GroEl, a strong bacterial expression promoter[20], was obtained from GenScript USA Inc. and transformed into Subcloning Efficiency™ DH5α™ Competent Cells (Life Technologies, Carlsbad, CA, USA) according to manufacturer's instructions. All subsequent cloning protocols were carried with the same cells.

All *E.coli* DH5α strains were stored on LB agar (10 g/L tryptone, 5 g/L yeast extract, 5 g/L NaCl, pH 7.5) plates, and cultured by inoculation in LB media (10 g/L tryptone, 5 g/L yeast extract, 5 g/L NaCl, pH 7.5) with appropriate antibiotic (Sigma) at 37^0C and 225 RPM overnight.

2.2.2 Genomic DNA and plasmid extraction

Genomic DNA of *S.ureae* was extracted by Wizard® Genomic DNA Purification Kit (Promega Corporation) according to the manufacturer's instruction. Concentration and quality

of the genomic DNA were assessed by UV absorbance and electrophoresis on 1% ultra pure agarose gel (Life Technologies).

Extraction of pUC57 and pAD123 and any recombinant plasmid subcloning products from *E.coli* Dh5α strain was accomplished by PureLink® Quick Plasmid Miniprep kit (Invitrogen®, Carlsbad, CA, USA) according to the manufacturer's instructions, and concentration and quality of the plasmid DNA were assessed by UV absorbance and electrophoresis on 1% agarose gel (Life Technologies).

2.2.3 GroEl Polymerase Chain Reaction (PCR)

The GroEl promoter was amplified from pUC57 using Phusion® High-Fidelity PCR kit (New England BioLabs) according to manufacturer's instructions.. A pair of oligonucleotide primers were designed (IDT) as follows: Forward primer: 5'-GGGCTATAGAATTCGAAAAGAATGATGTAAGC-3' containing EcoRI restriction site and Reverse primer 5'-TTTTATAGAGCTCTTCCTCCTTTAATTGGGC-3' containing SacI restriction site.

PCR conditions were: 98ºC (30 sec), 25-35 cycles 98º C (10 sec), 66.4º C (30 sec)and 72º C (15 sec), final extension 72º C (10 min). Amplified DNA of the GroEl promoter was visualized by electrophoresis on 1% agarose gel, and product was purified using the QIAquick Gel Extraction Kit (Qiagen, Germany).

2.2.4 Subcloning of GroEl promoter into pAD123 expression vector

Digests of GroEl promoter and pAD123 (EcoRI /SacI [NEB]; 37oC, 2hrs) were analyzed by electrophoresis on 1% ultra pure agarose gel (Life Technologies) purified by the QIAquick Gel Extraction Kit (Qiagen, Germany).

Products were ligated in a 20 µl volume containing 3:1 ratio of GroEl: pAD123 (50ng vector) using Quick T4 DNA ligase (NEB) according to manufacturer's instructions.

1uL ligation was transformed into competent *E.coli* DH5α cells (Life Technologies) according to the manufacturer's protocol and plated on Amp (100ug/mL) agar. Colonies were observed for fluorescence to confirm recombinant expression in pAD123 (GFP gene marker located downsteam of its MCS [20]).

For further manipulation, cells were inoculated in LB medium with incubationt at 37º C and 225 RPM overnight. Plasmid was harvested using PureLink® Quick Plasmid Miniprep kit (Invitrogen®, Carlsbad, CA, USA) according to the manufacturer's instructions. Stocks prepared included LB streaks stored at 4º C and glycerol stocks (15% glycerol) at -80oC.

2.2.5 Urease PCR reaction

Urease (UreA-G, A-C, D-G, AB, E) was amplified from *S.ureae* genomic DNA using Phusion® High-Fidelity PCR kit (New England BioLabs). Pairs of oligonucleotide primers were designed (IDT) and are summarized:

UreA-G (5kB) For: 5'-TTTTTATA / GAGCTC / ATGCGATTACTACCGCGTGA-3' (SacI)
Rev: 5'-TTTTTATA / GGTACC / ACACTCCAATGCGCGAACTA-3' (KpnI)

UreA-C (2.4kB) For: 5'-TTTTTATA/ GAGCTC / ATGCGATTACTACCGCGTGA-3' (SacI)
Rev: 5'-TTTTTATA / GGTACC / TTTCTTCACCTCAGAATAAGAAA -3' (KpnI)

UreD-G (2.6kB) For: 5'-TTTTTATA / GAGCTC / ATGCGATTACTACCGCGTGA-3' (KpnI)
Rev: 5'-TTTTTATA / TCTAGA / ACACTCCAATGCGCGAACTA-3' (XbaI)

UreAB (1.2kB) For: 5'- TTTTATA / GGTACC / AATCTTCGCCGAGAAACTGT-3' (KpnI)
Rev: 5'- TTTTATA / GGTACC / TCATTTTGTATTCCCGCCTC -3' (KpnI)

UreE (0.5kB) For: 5'- TTTTATA / GGTACC / ATGATTGTAGAAGTCTTA-3' (KpnI)
Rev: 5'- TTTTATA / GGTACC / TTAGTCATGGCTATGTCC-3' (KpnI)

PCR conditions were: 98ºC (30 sec), 25-35 cycles 98º C (10 sec), 55-69.0º C (30 sec) and 72º C (5 min), final extension 72º C (10 min). Product was visualized on 1% agarose gel, purified using the PureLink® Quick Gel Extraction Kit (Invitrogen® Carlsbad, CA, USA) and concentration estimated by UV absorbance. Recovered Urease (UreA-G) was digested with BamHI, HaeIII and EcoRI to confirm specificity of PCR reaction.

2.2.6 Transformation and Screen of UreA-G, UreA-C, UreD-G, UreAB and UreE in pAD123/pAD123-GroEl/pUC57

PCR extracts were digested with appropriate restriction enzymes (NEB) and ligated into pAD123, pAD123-GroEl or pUC57 using T4 DNA Ligase / T4 Quick DNA Ligase (NEB) or the DNA

Ligation Kit LONG by Takara according to manufacturer's instructions. Subsequently, transformation into competent *E. coli* Dh5a (Life Technologies) was performed to supplier's recommendations. The transformants selected on LB plates containing Amp were screened using restriction digest or colony PCR and gel analysis. Colony PCR was performed according to the protocol prepared by Yan Xu et al. of NEB[20] using standard *TAQ* DNA polymerase (NEB). Detection primers were designed (IDT) upsteam and downsteam of pAD123 MCS as follows: (Upstream) For: 5'- TGGGACAACTCCAGTGAAAA-3' ; (Downstream) Rev: 5'- TGCCACCTGACGTCTAAGAA-3'. Standard M13 primers (Thermofisher) were used for pUC57.

2.2.7 *Transformation Control on pAD123-GroEL (Lambda Phage HindIII in pAD123*-GroEL)

To determine any affect DNA fragment size may have on pAD123/pAD123-groEL ability to successfully replicate in *E. coli* hosts, Lamda Phage HindIII digest (18kB ; Takara) was combined with HindIII digested pAD123-GroEL with the DNA Ligation Kit LONG (Takara) or T4 DNA ligase (NEB) according to manufacturers recommendations. Transformants were grown on LB plates containing Amp and screened by restriction digest.

2.2.8 *Urease Enzyme Activity Assay*

All native ureolytic strains of *S. ureae, S. pasteurii, B. Megaterium, L. Sphaericus, B. subtilis* including *E. coli* Dh5a and its recombinants (UreAB, UreE) were measured for extent of urea hydrolysis according to a modified method prepared by Tugba et al[21]. Briefly, cultivation in modified ATCC 1832 medium (2.2.1) was performed overnight (30°/37°C, 225rpm, 50mL), and cultures re-suspended to an OD_{600} of 0.4 in phosphate buffered saline (PBS; 0.01M, pH 7.5). 30uL of each culture were innoculated into 300uL Stuart's Brother (SB; pH 7.0) in triplicate on a flat bottom 96-well plate. Wavelengths were measured every 12min, following brief shaking (3sec), at 560nm and 460nm for 12hrs on a SpextraMax M5 microplate reader. Samples were incubated at 30°C (*Sporosarcina*) or 37°C (*E. coli / Bacillus*). Standards of Jack Bean Urease (Type III; Sigma) were prepared (1U - 100U); (1U = 1uM of urease per minute) in PBS, innoculated in SB and run for 1 hour at 30°C alongside pH standards (1-10). Results were used

to create a standard activity curve of bacterial enzyme activity (U/mL). Negative controls were non-inoculated SB media.

2.3 RESULTS

2.3.1 PCR reaction of GroEl promoter

PCR amplification of the GroEl promoter gene from the pUC57 plasmid resulted in the production of a strong band region at 126 bp (Figure 2.1). Faint bands at approximately 0.5kB, 3kB, 10kB and greater than 20kB are visible. No band is present between lane 7 and 9.

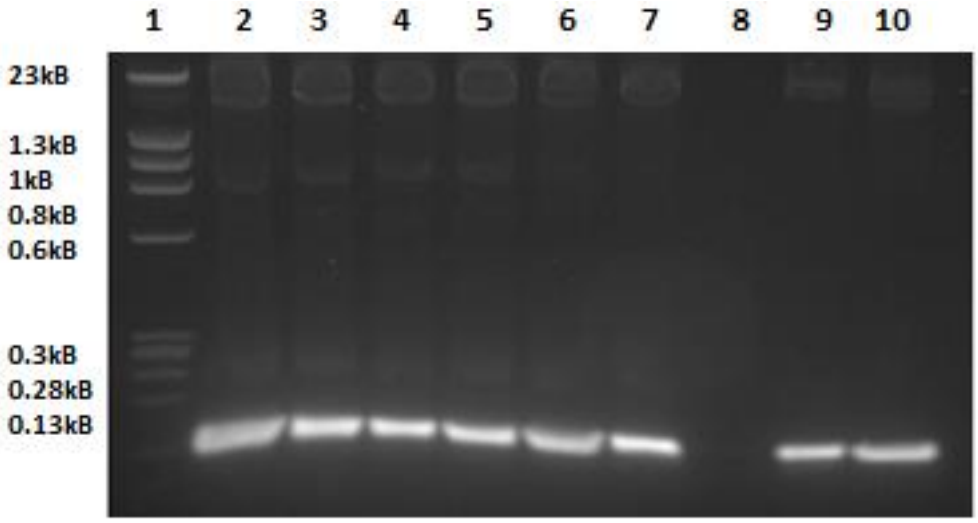

Figure 2.2: PCR amplification of GroEl promoter from pUC57 plasmid extracted from an overnight *E.coli* culture. The promoter was amplified from 100 ng of DNA. A broad range DNA molecular ladder (5 uL) was loaded in Lane 1, and 25 uL of the PCR product were loaded in Lanes 2-7, 9 and 10. A negative control was also loaded (lane 8; no polymerase). Recovery of PCR product was carried out on 2% agarose gel at 90V for 1 hour. Amplified GroEl PCR product appears around the 126 bp region. Positive control (pUC57, M13 primers) omitted.

2.3.2 Subcloning of GroEl in pAD123 expression vector

Ligated pAD123-GroEl appears around 5-6 Kbp region (Figure 2.2, lane 2-3). A fainter band around 0.4 Kbp was observed, corresponding to T4 quick ligase (NEB). Double digested

and undigested pAD123 visualized (Figure 3, lane 4-5) show bands at 5.9Kbp (lane 4, 5) and 23kB and greater (lane 5). Large bands in lane 5 correspond to different confirmations of circular plasmid (i.e. supercoiled, open circular).

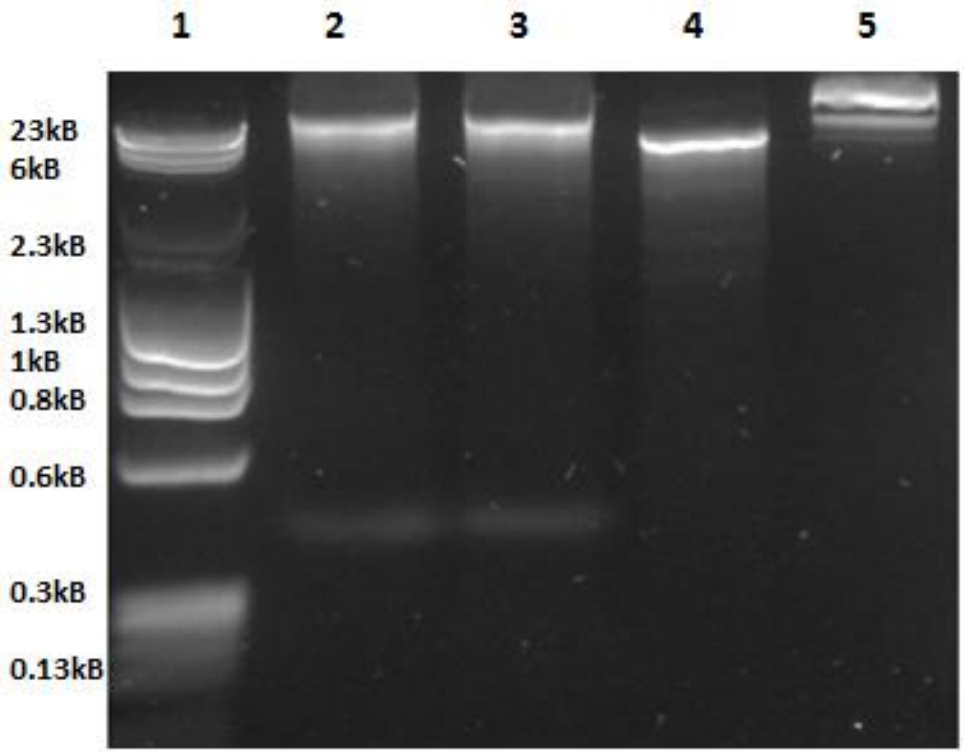

Figure 2.3: Digestion and ligation of pAD123-GroEl. Amplified GroEl was ligated into pAD123 in a 3:1 ratio. A broad range DNA molecular ladder (5 uL) was loaded (lane 1) along with 25 uL of the ligated pAD123-GroEl (lane 2, 3)). Doubled digested (KpnI/SacI) pAD123 (lane 4) and undigested pAD123 (lane 5) were also loaded. Fractionation of DNA was carried out on 1.5% agarose gel at 90V for 1 hour.

2.3.3 Urease UreA-G PCR reaction and product digest check

PCR amplification of various urease gene products (UreA-G, A-C, D-G, AB, E) from *S.ureae* genomic DNA resulted in production of bands in areas corresponding to the size of predicted urease fragments. A Representative UreA-G fragment PCR is shown in Figure 2.3.

Digested urease amplicon A-G is visualized in Figure 2.4 to yield bands of sizes predicted by the software Serial Cloner 2.6. Digestion with BamHI resulted in the two bands bands around 3.1Kb and 2.0. EcoRI yields one band at 2.6kB. HaeIII resulted in bands with sizes of 1.6Kb, 1.3Kbp, 0.8kBKb, 0.5kB-0.1kB; the upper three bands observed, the lower three observed as a streak. All digests, save for HaeIII visualize a band at 5kB.

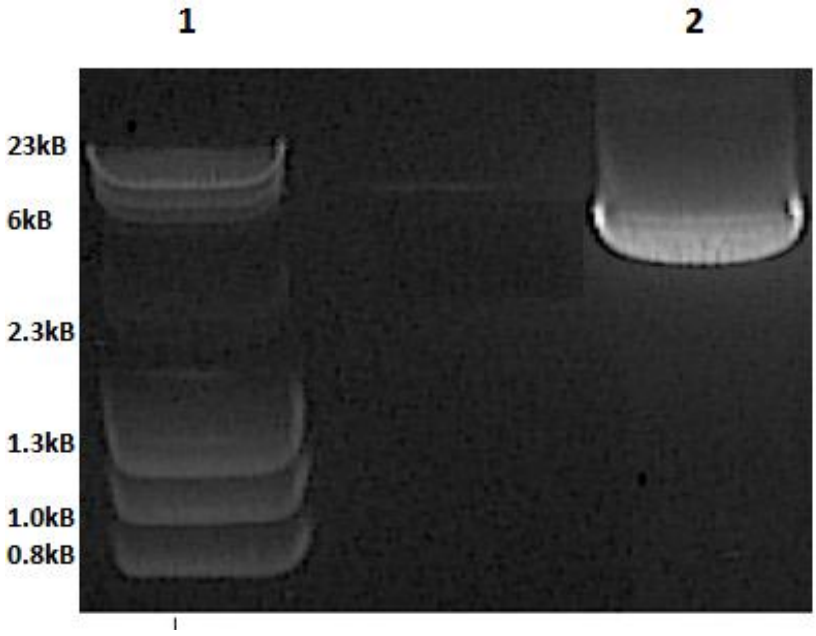

Figure 2.4: PCR amplification of the Urease gene from *S.ureae* genomic DNA extracted from an overnight *S.ureae* culture. The urease operon was amplified from 100 ng of DNA. A broad range DNA molecular ladder (5 uL) was loaded, and100 uL of the PCR product were loaded in the urease lane. Fractionation of the PCR product was carried out on 1.5% agarose gel at 90V for 1 hour. The amplified urease product appears around the 5 Kbp . Negative (no polymerase) and positive control (pUC57, M13 primers) omitted.

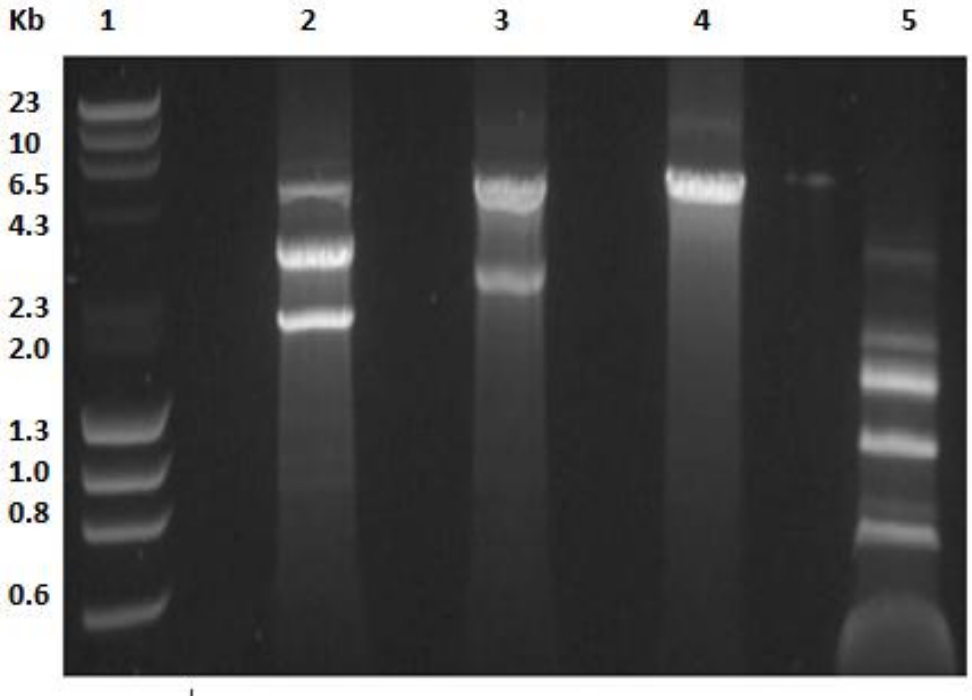

Figure 2.5: Single digests of urease (UreA-G) amplified from genomic *S.ureae* DNA. Single digests with BamHI, EcoRI, SacI and HaeIII (Lanes 2-5) were performed on 2ug of purified UreA-G in a total reaction volume of 50 uL,. 25 uL of each reaction were along with 5 uL of a broad range DNA molecular ladder (Lane 1). Fractionation of the digestion products was carried out on 0.85% agarose gel at 90V for 45 minutes. Band sizes were predicted using Serial Cloner 2.6.

2.3.4 Transforming UreA-G, UreA-C, UreD-G, UreAB, UreE (Colony PCR)

Colony PCR screens following transformation of pAD123-GroEL with UreA-G, A-C or D-G revealed only bright bands at less than 0.3kB. Figure 2.5 is a representative gel following pAD-GroEL transformation with UreAG. UreAB and UreE transformants following ligation into pAD-GroEL revealed bright bands at 1.3kB (UreAB trial; Lane 1, Figure 2.6) and 0.6kB (UreE trial; Lane 2/3, Figure 2.6). pAD123-GroEL only revealed a band at less than 0.3kB (Lane 4, Figure 2.6). Similar banding patterns were observed when transformation was attempted in pUC57 for UreAG/AC/DG v. UreAB/E (data not shown).

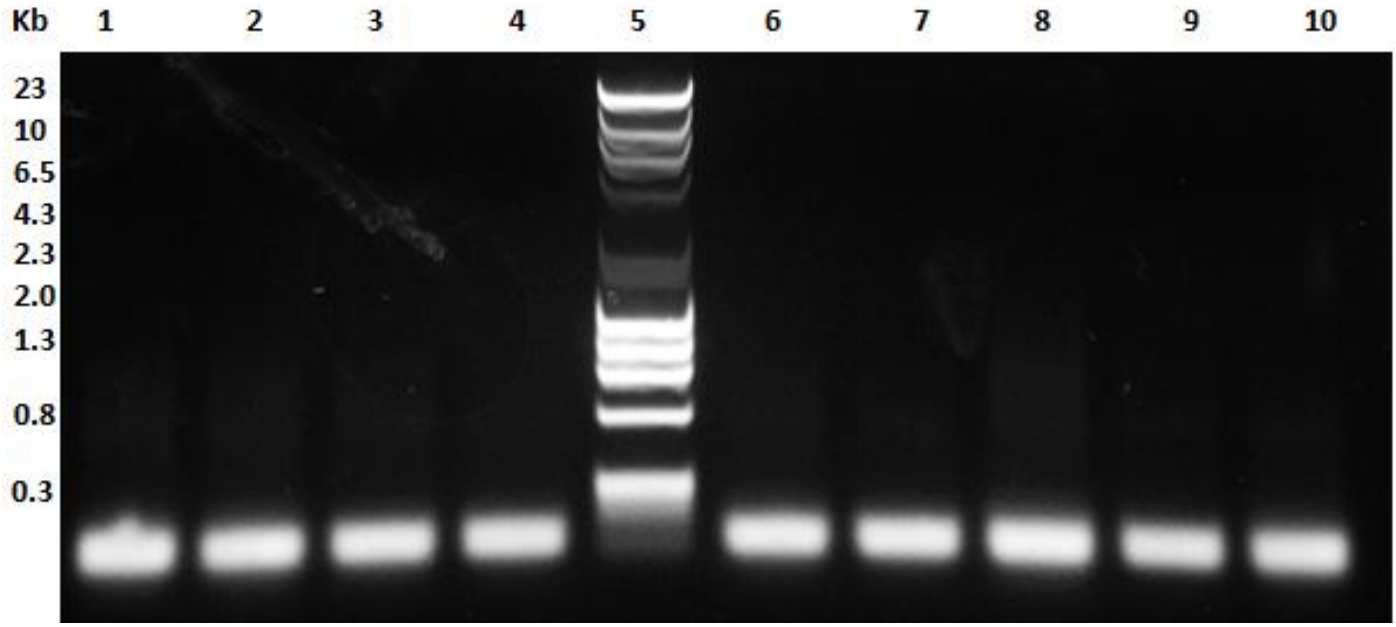

Figure 2.6: Colony PCR of candidate pAD123-GroEL-UreAG recombinants following transformation and incubation on LB-Amp. Putatitive recombinants (lanes 2-4,6-10) were loaded alongside a variable MW ladder (lane 5; NEB). Fragments were separated for 45 min at 110V on a 0.85% agarose gel. A positive control (Lane 1 pAD123-GroEL) was co-loaded. A negative control (no DNA) omitted.

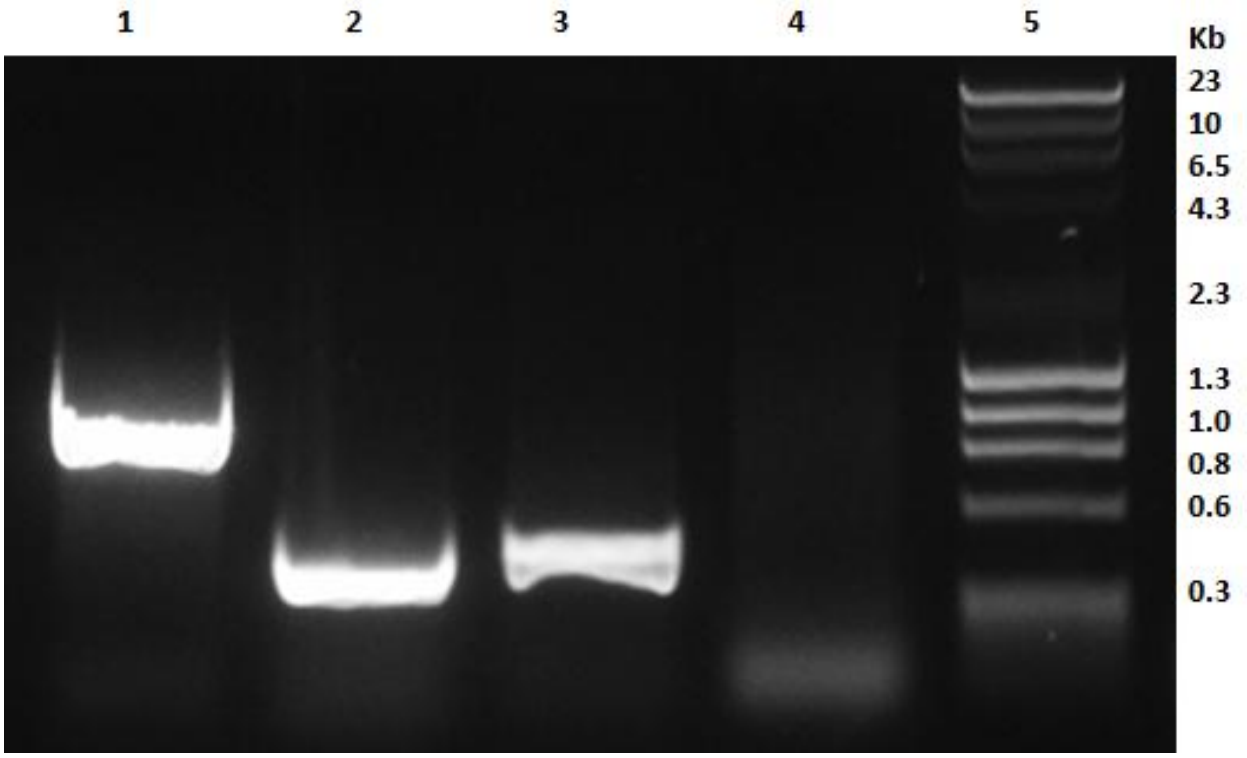

Figure 2.7: Screen of canadidate pAD123-GroEL-UreAB or UreE colonies following transformation and incubation on LB-Amp. Candidates were (lane 1-3) alongside a pAD123-GroEL only positive control (lane 4) and MW ladder (lane 5; NEB). Separation was for 45 min at 110V on a 0.85% agarose gel. Negative control (no DNA) omitted.

2.3.5 Lambda HindIII (Restriction Digest)

HindIII restriction digest of Lambda Phage DNA (18kB) and ligated into pAD123-groEL produced two band sizes (lane 1, figure 2.7) larger than pAD123-groEL (lane 6, figure 2.7) by itself. KpnI digests of pAD123-groEL with phage DNA (lane 2) revealed two fragments at 22kB and 1.5kB while pAD123-groEL alone produced a band at 6kB. HindIII digested pAD123-groEL-phage produced an 18kB fragment and a band a strong band 23kB (lane 4, figure 2.7). Undigested pAD123-groEL produced multiple bands between 6.5kB and 23kB representative of various plasmid orientation (linear, open circle, super coiled).

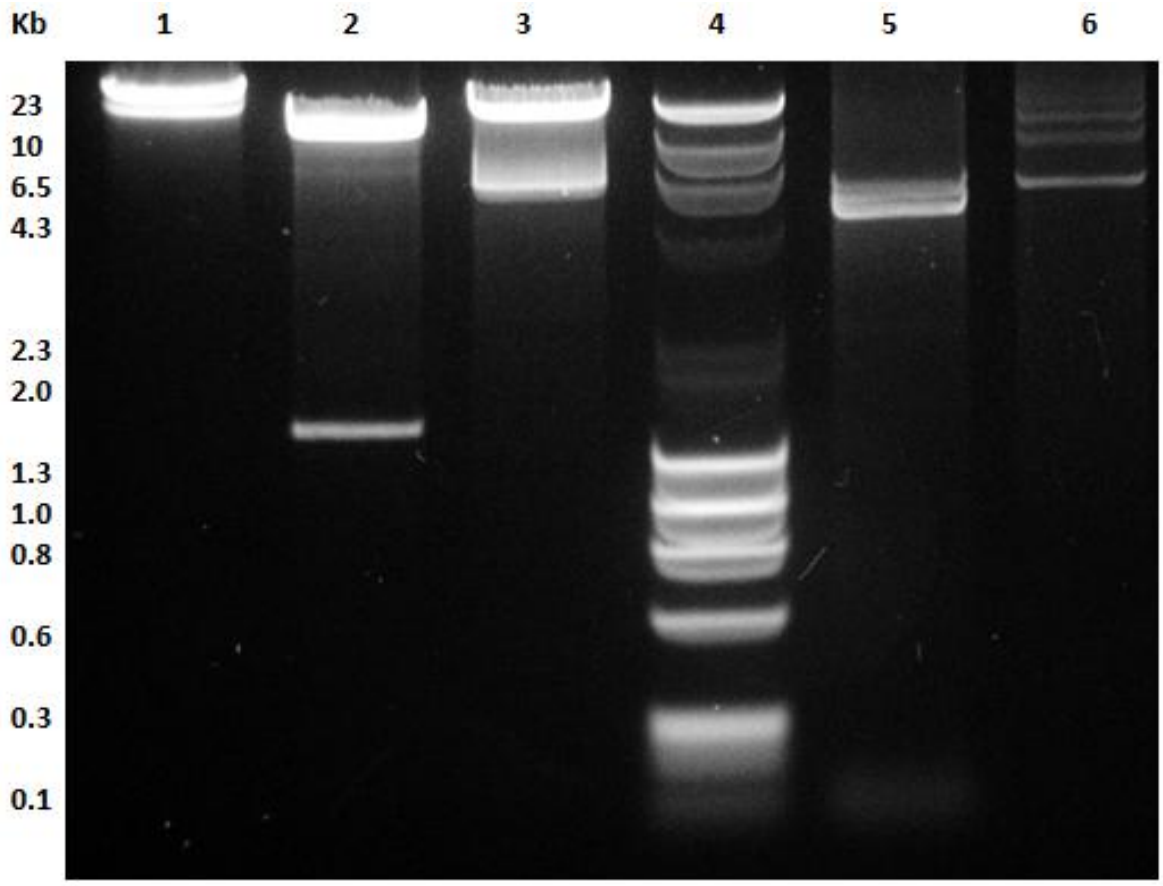

Figure 2.8: Restriction digest of pAD123-GroEL transformed with HindIII digested Lamda phage DNA (Takara LONG ligation kit, Clontech). Undigested pAD123-GroEL-Lamda (lane 1), KpnI digested pAD123-GroEL-Lambda, HindIII digested pAD123-GroEL-Lambda, KpnI digested pAD123-GroEL and undigested pAD123-GroEL are visualized. Digests were performed with 1ug of DNA (1hr) in 50uL with 20uL loaded. A variable molecular weight ladder (NEB) was co-loaded in lane 4. Fragments were separated for 1hr at 120V on a 1% agarose gel.

2.3.6 Urease enzyme activity assay

Standards of Jack bean urease (Figure 2.8, 1-100U/mL) show a logistic curve pattern with steeper curves apparent for higher activity conditions. From the standard curve, *Sporosarcina pasteurii* and *ureae* produced activity greater than 10 U/mL though the SE of *S. ureae* was higher than pasteurii without a significant difference between the two conditions ($p<0.05$). *Bacillus* species showed signicantly higher activity ($p<0.05$) compared to control with values ranging between 0.5 to just under 1.5 U/mL. However, they were significantly lower values compared to *Sporosarcina* species. *E. coli* conditions, native or recombinant, did not show a significant change from baseline (SB only) with values from 0.01 to nearly 0.50 U/mL (UreAB) observed.

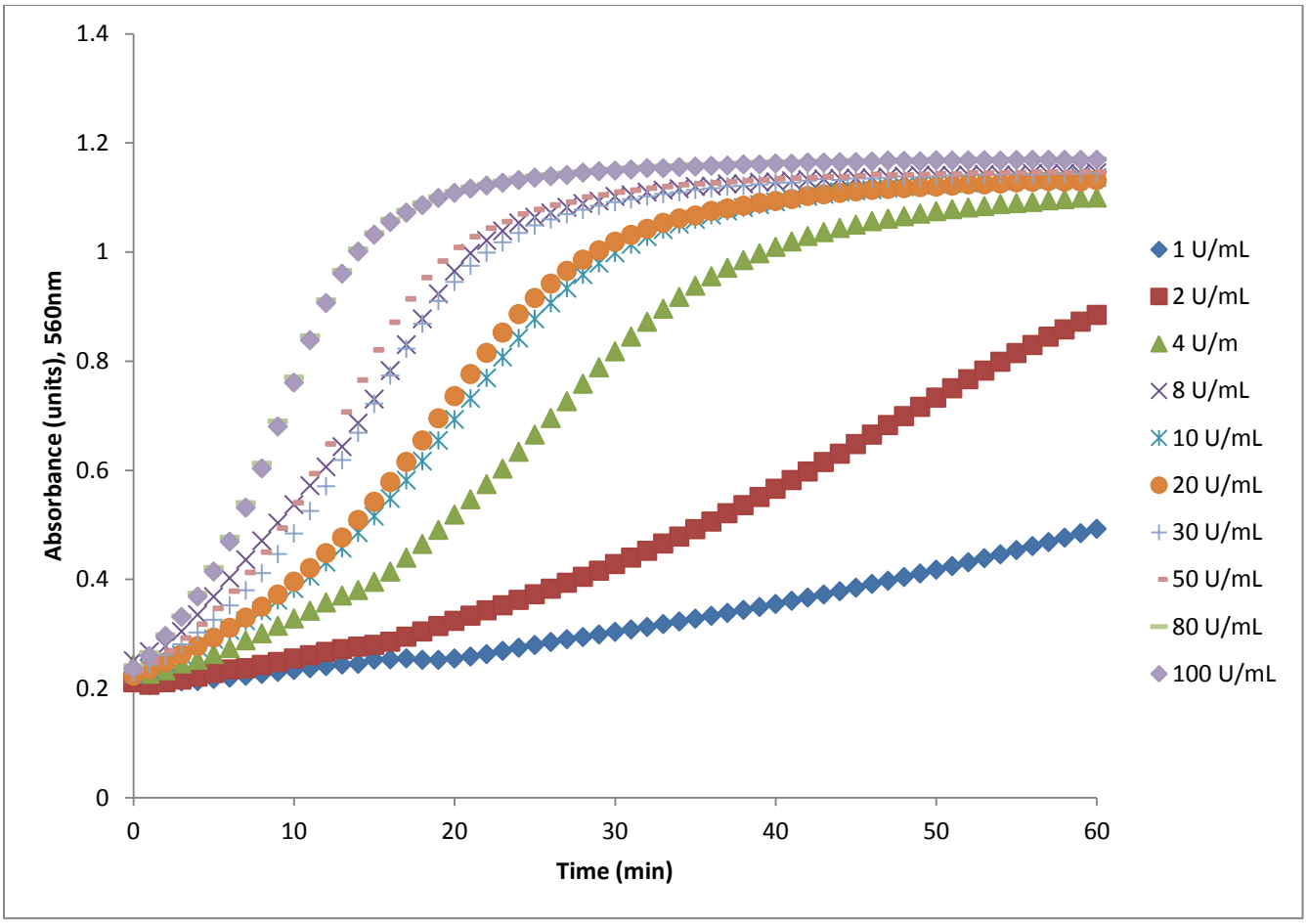

Figure 2.9: Absorbance curve of urease enzyme (Jack Bean Type III) at different activites (U/mL) measured at 560nm. Absorbance was read every minute for one hour while incubated at 30°C with brief shaking (3 sec) prior to each measurement. Rate was calculated at each time point as an average abs_{after} - abs_{bef} / t_{after} - t_{before} and the peak value for each standard reported on a rate vs time curve correlating standard urease activity to bacterial urease activity.

Table 2.1: Comparison of urease activity (U/mL) ahcieved by strains of Sporosarcina, Bacillus and E. coli with microplate assay method. Values (N=6) are reported as an average of two distinct trials, each measured in triplicate, with Standard Error (SE). One unit (U) is 1mM of urea degraded per minute. Innoculates were set at OD_{600} = 0.4 and run at 30°C (*Sporosarcina*) or 37°C (*Bacillus / E. coli*).

Strain	Activity (U/mL)
Sporosarcina pasteurii	12.55 ± 0.61
Sporosarcina ureae	11.42 ± 0.95
Bacillus megaterium	0.50 ± 0.07
Bacillus subtilis	0.78 ± 0.40
Lysinibacillus sphaericus	1.2 ± 0.29
Escherichia coli Dh5a	0.01 ± 0.04
Escherichia coli Dh5a (UreAB)	0.40 ± 0.31
Escherichia coli Dh5a (UreE)	0.01 ± 0.05
Control (SB Only)	0.00 +0.02

2.4 DISCUSSION

As the carbonatogenic activity of a bacterial strain is correlated to the efficiency of its urease enzyme[1, 2], it follows that the selection of the most carbonatogenic strain would allow for the optimum biomineralization of calcium carbonate applied to biogrouting, such that greater strength and cohesiveness of soil structure is achieved – the more $CaCO_3$ crystal bridges facilitate inter-particle contacts in sand, and therefore the more cohesiveness and shear strength of soil structures [2, 6, 18]. Therefore, the first goal of this study was to compare the different ureolytic strains in the literature to determine which strain has the highest MICP potential, as reflected in ammonia production over unit time. Comparisons in this study (Table 2.1) revealed that *S.ureae and S. pasteurii* had the highest urease activity (11.42 and 12.55 U/mL, respectively) as observed in the marked increase of ammonia concentration over time (Table 2.1) compared to *Bacillus* (0.5-1.5 U/mL), *E. coli* (0.0-0.5 U/mL) and baseline (0.0 U/mL). This supports *Sporosarcina* as a superior carbonatogenic strain compared to other candidates which is consistent with the literature[2,7.] However, the low urease activity of *Bacillus* conflicts with some literature and could be attributed to the use of genetically modified bacteria in other studies, as opposed to native strains in this study[8,9]. As native *S.ureae* and *S. pasteurii* to have the highest urease and, by inference, carbonatogenic activity of the examined strains, implementation of a urease overexpression system to increase urease amounts in these strains would be supported to yield the most beneficiary results for MICP.

With this in mind, the second aspect of the study was to develop an expression vector system capable of replication in *S.ureae* or *S. pasteurii* and which would increase urease activity above native values (Table 2.1). A recombinant vector with whole (UreAG) or partial (UreAC/DG/AB/E) was attempted and some success achieved with stability of UreAB and UreE successfully confirmed in *E. coli* Dh5a (Figure 2.6). Difficulties in stabilizing larger fragments of urease (UreAG,UreAC, UreDG) may be a result of rapid overexpression of protein resulting in toxic inclusion bodies within cell frameworks. These result when proteins cannot fold properly or accumulate too quickly in the cell[25]. Size can also be an issue, as larger DNA fragments can destabilize plasmids. However, a lamda phage fragment was successfully cloned (figure 2.6) in

pAD123-GroEL suggesting it is capable of holding large fragments with no disruption to its stability to replicate.) The GroEl promoter is a high bacterial expression promoter derived from *B.subtilis*[20] and exists as a constitutive (non-inducible) promoter in the current expression system. Insertion of is GroEl in the multiple cloning site (MCS) of pAD123 upstream of intended urease gene cluster fragments may destabilize larger fragments from successfully stabilizing in-vivo due to high, uncontrollable expression. Interestingly, stability in pAD123 without GroEL was not achieved suggesting that some, yet unknown mechanism, in spite of a lack of an promoter for constitutive expression was present. UreAB and UreE were selected at random from potential genes in the urease cluster and the sequences achieved stability. It is theorized that either UreC, D and G are expressed at toxic levels in *E. coli* or perhaps larger stretches of the cluster are naturally inhibited and destablized. *E. coli* can contain genes for a urease, however and in nitrogen rich conditions it is inhibited, if inherently active at all [26]. A colony PCR assay of E. coli Dh5a with primers internal to UreAG (data not shown) produced bright bands for urease indicating some regulation is maintained, particularly as no urease activity was observed in this study (Table 2.1). High nutrient LB media was used for recovery following DNA transformation which would encourage urease inhibition in *E. coli*. It is potentailly the case that a destabilization of a plasmid containing a working urease apoenzyme (UreAC), coenzyme (UreD-G) or holoenzyme (UreA-G) resulted. Since no significant urease activity for UreAB or UreE recombinants was observed it is surmised that no working urease was produced and thus these sequences were not inhibited by native *E. coli* mechanisms. Nevertheless, the presence of controlled, inducible expression in plasmids (e.g. pET series [Invitrogen]) is a common practice for gene expression and initial transformation stability into vectors[27]. This is proposed to be a promising next step to establish a full UreAG recombinant expression system in *E. coli*.

Additionally, since urease is a metalloenzyme containing a nickel dependent active site [17,18, 22], and other transition metals such as Cobalt and Iron have been observed to potentially supplement enzyme activity like nickel[15,18], investigation of nickel and other trace metals can be conducted as another potential source for enhancement of urease activity. Ultimately, the improvement of ureolytic activity of *S.ureae* /*S. pasteurii* could allow it to become an alternative, economic and superior bacterial strain for bio-grouting techniques of sand.

CHAPTER 3

OPTIMIZING THE EXPRESSION AND ACTIVITY OF UREASE IN *SPOROSARCINA* AND A SECOND GENERATION UREASE EXPRESSION SYSTEM WITH STRENGTH ASSESSMENT IN MODEL SAND

3.0 Introduction

Calcium carbonate ($CaCO_3$) is a mineral which is widely distributed on planet earth (Al-Thawadi et al., 2012). Production of calcium carbonate crystals can occur spontaneously from the reaction of carbonate (CO_3^{-2}) and calcium ions (Ca^{+2}) (Al-Thawadi et al. 2012). However, calcium carbonate precipitation can be mediated biologically. In fact, calcium carbonate production is a common method through which biological organisms create hard and rigid substances. For example, the mollusk shell and crustacean exoskeletons are primarily composed of various polymorphs of calcium carbonate (Ndao et al. 2010; Sato et al. 2011). Of particular importance to geotechnical interests, microbially induced calcite precipitation (MICP) has shown great promise in geotechnical and civil engineering practices (Cheng and Cord-Ruwisch 2012; Dejong et al. 2006; van Paassen et al. 2009).

Soils are susceptible to weathering and erosion which can greatly affect their mechanical properties (van Paassen 2009; De Muynck et al. 2010). With any civil engineering enterprise, the mechanics of the soil which lies beneath is an important consideration as soils often do not satisfy functional requirements (van Paassen et al. 2009). Soil stabilization is desirable for reasons including earthquake liquefaction prevention, land reclamation projects, and other engineering projects where soil performance is a concern (van Paassen et al. 2009). Superficial soil stabilization can be achieved using common approaches like compaction or mixing soils with lime or cement (Karol 2003). When stabilization is required at a depth, superficial techniques are insufficient and various procedures to ensure soil stability such as chemical grouts, jet grouting, deep soil mixing, etc., are used (Idriss and Boulanger 2008; van Paassen et al. 2009). However, since the area on which these methods can have an effect is limited to the proximity of the mixing equipment and due to short gel times of injected grouts, these methods are not suitable for treatment of large volumes (van Paassen et al. 2009).

Moreover, the chemical agents used are often costly and harmful to the environment due to pH fluctuations or toxic effects (van Paassen et al. 2009; Dejong 2006). An innovative alternative is the process of MICP which involves the use of endogenous soil microbes to achieve the same ends of soil stability without the negative environmental impacts (Dejong 2006).

Microbial processes have shown great promise in many fields. The process of microbial calcite precipitation has been used to reduce the porosity/permeability of subsurface formations (Ferris and Stehmeier 1992). MICP has been used as a means to remediate concrete structures and was found to increase the compressive strength of the material (Ramachandran et al. 2001). Although many biological processes lead to the precipitation of calcium carbonate, not all are suitable for ground reinforcement (van Paassen et al. 2009). Many of the bacteria used in MICP contain urease, an enzyme which catalyses the breakdown of urea, a common metabolic waste product. More specifically, the strain chiefly employed for MICP in the literature has been *Sporosarcina pasteurii* (Whiffin et al. 2007; Al-Thawadi 2008; Van Paassen et al. 2009). The mechanism of calcium carbonate precipitation as carried out by *S.pasteurii* begins with the catalysis of urea into ammonium and carbonate by the enzyme urease as seen in Eq.1 (Whiffin et al. 2007).

Eq.1: $CO(NH_2)_2 + 2H_2O \rightarrow 2NH_4^+ + CO_3^{2-}$

In a calcium rich environment, the carbonate ions produced, precipitate to form calcite crystals as seen in Eq.2.

Eq.2: $CO_3^{2-} + Ca^{2+} \rightarrow CaCO_3(s)$

Ureolytic bacteria have various mechanisms to regulate the expression of urease (Al-Thawadi 2008). *Sporosarcina pasteurii* is of particular interest for the purpose of calcite precipitation due to the mechanism of urease regulation which is constitutive. In other words, *S.pasteurii* expresses the urease enzyme regardless of environmental conditions (Al-Thawadi 2008). A closely related strain, *Sporosarcina ureae*, also has constitutive regulation of urease; however, it has not been characterised in terms of its MICP potential. One of the aims of this study is to characterize this strain in the context of MICP.

Several methods have been employed to optimize calcite precipitation such as manipulating the concentration of microbes and nutrients available to them; however, the method of optimization used in this study is to increase the solubility of urease. If the concentration of urease in solution can be increased, more enzymes will be available for urea catalysis. This will ultimately lead to an increase in calcite precipitation, causing increased strength of soils and at a more rapid pace.

Various methods exist to enhance in-vitro protein solubility. There are a number of solubility-enhancing peptide tags, e.g. glutathione S-transferase (GST), small ubiquitin-like modifier (SUMO) protein, maltose-binding protein (MBP), etc., which one can fuse to a protein of interest to increase solubility (Chantarasiri et al. 2012; Costa et al. 2014). The issue with peptide tags is their size is often large and can affect protein folding and functionality making them undesirable for industrial enzymes (Chantarasiri et al. 2012). Alternatively, the bioengineering of a protein of interest by site-directed mutagenesis presents itself as an ideal method to increase solubility. In 2006, Trevino and colleagues (Trevino et al. 2006) conducted a systematic investigation of the relative contributions of all twenty amino acids to protein solubility. The results of Trevino et al. suggested that aspartic acid, glutamic acid, and serine contribute significantly more favorably than the other hydrophilic amino acids to protein solubility (Trevino et al. 2006). Hydrophobic to hydrophilic amino acid mutations is generally the method to increase solubility; however, hydrophobic amino acids are found mostly in the core of a protein and changes to these could greatly affect protein structure (Trevino et al. 2006). Evidently, mutations to surface amino acids are a more viable option. Thus, the current study will also aim to substitute surface hydrophilic amino acids, which do not contribute to solubility, for hydrophilic amino acids which contribute more favorably to protein solubility (glutamic acid, aspartic acid, and serine) in the urease enzyme.

In summary, the proposed study has set out to achieve the following goals: (1) Extract the urease gene cluster (UreA-G) from the ureolytic strain, *S. ureae*, which is a close relative of *S.pasteurii*, (2) Transfer the gene cluster to an expression vector in *Escherichia coli* to allow for protein expression, (3) Make single amino acid changes to the urease gene by site-directed

mutagenesis in hopes of increasing in-vitro urease solubility, and (4) to analyze urease enzyme activity and solubility subsequent to amino acid substitutions and compare these results with the results obtained from wild-type urease in addition to several other ureolytic strains including *Lysinibacillus sphaericus*, *Bacillus subtilis*, and *Bacillus megaterium*.

3.1 MATERIALS AND METHODS

3.1.1 Ureolytic Bacteria, E.coli Strains, and Plasmids

Sporosarcina ureae (SL6708), *Bacillus subtilis* subsp. *subtilis* (Marburg NCIB3610^T), *Bacillus megaterium* (QMB1551), and *Lysinibacillus sphaericus* (WHO2297) were obtained from the Bacillus Genetic Stock Center (Columbus, Ohio). Bacteria were grown in LB media, by supplier's instructions or on modified ATCC1 1832 medium (2.2.1). *S. ureae* was grown additionally on agar plates composed of yeast extract (10g/L), TRIS (10g/L), 0.05M $(NH_4)_2SO_4$, agar (15g/L), pH 8.0 at 4°C.

E.coli strains DH10β, TOP10, and BL21 (DE3) were obtained from New England Bio Labs Inc. (NEB), Invitrogen, and Lucigen, respectively. All were grown in LB media unless specified by supplier. The pMiniT stability vector was obtained from NEB as part of the PCR Cloning Kit and the pET-28b(+) expression vector was obtained from a donation by the Boddy lab of uOttawa.

3.2.2 Genomic and Plasmid DNA Extraction

Genomic DNA of *S.ureae* was extracted by Wizard® Genomic DNA Purification Kit (Promega Corporation) according to the manufacturer's instruction. Concentration and quality of the genomic DNA were assessed by UV absorbance using the Thermo Scientific NanoDrop 2000 UV-Vis Spectrophotometer and by electrophoresis on 0.8% ultra-pure agarose gel (Thermofisher).

Extraction of plasmids pMiniT, and pET-28b(+), including their recombinant varieties, was accomplished by PureLink® Quick Plasmid Miniprep kit (Invitrogen®, Carlsbad, CA, USA), Clontech NucleoSpin Plasmid Miniprep Kit or Lab-Based Miniprep using Clontech Miniprep columns. Minprep solutions prepared according compositions provided by Epoch Life Sciences.

Concentration and quality of plasmid DNA was assessed by UV absorbance using the Thermo Scientific NanoDrop 2000 UV-Vis Spectrophotometer and/or electrophoresis on 0.8% agarose gel (Thermofisher).

3.2.3 Amplification of UreA-C and UreD-G

The sequences UreA-C and UreD-G were amplified from genomic DNA of *S.ureae* using the Phusion® High-Fidelity PCR kit (NEB). The PCR reaction was performed in a total volume of 50 µl containing 100 ng of DNA, 0.5 µM of each primer, 200 µM dNTPs, 10 µl of 5X Phusion High Fidelity buffer, and 1.0 U of Phusion DNA polymerase. A pair of oligonucleotide primers were designed and provided by Integrated DNA Technologies for each fragment. Forward primer for UreA-C: 5'-TATA/CCATGG/GA/CGATTACTACCGCGTGAA-3' (Tm = 63°C) containing NcoI restriction site and two additional base pairs which code for glycine (underlined) correcting for frame shift caused by NcoI restriction site containing ATG start codon and reverse primer for UreA-C: 5'-TATA/GCTAGC/TTTCTTCACCTCAGAATAAGAAA-3' (Tm = 59°C) containing NheI restriction site. Forward primer for UreD-G:

5'-TATA/GCTAGC/ATGATTGTAGAAGAAGTCTTAAT-3' (Tm = 52°C) containing NheI restriction site and reverse primer for UreD-G:

5'-TATA/GAGCTC/CTAGTACTTCCTTAAAAAACTTG-3' (Tm = 53°C) containing SacI restriction site.

PCR reaction was carried out with 25 cycles of denaturation at 98º C for 10 seconds, 66.4º C annealing for 30 seconds and 72º C extension for 15 seconds. The reaction was initiated at 98ºC for 30 seconds as initial denaturation before beginning the PCR cycle, and it was ended with a final extension at 72º C for 10 minutes in a thermal cycler (Eppendorf NA). The amplified DNA was visualized by electrophoresis on 0.8% agarose gel, and product was purified using the Clontech Nucleospin® Gel and PCR Clean-up kit.

3.2.4 Ligation of UreA-C and UreD-G into pMiniT and Transformation into DH10β E.coli

UreA-C and UreD-G sequences were transferred independently into pMiniT using the transformation protocol with the NEB PCR Cloning Kit. UreA-C and UreD-G amplicons were transformed into DH10β *E.coli.* The transformation of UreD-G was not observed in DH10β transformants, therefore, it was contained in a similar *E.coli* strain, TOP10 *E.coli* from Invitrogen.

3.2.5 Sub-cloning of UreA-C and UreD-G into pET-28b(+) and Transformation into TOP10 E.coli

DH10β *E.coli*, and TOP10 *E. coli* containing UreA-C and UreD-G in pMiniT, respectively, were grown over night; plasmid DNA was extracted using the Clontech NucleoSpin® Plasmid Miniprep Kit according to manufacturer instructions. The pMiniT plasmid containing UreA-C or UreD-G was digested with NcoI and NheI (UreA-C) or NheI and SacI (UreD-G) restriction sites in a total volume of 50 µl at 37º C for 2 hours. Digestion products were analyzed by electrophoresis on 0.8% agarose gel (Thermofisher) and bands of desired product were excised and purified using the Clontech Nucleospin® Gel and PCR Clean-up kit.

The UreA-C and UreD-G fragments were then subcloned into pET-28b(+) expression vector. The ligation reaction was prepared in 10µl volumes using 3:1 insert:vector, 1µl high concentration T4 DNA ligase (NEB®), and incubated at 4°C for 16hr with heat inactivation at 65°C for 10min. The recombinant pET-28b(+)-UreA-C and pET-28b(+)-UreD-G plasmids were transformed into TOP10 *E.coli* (Thermofisher) independently according to manufacturer protocol. Steps above were repeated to move UreD-G in pET-28b(+) to UreA-C in pET to form complete gene cluster pET28b(+).

Methods sections 2.2-2.5 can be summarized in Figure 1.

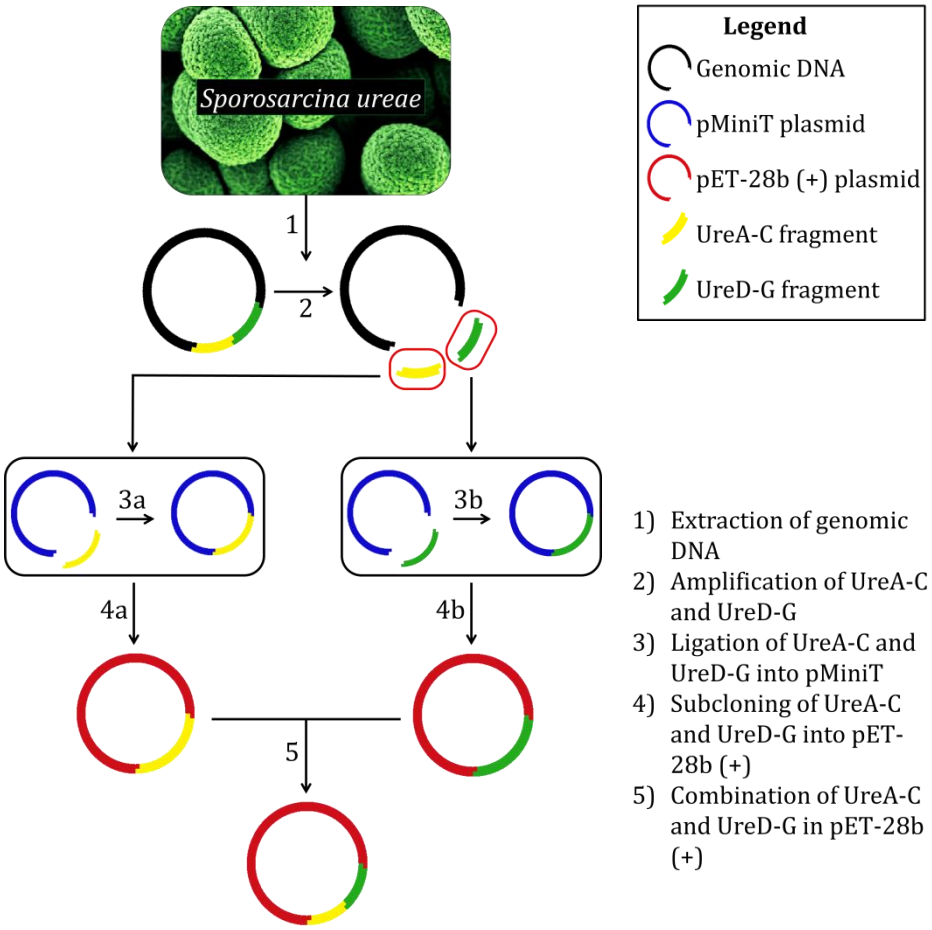

Figure 3.1. Flow diagram representing sections 2.2-2.5 of the methods. This figure illustrates the sequence of events which occurred from the genomic DNA extraction from *S. ureae* to having the full urease gene cluster within pET-28b (+).

3.2.6 Colony PCR Screening to Identify Recombinant Plasmids with DH10β and TOP10 Strains

Recombinant *E.coli* colonies were grown overnight at 37°C. After incubation, 25-100% of visible colonies from transformation plates were suspended in 50µL ddH2O (autoclaved), heated to 95°C for 10 minutes, and centrifuged at 13000RPM for 3 minutes. A 1µl sample of supernatant solution was transferred to a 10µl PCR tube. PCR was performed according to manufacturer instructions for NEB® *Taq*. Primers used in colony PCR are as follows. Forward primer for pMiniT: 5′-ACCTGCCAACCAAAGCGAGAAC-3′ (Tm = 61°C) and reverse primer for pMiniT: 5′-TCAGGGTTATTGTCTCATGAGCG-3′ (Tm = 57°C). Forward primer for pET-28b(+): 5’-

TAATACGACTCACTATAGGGG-3’ (Tm = 55°C) and reverse primer for pET-28b(+): 5’-GCTAGTTATTGCTCAGCG-3’ (Tm = 56°C). The same primers were used for sequencing analysis.

3.2.7 DNA Sequencing

Primers were designed with Serial Cloner and ordered through Integrated DNA technologies (ITG). Presence of UreA-C and UreD-G in pMiniT and UreA-C, UreD-G, and UreA-G in pET28b (+) confirmed by partial sequence at 5' and 3' ends of product utilizing sequencing primers of plasmid. The primers used for pMiniT detection and sequencing were those from the NEB® PCR Cloning kit. Sequencing was completed using the CEQ™ 8000 Genetic Analysis System by Beckman Coulter, Inc. or by the Applied Biosystems 3730 DNA Analyzer.

3.2.8 Protein Visualization for Determination of Amino Acid Changes

The Pymol software program was used to visualize the urease protein. The crystal protein structure was obtained from the Protein Data Bank website. Pymol’s mutagenesis function allows one to make amino acid changes in-silico and provides information concerning any stearic hindrance which may result from any particular mutation. To aid in the determination of which precise changes would be made, the primary structures of urease from five strains (*Sporosarcina ureae, Sporosarcina pasteurii, Bacillus subtilis, Bacillus megaterium,* and *Lysinibacillus sphaericus*) were aligned using the Clustal Omega multiple sequence alignment program on the European Bioinformatics Institute website (http://www.ebi.ac.uk/services). The alignment demonstrated which areas of the protein were conserved and which areas were variable. It was decided that the target areas for mutation should correspond to the variable regions to avoid compromising protein function. Furthermore, using the logic from Trevino et al. (amino acids aspartic acid, glutamic acid, and serine were found to contribute significantly more favorably than hydrophilic amino acids arginine, lysine, asparagine, threonine, and glutamine to protein solubility), in-silico mutations were done using Pymol. If minimal stearic hindrance resulted, this was seen as a potential candidate. Once two candidates had been chosen from each subunit of urease, the specific DNA changes were determined using Serial Cloner.

3.2.9 Site-directed Mutagenesis

Mutations performed according to manufacturer's instruction using the NEB® Q5® Site-Directed Mutagenesis Kit. A modification was made to the protocol whereby the DH5α cells provided were exchanged for DH10β or TOP10 *E.coli* cells during the transformation. Mutation from Asn110 (aAT) to Asp110 (gAT) in urease subunit beta involved the following primers: forward primer: 5'-GGGAGGCGGG**gAT**ACAAAATG-3' (Tm: 63°C) and reverse primer: 5'-AATGCTCCGTCTACTTTATTG-3' (Tm: 58°C). Mutation from Asn100 (aAT) to Asp100 (gAT) in subunit beta involved the following primers: forward primer: 5'- CGGTTTTCAC**gAT**AAAGTAGAC-3' (Tm: 55 °C) and reverse primer: 5'- TACACTTCTCTTTCTCCAG-3' (Tm: 55°C). Mutations were confirmed using sequencing primers upstream and/or downstream of codon change in sequence with the following UreB primer: 5'-TTTGATCGGGATGTGACGTA-3' (Tm = 60°C).

3.2.10 Protein Solubility Assay

Subsequent to sequencing confirmation of both rounds of site-directed mutagenesis in which Asn100 was substituted for Asp100 and Asn110 was substituted for Asp110, round 1, round 2, and unmodified urease in pET-28b (+) were transformed into the BL21-DE3 *E. coli* expression strain. Urease protein solubility was measured following the cell lysate preparation protocol (BioRad): cells were cultured overnight in 5mL LB (appropriate antibiotic added) at 37oC. 1mL of overnight culture was removed and added to 4mL fresh LB (appropriate antibiotic added), then cultured to a density of ~0.5 OD600 (1-2 million cells per ml). Tubes were labelled non-induced no site-directed mutagenesis (SDM), induced no SDM, induced SDM round one, and induced SDM round 2. All but the control were induced with IPTG for 3hrs at 37°C. 1mL of induced cells were centrifuged in a conical tube at 5000rpm for 5min. Supernatant was removed and pellet was washed with 5mL TBS (Tris-Buffered Saline), and then centrifuged at 5000rpm for 5 min. 1mL Triton X-100 lysis buffer was added. Lysate was incubated on ice with gentle shaking for 15 minutes then sonicated three times in two second bursts with one minute rest on ice between each two-second pulse. Lysate was then incubated on ice for an additional

15 minutes then centrifuged at 16000 x g for 10 minutes at 4ºC. Supernatant was collected (avoiding the pellet) into new microfuge tubes. A Bradford assay was conducted to determine protein concentration. A total amount of 50µg/20µl of protein was added to each lane and the gel was run for 5min at 50V, the 60 min at 150V.

3.2.11 Urease Quantification (Trace Metals and E. coli)

Incubation and innoculation conditions were followed as described in section 2.2.8 with the addition of trace metal incubation at 0.1, 1 and 10ppm $NiCl_2$, $FeCl_2$ and $CoCl_2$ for *Sporsosarcina ureae* at 30°C. Recombinant *E. coli* strains (second generation urease expression system) were run at 37°C and compared to *S. ureae*.

3.2.12 Bioconsolidation

Sand vessels (60x60x15mm) machined at uOttawa were packed with a sterile, silica sand (0.2mm to 75um grain size) to a final dry density of 2.50-2.55g/cm^3. Cells of *S. ureae* , S. pasteurii and recombinant *E. coli* (with 2nd generation SDM point changes) were prepared and inoculated modified ATCC1832 media as described in 2.2.1 and grown overnight. Cells were concentrated in cementation media (0.5M $CaCl_2$, 0.5M Urea, 10g/L Tris-HCl, 1g/L yeast extract, pH 7.5) to an OD_{600} = 0.5-0.7. A control with cementation media only was also run. All conditions were tested at ambient temperature 20-25°C. Vessels were injected twice with fresh cementation media at t=0 and t=24h. Treated sands were washed with approximately 30-40mL of PBS between injection. Final samples were flushed with dH_2O and dried at 45-60°C for 48h prior to storage at 20°C in plastic containers.

Dried sands (60x60x15mm) were placed into a direct shearing apparatus (Model: ELE-26-2112/02) and consolidated for 10min under a normal stress of 25kPa. Samples were sheared at a rate of 2.5mm/min under dry, drained conditions. Stress-strain curves were acquired via the LabView data acquisition software program and imported onto Excel software for analysis

3.3 RESULTS

3.3.1 Amplification of UreA-C and UreD-G from *S.ureae*

PCR amplification of the UreA-C (lane 2 and 4), UreD-G (lane 5), and UreD (lane 1) sequences from genomic DNA of native *S. ureae* resulted in the production of bands in the 2.4kBp, 2.5kBp, and 0.9kBp regions, respectively, as shown in Figure 2.

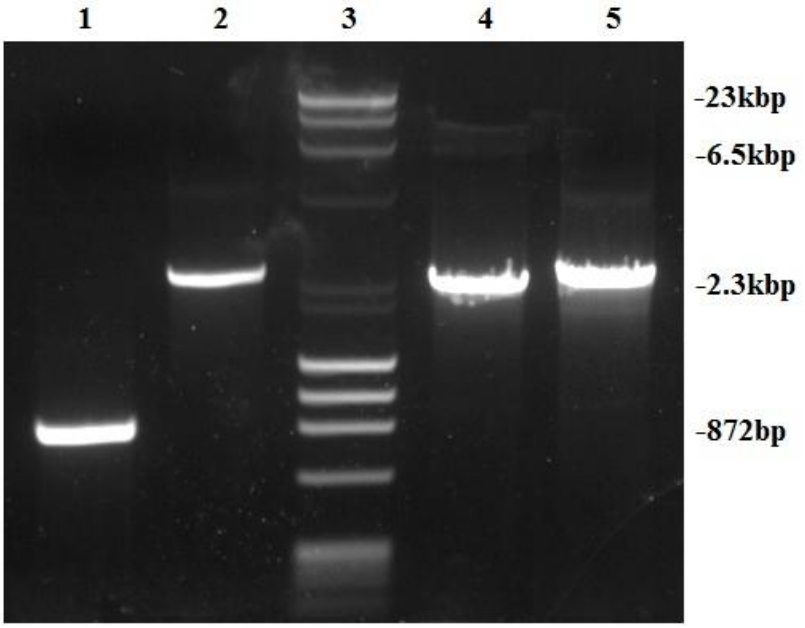

Figure 3.2: PCR amplification of UreA-C, UreD-G, and UreD from native *S. ureae*. A sample of 25 µl of each of the PCR products was loaded agarose gel wells, along with 5 µl of a broad range DNA molecular ladder (NEB) loaded in lane 3. Lane 1 contains UreD, lanes 2 and 4 contain UreA-C, and lane 5 contains UreD-G. Fractionation of the PCR products was carried out on 0.8% agarose gel at 90V for 5 minutes, then 120V for 35 minutes. Band sizes were predicted using Serial Cloner. Negative (no DNA) and positive (pet28b, T7 primers) omitted.

3.3.2 Colony PCR of UreA-C or UreD-G candidates

UreA-C or UreD-G was amplified from the pMiniT plasmid in DH10β *E.coli.* Gel fractionation following colony PCR of the selected colonies resulted in the production of bands in the 1.2kbp or 1.3kbp regions, respectively as shown in Figure 3. Bands are very bright and "horseshoe" shaped. Band smearing is present in lanes 1-4 and lanes 6-7 at roughly 700-100bp. There are also discernably brighter bands in lanes 3, 6, and 7 in the 300bp region.

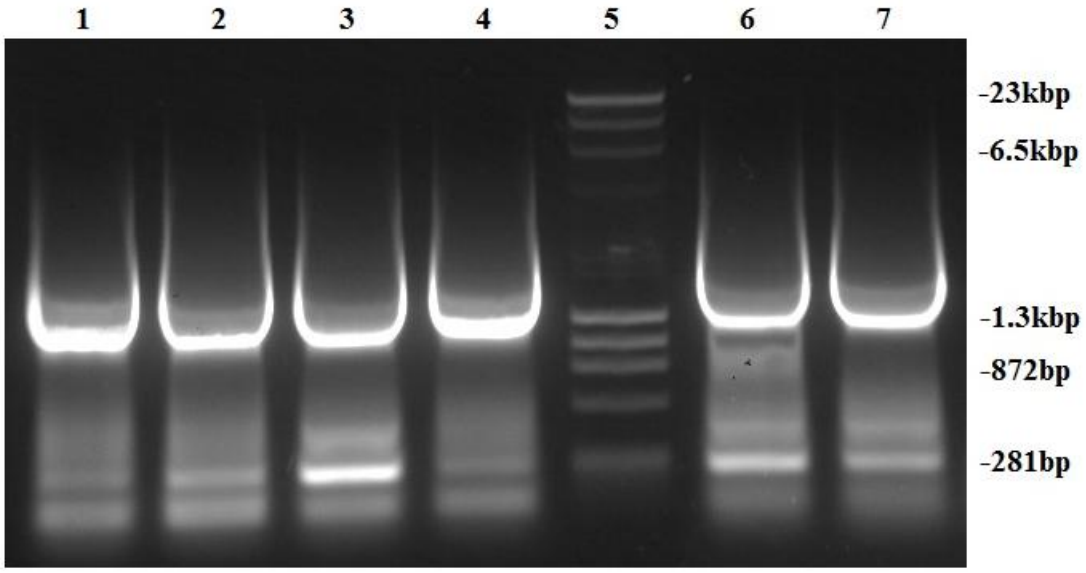

Figure 3.3: Colony PCR amplification of UreA-C or UreD-G from pMiniT plasmid. Lanes 1-4 contain UreA-C, lane 5 contains the broad range DNA ladder from NEB Phusion® PCR Kit, and lanes 6-7 contain amplified UreD-G. Fractionation of the PCR products was carried out on 0.8% agarose gel at 90V for 5 minutes, then 120V for 35 minutes. Negative (no DNA) and positive (no insert, pMiniT plasmid) omitted.

3.3.3 Digest of pMiniT containing UreA-C or UreD-G in DH10β

Following amplification (colony PCR from 3.2) of UreA-C or UreD-G from the pMiniT plasmid and gel fractionation, the desired bands were excised and purified. Purified DNA fragments were digested with BamHI and HindIII to ensure the presence of desired insert. Lanes 1-3 containing UreA-C digested by BamHI or HindIII resulted in the production of bands in the

2.2kbp and 400bp regions in lane 1, 2.0kbp and 500bp regions in lane 2, and 2.4kbp region in lane 3. Lanes 5-7 containing UreD-G digested by BamHI or HindIII resulted in the production of bands in the 2.5kbp, 1.7kbp, 0.9kbp, and 200bp regions in lane 5, 2.5kbp region in lane 6, and 2.6kbp region in lane 7.

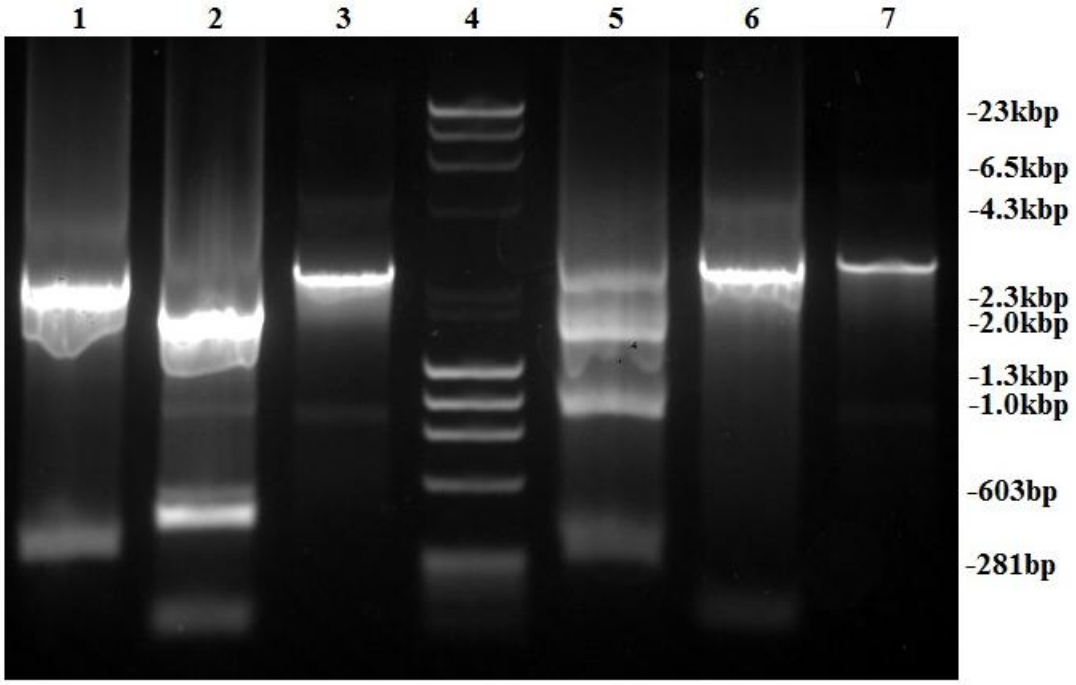

Figure 3.4: Digestion of colony PCR products (UreA-C or UreD-G) from pMiniT plasmid. Desired bands from colony PCR containing UreA-C or UreD-G gene fragments were excised and purified. Purified product was digested with BamHI and HindIII. Lanes 1-3 contain UreA-C digested by HindIII (1), BamHI (2), or undigested (3), while lanes 5-7 contain UreD-G digested by HindIII (5), BamHI (6), or undigested (7). Lane 4 contains the broad range DNA ladder from NEB Phusion® PCR Kit. Fractionation of digested PCR products was carried out on 0.8% agarose gel at 90V for 5 minutes, then 120V for 35 minutes.

3.3.4 Preparation of pET-28b(+) for UreA-C and UreD-G Ligation

The pET-28b(+) plasmid was digested with NheI and SacI in lane 2 and by NcoI and NheI in lane 3. These restriction enzyme locations were chosen to allow for the ligation of UreA-C and UreD-G fragments into pET-28b(+). Digestion resulted in the production of bands in the

4.5kbp region (lane 2) and the 4.2kbp region (lane 3). Bright bands are observed in both lanes; additionally, lane 3 has significant band streaking.

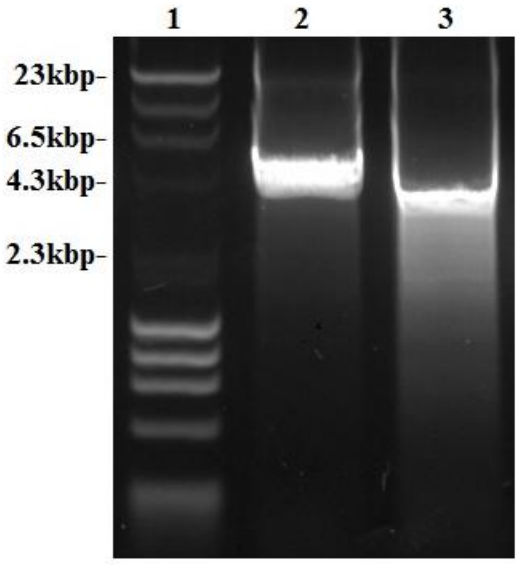

Figure 3.5: Preparatory gel of pET-28b(+) prior to UreA-C and UreD-G ligation. The pET-28b(+) plasmid was digested by NheI and SacI in lane 2 and by NcoI and NheI in lane 3. Lane 1 contains the broad range DNA ladder from NEB Phusion® PCR Kit. Fractionation of digested products was carried out on 0.8% agarose gel at 90V for 5 minutes, then 120V for 35 minutes.

3.3.5 Confirmation of subcloned UreA-C and UreD-G into pET-28b(+) restriction digest.

Recombinant DH10β containing UreA-C and TOP10 *E.coli* colonies containing UreD-G inserts in pET-28b(+) were grown on kanamycin selection plate. Colony PCR was conducted on sample colonies and they were analyzed by gel fractionation. PCR products were then purified and digested using XbaI or XhoI. Digestion resulted in the production of a bright band in the 2.0kbp region and a faint band in the 500bp region in lane 1, two bright bands in the 1.1kbp and 1.5kbp regions in lane 2, and one bright band in the 2.5kbp region in lane 3.

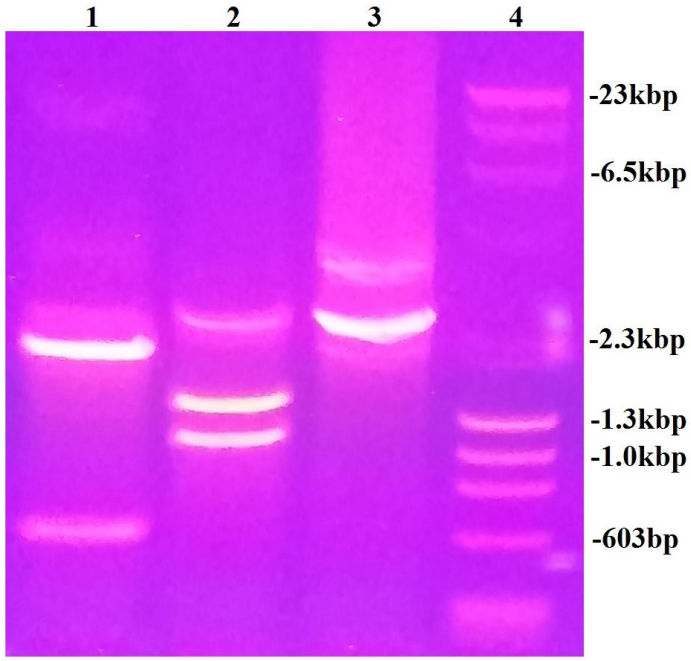

Figure 3.6: Digestion of recombinant pET-28b(+) plasmid containing UreA-C or UreD-G insert. Candidate colonies were selected after growing overnight on kanamycin plates. Colony PCR was performed on select colonies to amplify UreA-C or UreD-G. The UreD-G amplicon in lanes 1-2 was digested by XbaI (lane 1) or XhoI (lane 2). Lane 3 contains the UreA-C amplicon from colony PCR candidate digested by XhoI. Lane 4 contains the broad range DNA ladder from NEB Phusion® PCR kit. Fractionation of digested products was carried out on 0.8% agarose gel at 90V for 5 minutes, then 120V for 35 minutes.

3.3.6 Combinatorial ligation of UreA-C and UreD-G in pET-28b (+) expression vector

Colony PCR was performed to amplify the pET-28b (+) plasmid containing UreA-G. The PCR product was then digested using NheI and SacI. These restriction sites were chosen to excise the UreD-G fragment from the pET-28b (+) and UreA-C sequence. Digestion in panel A resulted in the production of one bright band in the 11.0kbp region and one faint band in the 5.0kbp region in lanes 1-3 and 5. In lane 6, two bright bands are observed in the 13.0kbp and 11.0kbp regions. Panel B containing undigested plasmid resulted in the production of bands in the 13.0kbp and 10.0kbp regions in lanes 1-3 and 5. In lane 6, one bright band is observed in the 14kbp region and a faint band is observed in the 7.0kbp region.

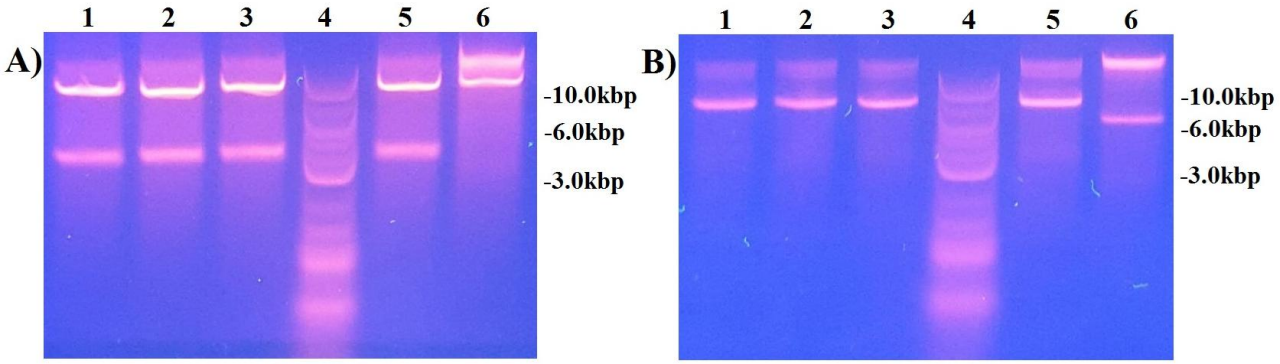

Figure 3.7: Digest of pET-28b(+) containing UreA-G. TOP10 *E. coli* colonies were grown overnight on kanamycin selection plates. Colonies were selected at random for colony PCR. The full pET-28b(+) plasmid containing UreA-G was amplified and digested using NheI and SacI. Panel A consists of the following: digest samples of pET-28b(+) containing UreA-G in lanes 1-3 and 5, digest sample of pET-28b(+) containing UreA-C (control) in lane 6. Panel B consists of the following: undigested UreA-G in lanes 1-3 and 5, undigested UreA-C in lane 6. Both panel A and B have the Quick-Load Purple 2-Log DNA Ladder from NEB in lane 4. Negative (no DNA) and positive (Lamda fragment) controls omitted.

3.3.7 Colony PCR of round 1 site-directed mutagenesis (SDM) of UreA-G in pET-28b (+)

Following identity confirmation of UreA-G in pET-28b (+), the first round of site-directed mutagenesis was conducted which resulted in the substitution of Asn110 to Asp110 of urease subunit beta. Modified UreA-G in pET-28b (+) was transformed into TOP 10 *E. coli*. Colony PCR was conducted in which the pET-28b (+) plasmid containing UreA-G was amplified. Gel fractionation following colony PCR of the selected colonies resulted in the production of bands in the 11.0kbp region in lanes 1, 2, 4, and 5. This was repeated for a second round of SDM (data not shown).

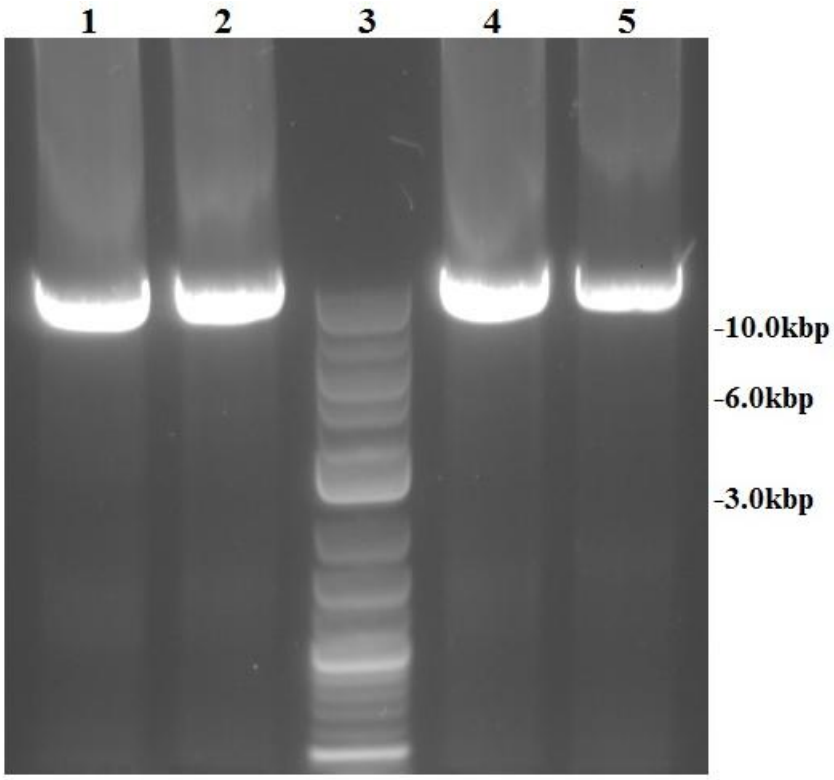

Figure 3.8: Colony PCR amplification of pET-28b (+) plasmid containing modified UreA-G. TOP10 *E. coli* colonies were grown overnight on kanamycin plates. Colony PCR was conducted in which the pET-28b (+) plasmid containing modified UreA-G was amplified. Lanes 1, 2, 4, and 5 contain UreA-G, lane 3 contains the Quick-Load Purple 2-Log DNA Ladder from NEB. Fractionation of the PCR products was carried out on 0.8% agarose gel at 90V for 5 minutes, then 120V for 35 minutes. Negative(no DNA) and positive (Lambda fragment) controls omitted.

3.3.8 Urease solubility assay

Subsequent to the sequencing confirmation of the second round of site-directed mutagenesis in which Asn100 was substituted for Asp100, round 1, round 2, and unmodified urease in pET-28b (+) were induced to express their respective urease enzyme in BL21-DE3 *E. coli*. SDS-Page gel analysis was conducted which resulted in 3 bands which appear to become brighter as we go from un-induced no SDM (1) to induced SDM round 2 (4) in the 197kDA, 60kDa, and 26kDa regions. There are several bands present in lane 1 which become progressively fainter in lanes 2-4 in the 70-90kDa range.

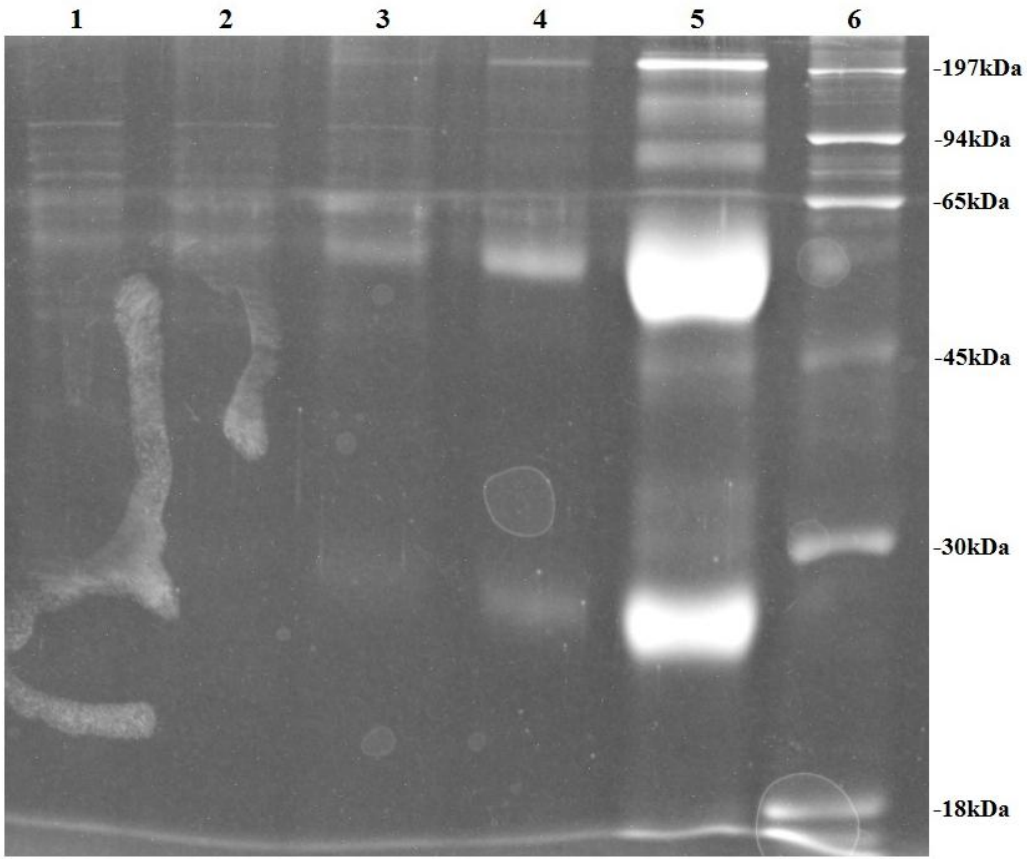

Figure3.9: SDS-Page gel illustrating urease protein fragment solubility. Subsequent to cell induction, a Bradford assay was conducted to ensure the total amount of protein per lane was 50µg/20µl. Lane 1 contains native urease from un-induced BL21-DE3 *E.coli*, lane 2 contains native urease from induced BL21-DE3 *E.coli*, lane 3 contains urease with Asp110 substitution from BL21-DE3 *E. coli*, lane 4 contains urease with Asp100 and Asp110 substitutions from BL21-DE3 *E. coli*, lane 5 contains bovine gamma globulin (control), and lane 6 contains the PAGEmark™ Unstained Marker from GBioSciences.

3.3.9 Urease quantification assay

Metal conditions of 0.1ppm $NiCl_2$ and 1/0.1ppm $FeCl_2$ maintained urease activities between 10 - 16 U/mL for *S. ureae*. Conversely, all other trace metals conditions led to values below 10 U/mL and particularly for all $CoCl_2$ conditions, values were near 0 U/mL. E. coli with a pET28(b)-UreAG expression mechanism produced values near but above zero prior to mutagenic changes and upwards of 15 U/mL for the system when two amino acid changes were applied to the UreB subunit of the urease expression gene cluster. This condition produced the highest observed activity of all measured.

Table 3.1 Comparison of urease activity (U/mL) ahcieved by Sporosarcina ureae and E. coli of second generation urease exression system. S. ureae was innoculated with trace metal enriched SB. Values (N=3) are reported as ±standard deviation (SD). One unit (U) is 1mM of urea degraded per minute. Innoculates were set at OD_{600} = 0.4 and run at 30°C (*Sporosarcina*) or 37°C (*Bacillus / E. coli*). SDM 1 and 2 refer to amino acid changes made on UreB subunit.

Condition	Activity (U/mL)
$NiCl_2$ (ppm)	
10	0.00 ± 0.00
1	10.55 ± 0.85
0.1	13.65 ± 0.21
$FeCl_2$ (ppm)	
10	7.55 ± 0.03
1	12.48 ± 0.95
0.1	14.31 ± 0.08
Co (ppm)	
10	0.05 ± 0.01
1	0.01 ± 0.05
0.1	0.00 ± 0.00
E. coli (pET28(b)-UreAG)	
No SDM	0.15 ± 0.09
SDM 1	12.74 ± 0.08
SDM 2	15.56 ± 1.39

3.3.10 Bioconsolidation of Model Sand

Sands treated with *Sporosarcina* induced soil strengths of neat 100kPa and greater than 5 times the value observed for control only conditions (85-90kPa v 16.90kPa). Despite a high activity rate in 3.3.9 the *E. coli* SDM 2 derivative induced a shear strength of 20kPa nearest that of control values observed. A broad range of soil strengths were observed for *Sporosarcina* conditions with the SD values equal to greater than half the mean strength in the condition for *S. ureae* (85kPa v 45kPa).

Table 3.2 Peak shear strength, τ (kPa) of stabilized silica sands (60x60x15mm) treated under various cementation conditions (100% saturation). All values (N=2-3) represent those from conditions carried out at room temperature (20-25°C) for 48 hours with two injections, unless otherwise stated. Data is presented as the mean ± SD. * $p < 0.05$ against two-tailed, unpaired t-test against 0.5M Urea-$CaCl_2$ (2-injection). Values derive from soil samples consolidated with a normal load of 25kPa prior to shearing.

Strain	Strength (kPa)
Sporosarcina pasteurii	85.97 ± 45.41
Sporosarcina ureae	90.42 ± 12.93
E. coli (SDM 2)	20.24 ± 3.20
Control (media only)	16.90 ± 0.9

3.4 DISCUSSION

In this second aspect of the investigation a chief goa wasl to extract the urease gene cluster from native *S. ureae* to allow for subsequent insertion into an *E. coli* expression system. The amplification of whole fragment UreA-G sequence and its ligation into the pMiniT stability vector was unsuccessful. This may have been due to the large size of the UreA-G insert (~5.6kbp) relative to the pMiniT plasmid (2525bp). However, the fragment when amplified as a pair of sequences, UreA-C (apoenzyme cluster) and UreD-G (co-enzyme cluster), of roughly equivalent size (2379bp and 2610bp) successfully stabilized in pMiniT (DH10β host).

The pMiniT plasmid contains ampicillin resistance in addition to a toxic minigene which, when expressed, is lethal to cells. This allows for a thorough double selection process in which only cells with the plasmid containing the insert are selected. The ligation of UreA-C and UreD-G into pMiniT was confirmed by colony PCR (Figure 3.3) and enzyme digest (Figure 3.4). Of note, it is observed in Figure 3.2 that bands for UreA-C are in the 1.2kbp region and the slightly larger UreD-G sequence is observed in the 1.3kbp region. The smaller band size observed is likely caused by overloading of the gel lanes with DNA which causes the bands to travel further down the gel than expected. Thus, a second confirmation analysis was done using a restriction enzyme digest (Figure 3.4). Serial Cloner predicted the digestion of UreA-C to produce bands in the 1970bp and 409bp regions for BamHI digest and bands in the 2175bp and 204bp region for HindIII digest. The digestion of UreD-G was predicted to produce one band in the 2.6kbp region for BamHI digest and bands in the 1642bp, 831bp, and 137bp regions for HindIII digest. The observed banding pattern in Figure 3.4 is consistent with expected bands predicted by Serial Cloner indicating that the desired sequence was present in pMiniT. The faint bands at the bottom of lane 2 and 6 are perhaps artifacts carried over from gel extraction of the bands following colony PCR or perhaps erroneous digest sequences added due to polymerase replication error (this is unlikely due to high fidelity of NEB Phusion®). The top band observed in lane 5 is likely uncut UreD-G due to incomplete digestion. This is supported by the similarity of band size as compared to the undigested UreD-G fragment in lane 7.

Following the creation of recombinant pMiniT-UreAG, transfer of the urease gene cluster into an expression vector was undergone. pET-28b (+) vector was chosen as the expression vector which contains kanamycin resistance and the T7 expression system. The T7 expression system contains the *lac* repressor which allows for induction by IPTG. The UreA-C and UreD-G fragments were successfully ligated into pET-28b (+) as confirmed by restriction enzyme digests (Figure 3.6). Serial Cloner predicted the digestion of UreD-G to produce bands in the 2097bp and 513bp regions for XbaI digest (lane 1) and bands in the 1531bp and 1079bp region for XhoI digest (lane 2). The digestion of UreA-C was predicted to produce one band in the 2.4kbp region for XhoI digest (lane 3) as UreA-C does not contain a XhoI restriction site. The observed banding pattern in Figure 3.6 is consistent with expected bands predicted by Serial Cloner indicating that the desired sequences were present in pET-28b (+).The top band present in lane 2 is likely uncut UreD-G as it is consistent in size with undigested UreD-G (2610bp). These fragments (UreA-C and UreD-G) were then successfully combined to form the full urease gene cluster (UreA-G) in pET-28b (+) confirmed also by restriction enzyme digests (Figure 3.7). The size of the full pET-28b (+) plasmid containing UreA-G is 10357bp as predicted by Serial Cloner. The restriction enzyme digest by NheI and SacI is designed to excise the UreD-G fragment from the amplified pET-28b (+) containing UreA-G. Thus, in lanes 1-3 and 5 of panel A, one should observe bands in the 7747bp and 2610bp regions. In Figure 3.7 bands are observed in the 10.0kbp and 5.0kbp regions. This discrepancy may be due to issues with loading the ladder as both bands are equally discrepant from expected sizes. As a result, sequencing was done to confirm the presence of UreA-G in pET-28b (+).

The second goal in part two of the study was to introduce amino acid substitutions into the primary structure of the urease enzyme to improve activity via solubility gains. This is expected to increase enzyme concentration in solution and lead to enhanced carbonatogenesis (as the limitation exerted by enzyme saturation would be reduced). Site-directed mutagenesis was conducted to convert Asn100 and Asn 110 to Asp100 and Asp110. Colony PCR was conducted on both round 1 and round 2 SDM as seen in Figure 8 which is a representative colony PCR of only the first round of SDM. The band size predicted (pET-28b (+) + UreA-G) was 10.4kbp. As one can observe in lanes 1-2 and 4-5 the bands produced are consistent with

predictions. Both mutations were confirmed as well with partial Sanger sequencing (View Appendix).

The final goal of this study was to analyze urease enzyme activity and solubility subsequent to amino acid substitutions and compare these results with the results obtained from native strains in part one of the investigation. Finally to apply the method to a model sand treatment. Enzymatic enhancement of urease was observed (Figure 3.9) for nickel and iron enrichment equal to or less than 1ppm. Urease is a metalloenzyme dependent on nickel for activity. Iron may also aid in coenzyme activity. Cobalt was detrimental to urease rates perhaps due to other toxic effects on the cell. At least partial gene expression was observed by SDS-PAGE following induction of recombinant *E. coli* clones (Figure 3.8). Although nothing conclusive can be drawn without a western blot there are several interesting observations. There are three bands present in lanes 1-4 which become brighter from un-induced no SDM (lane 1) to induced SDM 2 (lane 4). These bands are observed in the 197kDa, 60kDa, and 27kDa regions. UreA-G protein complex is 182kDa which is reasonably close in size to the thin top band present in lanes 1-4 in the 197kDa region. This band is brightest in the second round SDM lane (4) which may provide weak evidence for an increase in solubility as the total amount of protein present in each lane was standardized by Bradford assay. Both mutations were introduced into subunit beta which is 11.92kDa; however, no band is capable of being seen on the SDS-page gel at this size. The bands which become progressively brighter in the 60kDa and 27kDa regions are unknown; however, could be a number of combinations of subunits A-G. Moreover, bands in the 70-90kDa range are observed in lane 1 which become progressively fainter in lanes 2-4. These bands are perhaps cellular proteins present in the BL21-DE3 *E. coli*. This is supported by the fact that, once induced, the cell's protein profile changes as the protein of interest (in this case UreA-G) is overexpressed.

Model sand treatment of Sporosarcina produced a binding strength significantly greater ($p<0.05$) by a two tailed t-test compared to *E. coli* and media controls. Surprisingly E. coli (SDM 2, Table 3.1) attaining the highest urease activity recorded did not produce meaningful MICP activity in sands. It is proposed the cementation media was severely lethal to E. coli compared

to *Sporosarcina.* Effluent withdrawn from columns and platted on LB (Sporosarcina) or LB-Kan (E. coli) at t = 0, 4, 16, 24 and 48 hrs (data not shown) indicated colony forming units decreased by 50% for *E. coli* at the 4 hr mark while only 15% decrease was observed for *Sporosarcina*. It is suggested the Gram negative wall of *E. coli* may not withstand effectively the conditions required for MICP compared to *Sporosarcina*.

In review, recombinant studies of urease expression have been studied in the literature (Karimi and Marjan 2001). However, with respect to applications in bio-cementation, the controlled overexpression of the full urease gene cluster (UreA-G) from *E. coli* to a Gram positive, ureolytic host (*S. ureae*) is poorly studied. However, only one study found had succeeded in expressing the full urease gene cluster in *Campylobacter sputorum*, which is a Gram negative strain (Nakajima et al. 2014). Interestingly, urease overexpression of the partial gene cluster (UreA and UreB) in Gram negative hosts of *Helicobacter pylori* have been achieved for medical application (Karimi and Marjan 2001). Targeted, rationalized site-directed mutagenesis of urease apoprotein residues is another unique venture in this area of research. According to the current literature review, only random mutagenesis of Gram positive strains (Achal et al. 2009) has been undergone with success.

The future goals following from this study include conducting further site-directed mutagenesis in sites which have already been started and which were determined with in-silico analysis using pymol in urease subunits A and C. The further amino acid changes are expected to continue to increase enzyme solubility. Once desired mutations are produced, the ureolytic activity is to be tested by the modified method by Okyay et al and described in section 2.2.8. Other tests such as Western blotting and Mass Spectrometry can be done to ensure that presence of the urease gene cluster from SDS-Page analysis (Nakajima et al. 2014). Moreover, another major future goal involves shuttling the modified urease enzyme to a final, Gram positive and highly ureolytic hosts of *Sporosarcina* to allow for overexpression of the urease gene cluster in tandem with native expression levels. Expression of the pLAM1 shuttle plasmid (*E. coli* to Gram positive) has been achieved in *S. ureae* cells. The pLAM1 vector is a modified version of the vector pHCMC04. The modification makes it more stable in *E. coli* hosts prior to

shuttling it to Gram positive hosts (Nguyen et al. 2005). Cloning of the modified urease gene cluster into the pLAM1 plasmid is already partly achieved as well, with UreDG transformed stably in Top 10 *E. coli* as confirmed by colony PCR and DNA sequencing (data not shown).

SUMMARY

The present study was chiefly completed to assess MICP as a method for the strength enhacement of loose, sandy soils for improved engineering capability. This was undergone in two main parts by: (1) selection of a high activity, Gram positive host among those previously studied in the literature and (2) optimize urease activity and expression by trace metal enrichment, establishment of a urease overexpression system and induction of structural urease changes at the amino level.

In the first part of this study, *Sporosarcina and Bacillus* were compared with respect to the ureolytic activity of the urease enzyme. Species of *Sporosarcina* were observed to have higher ammonia production over time compared to others. Moreover, as an introduction to the construction of a recombinant expression vector containing the urease gene cluster a first generation expression system containing UreAB or UreE in pAD123-GroEL was attained. No significant activity was observed in the primary generation of recombinants and larger fragments of UreA-G, A-C and D-G were not attainable despite various strategies. Investigation with a Lambda Phage fragment provided evidence the cloning issue was not restricted by fragment size but rather composition, requiring either an alternative host to *E. coli* theorized to inhibit initial stability of plasmids with whole fragments or a plasmid with high inducibility. A next generation recombinant system containing UreA-G in pET28(b) was then achieved entering the second aspect of the study and with these points in mind. Nickel and iron metal enrichment (0.1-1ppm) was supported to improve unease activity in *Sporosarcina ureae* indicating media with these metals would benefit MICP positively. Site directed changes at the UreB subunit induced a urease activity in *E. coli* equal to or greater than *Sporosarcina* however, its apparent inability to survive cementation conditions did not allow for meaningful MICP in treated sands. This suggests a high ureolytic activity does not always directly correlate to MICP ability. Thus, the main goals of the study were achieved; however, future work will involve characterizing the recombinant urease activity for MICP following the transformation of the pET-28b (+) plasmid containing UreA-G into a Gram-positive host such as *Sporosarcina*. Work is already being undergone to achieve this with the inducible plasmid pLAM. Overall, the study

provides valuable insight assessing the ability to finalize a field ready method for MICP as a method for strength enhancement of sandy soils in construction or nature.

REFERENCES

5.1 Chapter 1

1. Rolf, S.A., and Lu¨ttge A."Calcium Carbonate Formation and Dissolution". Chem. Rev. 2007, 107, 342−381
2. Tegethoff, W., and Kroker, J.R.E. Calcium carbonate from the Cretaceous Period into the 21st Century. B.V. 2001
3. Rodriguez-Navarro, C., et al. " Conservation of Ornamental Stone by *Myxococcus xanthus*-Induced Carbonate Biomineralization" Appl. Environ. Microbiol. April 2003 vol. 69 no. 4 2182-2193
4. Morse, J. W., and Mackenzie, F.T. "Geochemistry of Sedimentary Carbonates". Elsevier: Amsterdam, 1990
5. Mackenzie et al. ReV. Mineral. 1983, 11, 97.
6. E. P. Burford, S.H., and Gadd, G.M. "Biomineralization of fungal hyphae with calcite (CaCO3) and calcium oxalate mono- and dihydrate in carboniferous limestone microcosm". Geomicrobiology Journal, 23(8):599–611, 2006.
7. Versteegen, A. "Biotic and Abiotic Controls on Calcium Carbonate Formation in Soils". PhD Thesis (2010).
8. Kamkha, M.A., et al. "Effect of pH on the Kinetics of Mass Crystallization of Calcium Carbonate". Kinetics and Catalysis, v. 30, n. 1, p. 62 – 67 (1989).
9. Dickinson, S.R., et al. "Controlling the Kinetic versus Thermodynamic Crystallisation of Calcium Carbonate". Journal of Crystal Growth, v. 244, p. 369 – 378 (2002).
10. Marion, G.M., et al. "Precipitation of solid phase calcium carbonates and their effect on application of seawater Sa-T-P models". Ocean Sci, 5, 285-91 (2009).
11. Gower, L.B. "Review Biomimetic model systems for investigating the amorphous precursor pathway and its role in biomineralization." *Chem Rev*. 108.11 (2008): 4551-627. Print.
12. Rybacki, A.S. "Calcium carbonate precipitation mechanisms and geochemical analysis of particulate material found within the waters of Maramec Spring, St James, Missouri". MSc. Thesis (2010).
13. Marion, G.M., et al. "Precipitation of solid phase calcium carbonates and their effect on application of seawater Sa-T-P models". Ocean Sci, 5, 285-91 (2009).
14. Dove, P.M. and Hochella, M.F. "Calcite Precipitation Mechanisms and Inhibition by Orthophosphate: In Situ Observations by Scanning Force Microscopy" Geochimica et Cosmochimica Acta, v. 57, p. 705 – 714 (1996).

15. Gómez-Morales, J., et al. "Nucleation of Calcium Carbonate at Different Initial pH Conditions". Journal of Crystal Growth, v. 169, p. 331 – 338 (1996).
16. Dreybrodt, W., et al. "Precipitation Kinetics of Calcite in the System CaCO3-H2O-CO2: The Conversion to CO2 by the Slow Process of H+ + HCO3 - → CO2 + H2O as a Rate Limiting Step" Geochimica et Cosmochimica Acta, v. 61, n. 18, p. 3897 – 3904 (1997).
17. Ferris, F.G., et al. "Metallic ion binding by Bacillus subtilis-Implications for the fossilization of microorganisms". Geology 16: 149–152 (1988).
18. Bazylinski D. and Frankel R. (2003) Biologically Induced Mineralization by bacteria, Reviews in Mineralogy and Geochemistry 54:95-114.
19. Lowenstam, H.A., and S. Weiner (1989) On Biomineralization, Oxford University Press, New York.
20. Stocks-Fischer S., et al. "Microbiological precipitation of CaCO3". Soil Biology and Biochemistry 31(11): 1563-1571 (1999).
21. Ferris, F. G., et al. "Iron-silica crystallite nucleation by bacteria in a geothermal sediment". Nature, 320: 609-611 (1987).
22. Fortin, D., and Beveridge, T.J. "Mechanistic routes to biomineral surface development. In: Biomineralization: From Biology to Biotechnology and Medical Applicatio" Bäuerlein E (ed) Wiley-VCH, Weinheim, Germany, p 7–2 (2000).
23. Pellerin, A. "Endostramatolites: Life in Extreme Environments and Lessons for the Detection of Life on Mars". MSc. Thesis. University of Ottawa, 2014.
24. Mann, S. "*Biomineralization: principles and concepts in bioinorganic materials chemistry"* Oxford, United Kingdom: Oxford University Press, 2001. Print.
25. Reid R.P. et al. "The role of microbes in accretion, lamination and early lithification of modern marine stromatolites". *Nature*, v.406, p.989 (2000).
26. Barabesi C., et al. "Bacillus subtilis Gene Cluster Involved in Calcium Carbonate Biomineralization". Journal of Bacteriology 189(1): 228–235 (2007).
27. Whiffin, V.S., and L.A. van Paassen, and M.P. Harkes. "Microbial carbonate precipitation as a soil improvement technique." *Geomicrobiology Journal*. 24.5 (2007): 417-423.
28. Southam G."Bacterial surface-mediated mineral formation". Environmental Microbe-Mineral Interactions. Lovley DR (ed) ASM Press, Washington, DC, p 257–276 (2000).
29. van Paassen, L.A., et al. "Potential soil reinforcement by biological denitrification". Ecological Engineering 36 (2010) 168–175
30. Krumbein W.E., et al. "Solar Lake (Sinai) Stromatolitic cyanobacterial mats". Limnology and Oceanography 22(4):635-656 (1977).
31. *Zumft, W. "Cell biology and molecular basis of denitrification". Microbiol. Mol. Biol. Rev **61**: 533–616 (1997).*

32. Whiffin, V.S. "Microbial CaCO3 precipitation for the production of biocement". Ph.D thesis (2004) Murdoch University, Perth, Western Australia, p. 154.

33. Sylvia, D.M., et al. "Principles and application of soil microbiology". 2nd edition.Pearson. New Jersey (2005)

34. Konieczna, I., et al. "Bacterial Urease and its Role in Long-Lasting Human Disease". Curr Protein Pept Sci. 2012 Dec; 13(8): 789–806.

35. Meldrum, F.C., and H. Colfen. "Review Controlling mineral morphologies and structures in biological and synthetic systems.." *Chem Rev*. 108.11 (2008): 4332-432. Print.

36. Kang, C-H., et al. "Soil Bioconsolidation Through Microbially Induced Calcite Precipitation by Lysinibacillus sphaericus WJ-8". Geomicrobiology Journal, 33:6, 473-478 (2016).

37. Lian, B., et al. "Carbonate biomineralization induced by soil bacterium Bacillus megaterium. Geochim Cosmochim Acta 70:5522–5535 (2008).

38. Casagrande, A. "Liquefaction and cyclic deformation of sands: A critical review". *Harvard Soil Mechanics Series No. 88* (1976).

39. Chu, J., et al. "Use of Microbial Technology in Geotechnical Engineering". *Second International Conference on Geotechnique, Construction Materials and Environment (2012)*

40. "Christchurch areas to be abandoned". *The New Zealand Herald*. NZPA. 7 March 2011. Retrieved June 22, 2016.

41. Thenhaus, P.C., et al. "Spatial and temporal earthquake clustering: part 1". EQECAT Inc. Publications 1, 1-12 (2008).

42. Bleskina, N.A. "Carbamide-Resin Stabilization of Sandy Soils". Soil Mechanics and Foundation Engineering, Vol. 45, No. 2, 2008 ;

43. Goffend, L.O., et al. "Nerve conduction, visual evoked responses and electroretinography in tunnel workers previously exposed to acrylamide and N-methylolacrylamide containing grouting agents." Neurotoxicity and Teratology 30, 186- 194 (2008).

44. Muynck, W.D., et al. "Bacterial carbonate precipitation improves the durability of cementitious materials," *Cem. Concr. Res.,* vol. 38, pp. 1005-1014, 2008.

45. Sarda, D.H., et al. "Biocalcification by Bacillus pasteurii urease: a novel application," *J. Ind. Microbiol Biotechnol.,* vol. 36, pp. 1111-1115, 2009.

46. Qian, W.L.C., and R. Wang, "Study on soil solidification based on microbiological precipitation of CaCO3," *Sci. China Technol. Sci.,* vol. 53, pp. 2372-2377, 2010.

47. F.G. Ferris, et al. "Bacteriogenic Mineral Plugging". Journal of Canadian Petroleum Society. 36, 9. 1997.

48. Mitchell, A.C., and Ferris, F.G. "Effect of Strontium Contaminants upon the Size and Solubility of Calcite Crystals Precipitated by the Bacterial Hydrolysis of Urea". *Environ. Sci. Technol.*, **2006**, *40* (3), pp 1008–1014

49. Woodhead A., et al. "Microbial Enhancement of Oil Recover" Dev. Petroleum Science. 1992.
50. Mitchell, K., and Santamarina, J.C., "Biological Considerations in Geotechnical Engineering," *J. Geotech. Geoenviron. Eng.,* vol. 131, pp. 1222-1233, 2005.
51. Van Paassen, L.A., et al. "Potential soil reinforcement by biological denitrification". Ecological Engineering 36 (2010) 168–175
52. Wei-Soon N., et al. "An Overview of the Factors Affecting Microbial-Induced Calcite Precipitation and its Potential Application in Soil Improvement" World Academy of Science, Engineering and Technology 62 2012
53. Al-Thawadi, S., and Cord-Ruwisch, R. 2012. Calcium carbonate crystals formation by ureolytic bacteria isolated from Australian soil and sludge. Journal of Advance Science and Engineering Research, **2**(1): 13–26
54. Achal, V., et al. "Strain improvement of *Sporosarcina pasteurii* for enhanced urease and calcite production" J Ind Microbiol Biotechnol (2009) 36:981–988.
55. Bergdale, T.E. et al. "Engineered biosealant strains producing inorganic and organic biopolymers". Journal of Biotechnology 161 (2012) 181–189
56. Lodish H, Berk A, Zipursky SL, et al. "Molecular Cell Biology". W.H. Freeman, New York. 4th Edition. 2000.
57. Turgeon, N., et al. "Elaboration of an electroporation protocol for Bacillus cereus ATCC 14579". Journal of Microbiological Methods 67 (2006) 543–548
58. Kim, J.K., et al. "Biosynthethesis of Active *Bacillus subtilis* Urease in the absence of known urease accessory proteins". J. Bacteriol. **October 2005** vol. 187 no. 20 **7150-7154**

5.2 Chapter 2

1. Van Paassen L. A. 2009 *Biogrout, ground improvement by microbial induced carbonate precipitation*, 202 pp. PhD thesis, Department of Biotechnology, Delft University of Technology, The Netherlands. Print.
2. Rodriguez-Navarro, C., F. Jroundi, M. Schiro, et al. "Influence of Substrate Mineralogy on Bacterial Mineralization of Calcium Carbonate: Implications for Stone Conservation." *Appl Environ Microbiol*. 78.11 (2012): 4017-4029. Print.
3. De Muynck, W., N. De Belie, and W. Verstraete. "Microbial carbonate precipitation in construction materials: a review." *Ecol. Eng*. 36. (2010): 118-36. Print.
4. Al-Thawadi, S.M. "Ureolytic bacteria and calcium carbonate formation as a mechanism of strength enhancement of sand". *Journal of Advance Science and Engineering Research*. 1. (2011): 98-114. Print.
5. Bang S.S., Ramakrishnan. V. "Microbiologically-enhanced crack remediation (MECR)". *Proceedings of the international symposium on industrial application of microbial genomes*. (2001): 3–13. Print.
6. Whiffin, V.S., L.A. van Paassen, and M.P. Harkes. "Microbial carbonate precipitation as a soil improvement technique." *Geomicrobiology J*. 24.5 (2007): 417-423. Print.
7. Al-Thawadi, S., and R. Cord-Ruwisch. "Calcium carbonate crystals formationby ureolytic bacteria isolated from Australian soil and sludge." *Journal of Advance Science and Engineering Research*. 2.1 (2012): 13-26. Print.
8. Hammes, F., N. Boon, G. Clement, et al. "Strain-specific ureolytic microbial calcium carbonate precipitation."*Applied and Environmental Microbiology* . 69. (2002): 4901-9. Print.
9. Mann, S. *Biomineralization: principles and concepts in bioinorganic materials chemistry.* Oxford, United Kingdom: Oxford University Press, 2001. Print
10. Gower, L.B. "Review Biomimetic model systems for investigating the amorphous aprecursor pathway and its role in biomineralization." *Chem Rev*. 108.11 (2008): 4551-627. Print.
11. Meldrum, F.C., and H. Colfen. "Review Controlling mineral morphologies and structures in biological and synthetic systems.." *Chem Rev*. 108.11 (2008): 4332-432. Print.
12. Beveridge, T.J. "Review Role of cellular design in bacterial metal accumulation and mineralization.." *Annu Rev Microbiol*. 43. (1989): 147-71. Print.
13. Carter, E.L., N. Flugga, and R.P. Hausinger. "Interplay of metal ions and urease" *Metallomics*. 1.3 (2009): 207-221. Print.
14. Jahns, T. "Ammonium/urea-Dependent Generation of a Proton Electrochemical Potential and Synthesis of ATP in Bacillus Pasteurii." *J Bacteriol.* 178.2 (1996): 403–409. Print.
15. Dick, J., W. De Windt, B. De Graef, et al. "Bio-deposition of a calcium carbonate layer on degraded limestone by Bacillus species." *Biodegradation*. 17. (2006): 357-67. Online.
16. Tobler, D.J., Cuthbert, M.O., Greswell, R.B., et al. "Comparison of rates of ureolysis between Sporosarcina pasteurii and an indigenous groundwater community under conditions required to precipitate large volumes of calcite". *Geochimica et Cosmochimica Acta* 75.11 (2011): 3290-3301. Print.
17. Farrugia, Mark A., Lee Macomber, and Robert P. Hausinger. "Biosynthesis of the Urease Metallocenter." *J Biol Chem.* 288.19 (2013): 13178–13185. Print.

18. Park, I.S., L.O. Michel, R.P. Hausinger, et al. "Characterization of the mononickel metallocenter in H134A mutant urease." *J Biol Chem*. 271.3 (1996): 18632-7. Print.
19. Dunn, A.K., Handelsman, J. “A vector for promoter trapping in *Bacillus cereus*”. *Gene* 226 (1999): 297-305. Print.
20. Horzempa, J., Tarwacki, D.M., *et al*. “Characterization and application of a glucose-repressible promoter in *Francisella tularensis*”. *Appl Environ Microbiol*. 74.4 (2008): 2161-2170.
21. HACH, Inc. "Salicylate Method - Nitrogen, Ammonia (0.50mg/L)." *HACH DR2700 Technical Manual* . 2013.
22. Zambelli, B., Musiani, F., Benini, S., Ciurli, S. “Chemistry of Ni^{2+} in urease: sensing, trafficking, and catalysis”. *Accounts of chemical research*. 44.7 (2011): 520-530. Print.
23. Tugba, O.O., and Rodrigues, D.F. "High throughput colorimetrc assay for rapid urease activity quantification" Journal of Microbiological Methods 95 (2013) 324–326.
24. Whitaker, Justin. "Bio-mediated calcium carbonate production as method for improving the liquefaction resistance of loose sands". Hnrs. Thesis. University of Ottawa, 2014.
25. Kiem, V., et al. 'The functional expression of toxic genes...". Anal Biochem. 2009 Oct 15; 393(2): 234–241.
26. Collins, C.M. and Falkow, S. "Genetic evidence of *E. coli* urease genes:..." J. Bacteriology, Dec. 1990, p. 7138-7144
27. Rosano, G.L., and Ceccarelli, E.A. "Recombinant protein expression is Escherichia coli: advances and challenges'. Front Microbiol. 2014; 5: 172.

5.3. Chapter 3

1. Achal, V., A. Mukherjee, P. C. Basu, and M. Sudhakara Reddy. 2009 "Strain Improvement of Sporosarcina Pasteurii for Enhanced Urease and Calcite Production." *Journal of Industrial Microbiology & Biotechnology* 36.7: 981-88. Web.
2. Al-Thawadi, S., and R. Cord-Ruwisch. 2012 "Calcium carbonate crystals formation by ureolytic bacteria isolated from Australian soil and sludge." *Journal of Advance Science and Engineering Research.* 2.1: 13-26.
3. Al-thawadi, Salwa. 2008 “High Strength In-situ Biocementation of Soil by Calcite Precipitating Locally Isolated Ureolytic Bacteria.” Thesis. Murdoch University, 2008. Perth: Murdoch U, 2008. Print.
4. Chantarasiri, Aiya, Vithaya, Meevootisom, Duangnate, Isarangkul, and Suthep Wiyakrutta. 2012 "Effective Improvement of D -Phenylglycine Aminotransferase Solubility by Protein Crystal Contact Engineering." *J Mol Microbiol Biotechnol Journal of Molecular Microbiology and Biotechnology* 22.3: 147-55. Web.
5. Cheng, Liang, and Ralf Cord-Ruwisch. 2012 "In Situ Soil Cementation with Ureolytic Bacteria by Surface Percolation." *Ecological Engineering* 42: 64-72. Web.
6. Costa, Sofia, André Almeida, António Castro, and Lucília Domingues. 2014 "Fusion Tags for Protein Solubility, Purification and Immunogenicity in Escherichia Coli: The Novel Fh8 System." *Frontiers in Microbiology* 5: n. pag. Web.
7. Dejong, Jason T., Michael B. Fritzges, and Klaus Nüsslein. 2006 "Microbially Induced Cementation to Control Sand Response to Undrained Shear." *J. Geotech. Geoenviron. Eng. Journal of Geotechnical and Geoenvironmental Engineering* 132.11: 1381-392. Web.
8. De Muynck, Willem, Nele De Belie, and Willy Verstraete.2010 "Microbial Carbonate Precipitation in Construction Materials: A Review." *Ecological Engineering* 36.2: 118-36. Web.
9. Ferris, Frederick G., and Lester G. Stehmeier. Bacteriogenic Mineral Plugging. Husky Oil Operations Ltd., assignee. Patent US5143155 A. 1 Sept. 1992. Print.
10. Idriss, I. M., and Ross W. Boulanger. 2008 “Soil Liquefaction during Earthquakes.” Oakland, CA: Earthquake Engineering Research Institute. Print.
11. Karimi, Mohsen, and Marjan Mohammadi. 2001 "Cloning and Expression of Recombinant Helicobacter Pylori Urease A and B Subunits as a Putative Vaccine." *Iranian Biomedical Journal* 5: 107-11. Web. 24 Apr. 2016.
12. Karol, R. H. 2003 *Chemical Grouting and Soil Stabilization.* New York: M. Dekker, Print.
13. Kotait, Maryam. Investigating the Over Expression of UreA-G for Increased Ureolytic Activity in Sporosarcina Ureae. Thesis. University of Ottawa, 2015.
14. Nakajima, T., T. Kuribayashi, S. Yamamoto, J. E. Moore, and B. C. Millar. 2014 "Construction and Expression of a Recombinant Urease Gene Cluster from

Campylobacter Sputorum Biovar Paraureolyticus." *British Journal of Biomedical Science* 71.2: 58-65. Web. 25 Apr. 2016.

15. Ndao, Moise, Ellen Keene, Fairland F. Amos, Gita Rewari, Christopher B. Ponce, Lara Estroff, and John Spencer Evans. 2010 "Intrinsically Disordered Mollusk Shell Prismatic Protein That Modulates Calcium Carbonate Crystal Growth." *Biomacromolecules* 11.10: 2539-544. Web.
16. Nguyen, Hoang Duc, Quynh Anh Nguyen, Rita C. Ferreira, Luis C.s. Ferreira, Linh Thuoc Tran, and Wolfgang Schumann. 2005 "Construction of Plasmid-based Expression Vectors for Bacillus Subtilis Exhibiting Full Structural Stability." Plasmid 54.3: 241-48. Web.
17. Okyay, Tugba Onal, and Rodrigues, Debora F. 2013 "High Throughput Colorimetric Assay for Rapid Urease Activity Quantification." Journal of Microbiological Methods 95.3: 324-26. Web.
18. Ramachandran, Santhosh K., V. Ramakrishnan, and Sookie S. Bang. 2001 "Remediation of Concrete Using Microorganisms." *ACI Materials Journal* MJ 98.1: n. pag. Web. 9 Mar. 2016.
19. Sato, Ai, Seiji Nagasaka, Kazuo Furihata, Shinji Nagata, Isao Arai, Kazuko Saruwatari, Toshihiro Kogure, Shohei Sakuda, and Hiromichi Nagasawa. 2011 "Glycolytic Intermediates Induce Amorphous Calcium Carbonate Formation in Crustaceans." *Nature Chemical Biology* 7.4: 197-99. Web.
20. Trevino, Saul R. 2006 "Amino Acid Contribution to Protein Solubility: Asp, Glu, and Ser Contribute More Favorably than the Other Hydrophilic Amino Acids in RNase Sa." *Journal of Molecular Biology.* U.S. National Library of Medicine. Web. 20 Mar. 2016.
21. Van Paassen, L. A., M. P. Harkes, G. A. Van Zwieten, and W. H. Van Der Zon. 2009 "Scale up of BioGrout: A Biological Ground Reinforcement Method." *ResearchGate.* IOS Press. Web. 02 Mar. 2016.
22. Whiffin, Victoria S., Leon A. Van Paassen, and Marien P. Harkes. 2007 "Microbial Carbonate Precipitation as a Soil Improvement Technique."*Geomicrobiology Journal* 24.5: 417-23. Web.

APPENDIX

6.1 Chapter 2

5'-- GAATTCGAGC TCGGTACCCG GGGATCCTCT AGATTTAAGA AGGAGATATA CATATGAGTA

61 AAGGAGAAGA ACTTTTCACT GGAGTTGTCC CAATTCTTGT TGAATTAGAT GGTGATGTTA

121 ATGGGCACAA ATTTTCTGTC AGTGGAGAGG GTGAAGGTGA TGCAACATAC GGAAAACTTA

181 CCCTTAAATT TATTTGCACT ACTGGAAAAC TACCTGTTCC ATGGCCAACA CTTGTCACTA

241 CTTTCGGGTA TGGTGTTCAA TGCTTTGCGA GATACCCAGA TCATATGAAA CAGCATGACT

301 TTTTCAAGAG TGCCATGCCC GAAGGTTATG TACAGGAAAG AACTATATTT TTCAAAGATG

361 ACGGGAACTA CAAGACACGT GCTGAAGTCA AGTTTGAAGG TGATACCCTT GTTAATAGAA

421 TCGAGTTAAA AGGTATTGAT TTTAAAGAAG ATGGAAACAT TCTTGGACAC AAATTGGAAT

481 ACAACTATAA CTCACACAAT GTATACATCA TGGCAGACAA ACAAAAGAAT GGAATCAAAG

541 TTAACTTCAA AATTAGACAC AACATTGAAG ATGGAAGCGT TCAACTAGCA GACCATTATC

601 AACAAAATAC TCCAATTGGC GATGGCCCTG TCCTTTTACC AGACAACCAT TACCTGTCCA

661 CACAATCTGC CCTTTCGAAA GATCCCAACG AAAAGAGAGA CCACATGGTC CTTCTTGAGT

721 TTGTAACAGC TGCTGGGATT ACACATGGCA TGGATGAACT ATACAAATAA ATCTCCTGCA

781 GGCATGCAAG CTTGAGTAGG ACAAATCCGC CGAGCTTCGA CGAGATTTTC AGGAGCTAAG

841 GAAGCTAAAA TGGAGAAAAA AATCACTGGA TATACCACCG TTGATATATC CCAATGGCAT

901 CGTAAAGAAC ATTTTGAGGC ATTTCAGTCA GTTGCTCAAT GTACCTATAA CCAGACCGTT

961 CAGAACAAAG AATACAAGAA AATATTTACA AAAAATCAAT TTAACAATTC CTTAAAACAT

1021 GCAGGAATTG ACGATTTAAA CAATATTAGC TTTGAACAAT TCTTATCTCT TTTCAATAGC

1081 TATAAATTAT TTAATAAGTA AGTTAAGGGA TGCATAAACT GCATCCCTTA ACTTGTTTTT

1141 CGTGTGCCTA TTTTTTGTGA ATCGCTAAGA AACCATTATT ATCATGACAT TAACCTATAA

1201 AAATAGGCGT ATCACGAGGC CCTTTCGTCT CGCGCGTTTC GGTGATGACG GTGAAAACCT

1261 CTGACACATG CAGCTCCCGG AGACGGTCAC AGCTTGTCTG TAAGCGGATG CCGGGAGCAG

1321 ACAAGCCCGT CAGGGCGCGT CAGCGGGTGT TGGCGGGTGT CGGGGCTGGC TTAACTATGC

1381 GGCATCAGAG CAGATTGTAC TGAGAGTGCA CCATACAAAA CATATTTCAA CACAATACAA

1441 ATGGGTTAGT TAAAAAAGCA GGCCTTCTAA AGGTCTGCTT TTTTTATTTG ATTATGTAAT

1501 TTTTAATGCC AGGATGCCAA TAAGCCATAA CCTCAAATGC ACCATTTGCA ACCTCGTCAT

1561 CTTCTTCCTC AATCTTGACC AGATCGCCGT CCTCCGCATC ACCAAGATTC AGCTCTTTAT

1621 GTATCTCCTT CAAAATGCCA CCGTATCCAA TTAACCTTCG AGCTGCCAAC GCATCATCCA

1681 AGTAAAGCAC CGTGTTCAGA TTGTCTTCAG TCACCTTATT ACCGCGCACA CAATCCGTAT

1741 CCTTAACCGG ATATTTAGAG ATTTCGCGAA CAGCTTTTTG CTCCATCATT GCGTTCCGCA

1801 CATCGTTTTC AATCTGTTCA GCGTCAATCT TAGCTTTACC TTTCACTCGA CGAATATCGA

1861 CAATTGGAGT GTAATCCAAT TTCATCGCCT TTTTCCAAAG GCTCGTCCAC TCCGCCTGCT

1921 TAATATAGTT TTTCCCAAAA TAATTTTTCC TTACTGGTAT CAACACATGA AAATGAGGAT

1981 GATATGTATC TTCTTCATGA TTTTTGGTAA TCTCTAAAGC TCTGAAAAAT CCAAGAACCG

2041 AAGTTTTTAC TTTTTTGTAC TGGAACAGTT TCCTAAAGCC TTCCATCATC GCAGAAATTT

2101 GTGGCTTCAG CCGTTCTCCC TTTACATTTC GAATCGTCAG CGTGAGAAAA ATCCATCCGC

2161 AGCCGTACTG TCTATTGGCT TCCTCTACGA TCAACTTATT GTGATAAGCA ATTTTTAACG

2221 ACCTGCGCCA CGCACACATC GGACATAACC TCACTTTACA AAAATGGGCT TGATACAGTT

2281 TTAACTTGCC CGTCTCCGGG TCTCTCTTAA ACGAAAGATA CTCTGCACAA CTAATTAGTT

2341 TTTCAGCCTT TTTGCCATAG TAAGGTGCCC CAATCTTACT CTCTAACGCT TCGTAATGCT

2401 CCGCCATGAG GTTCGTCCGT CTCTTTTTCC CCTTCCAATC CCGCTTTTTA CCTGTTGCGG

2461 TTTTATCTTC GAGGATGCTA TAATCATTTT CAGATGAATA AATCAACAAA AAAACTCCTT

2521 CTGAGCTAGT TCTCTAGCAT TCTATTATTT TGATTCGACA CCTTAATAAT AGCAGAAGGA

2581 GTTTTTACCT GTCAAAGAAC CATCAAACCC TTGATACACA AGGCTTTGAC CTAATTTTGA

2641 AAAATGATGT TGTTTCTATA TAGTATCAAG ATAAGAAAGA AAAGGATTTT TCGCTACGCT

2701 CAAATCCTTT AAAAAAACAC AAAAGACCAC ATTTTTTAAT GTGGTCTTTA TTCTTCAACT

2761 AAAGCACCCA TTAGTTCAAC AAACGAAAAT TGGATAAAGT GGGATATTTT TAAAATATAT

2821 ATTTATGTTA CAGTAATATT GACTTTTAAA AAAGGATTGA TTCTAATGAA GAAAGCAGAC

2881 AAGTAAGCCT CCTAAATTCA CTTTAGATAA AAATTTAGGA GGCATATCAA ATGAACTTTA

2941 ATAAAATTGA TTTAGACAAT TGGAAGAGAA AAGAGATATT TAATCATTAT TTGAACCAAC

3001 AAACGACTTT TAGTATAACC ACAGAAATTG ATATTAGTGT TTTATACCGA AACATAAAAC

3061 AAGAAGGATA TAAATTTTAC CCTGCATTTA TTTTCTTAGT GACAAGGGTG ATAAACTCAA

3121 ATACAGCTTT TAGAACTGGT TACAATAGCG ACGGAGAGTT AGGTTATTGG GATAAGTTAG

3181 AGCCACTTTA TACAATTTTT GATGGTGTAT CTAAAACATT CTCTGGTATT TGGACTCCTG

3241 TAAAGAATGA CTTCAAAGAG TTTTATGATT TATACCTTTC TGATGTAGAG AAATATAATG

3301 GTTCGGGGAA ATTGTTTCCC AAAACACCTA TACCTGAAAA TGCTTTTTCT CTTTCTATTA

3361 TTCCATGGAC TTCATTTACT GGGTTTAACT TAAATATCAA TAATAATAGT AATTACCTTC

3421 TACCCATTAT TACAGCAGGA AAATTCATTA ATAAAGGTAA TTCAATATAT TTACCGCTAT

3481 CTTTACAGGT ACATCATTCT GTTTGTGATG GTTATCATGC AGGATTGTTT ATGAACTCTA

3541 TTCAGGAATT GTCAGATAGG CCTAATGACT GGCTTTTATA ATATGAGATA ATGCCGACTG

3601 TACTTTTTAC AGTCGGTTTT CTAATGTCAC TAACCTGCCC CGTTAGTCGC CATTCGCCAG

3661 CTGCCTCGCG CGTTTCGGTG ATGACGGTGA AAACCTCTGA CACATGCAGC TCCCGGAGAC

3721 GGTCACAGCT TGTCTGTAAG CGGATGCCGG GAGCAGACAA GCCCGTCAGG GCGCGTCAGC

3781 GGGTGTTGGC GGGTGTCGGG GCGCAGCCAT GACCCAGTCA CGTAGCGATA GCGGAGTGTA

3841 TACTGGCTTA ACTATGCGGC ATCAGAGCAG ATTGTACTGA GAGTGCACCA TATGCGGTGT

3901 GAAATACCGC ACAGATGCGT AAGGAGAAAA TACCGCATCA GGCGCTCTTC CGCTTCCTCG

3961 CTCACTGACT CGCTGCGCTC GGTCGTTCGG CTGCGGCGAG CGGTATCAGC TCACTCAAAG

4021 GCGGTAATAC GGTTATCCAC AGAATCAGGG GATAACGCAG GAAAGAACAT GTGAGCAAAA

4081 GGCCAGCAAA AGGCCAGGAA CCGTAAAAAG GCCGCGTTGC TGGCGTTTTT CCATAGGCTC

4141 CGCCCCCCTG ACGAGCATCA CAAAAATCGA CGCTCAAGTC AGAGGTGGCG AAACCCGACA

4201 GGACTATAAA GATACCAGGC GTTTCCCCCT GGAAGCTCCC TCGTGCGCTC TCCTGTTCCG

4261 ACCCTGCCGC TTACCGGATA CCTGTCCGCC TTTCTCCCTT CGGGAAGCGT GGCGCTTTCT

4321 CAATGCTCAC GCTGTAGGTA TCTCAGTTCG GTGTAGGTCG TTCGCTCCAA GCTGGGCTGT

4381 GTGCACGAAC CCCCCGTTCA GCCCGACCGC TGCGCCTTAT CCGGTAACTA TCGTCTTGAG

4441 TCCAACCCGG TAAGACACGA CTTATCGCCA CTGGCAGCAG CCACTGGTAA CAGGATTAGC

4501 AGAGCGAGGT ATGTAGGCGG TGCTACAGAG TTCTTGAAGT GGTGGCCTAA CTACGGCTAC

4561 ACTAGAAGGA CAGTATTTGG TATCTGCGCT CTGCTGAAGC CAGTTACCTT CGGAAAAAGA

4621 GTTGGTAGCT CTTGATCCGG CAAACAAACC ACCGCTGGTA GCGGTGGTTT TTTTGTTTGC

4681 AAGCAGCAGA TTACGCGCAG AAAAAAAGGA TCTCAAGAAG ATCCTTTGAT CTTTTCTACG

4741 GGGTCTGACG CTCAGTGGAA CGAAAACTCA CGTTAAGGGA TTTTGGTCAT GAGATTATCA

4801 AAAAGGATCT TCACCTAGAT CCTTTTAAAT TAAAAATGAA GTTTTAAATC AATCTAAAGT

4861 ATATATGAGT AAACTTGGTC TGACAGTTAC CAATGCTTAA TCAGTGAGGC ACCTATCTCA

4921 GCGATCTGTC TATTTCGTTC ATCCATAGTT GCCTGACTCC CCGTCGTGTA GATAACTACG

4981 ATACGGGAGG GCTTACCATC TGGCCCCAGT GCTGCAATGA TACCGCGAGA CCCACGCTCA

5041 CCGGCTCCAG ATTTATCAGC AATAAACCAG CCAGCCGGAA GGGCCGAGCG CAGAAGTGGT

5101 CCTGCAACTT TATCCGCCTC CATCCAGTCT ATTAATTGTT GCCGGGAAGC TAGAGTAAGT

5161 AGTTCGCCAG TTAATAGTTT GCGCAACGTT GTTGCCATTG CTGCAGGCAT CGTGGTGTCA

5221 CGCTCGTCGT TTGGTATGGC TTCATTCAGC TCCGGTTCCC AACGATCAAG GCGAGTTACA

5281 TGATCCCCCA TGTTGTGCAA AAAAGCGGTT AGCTCCTTCG GTCCTCCGAT CGTTGTCAGA

5341 AGTAAGTTGG CCGCAGTGTT ATCACTCATG GTTATGGCAG CACTGCATAA TTCTCTTACT

5401 GTCATGCCAT CCGTAAGATG CTTTTCTGTG ACTGGTGAGT ACTCAACCAA GTCATTCTGA

5461 GAATAGTGTA TGCGGCGACC GAGTTGCTCT TGCCCGGCGT CAACACGGGA TAATACCGCG

5521 CCACATAGCA GAACTTTAAA AGTGCTCATC ATTGGAAAAC GTTCTTCGGG GCGAAAACTC

5581 TCAAGGATCT TACCGCTGTT GAGATCCAGT TCGATGTAAC CCACTCGTGC ACCCAACTGA

5641 TCTTCAGCAT CTTTTACTTT CACCAGCGTT TCTGGGTGAG CAAAAACAGG AAGGCAAAAT

5701 GCCGCAAAAA AGGGAATAAG GGCGACACGG AAATGTTGAA TACTCATACT CTTCCTTTTT

5761 CAATATTATT GAAGCATTTA TCAGGGTTAT TGTCTCATGA GCGGATACAT ATTTGAATGT

sdcsdc ATTTAGAAAA ATAAACAAAT AGGGGTTCCG CGCACATTTC CCCGAAAAGT GCCACCTGAC

5881 GTCTAAGAAA CCATTATTAT CATGACATTA ACCTATAAAA ATAGGCGTAT CACGAGGCCC

5941 TTTCGTCTTC AA – 3’

Figure 6.1. DNA sequence of promoter-trap expression vector pAD123 (5953 bp). This vector was constructed from pKK232-9 (GenBank accession number: U13859), pHP13 (GenBank accession number: DQ297764) and pFPV25 (GenBank accession number U73901). Key features of pAD123 include the coding sequence for beta-lactamase which confers ampicillin resistance, derived from pKK232-9 (highlighted in green, promoter underlined), as well as the sequence for chloramphenicol resistance (highlighted in blue) derived from pHP13, and a promoterless gene encoding mutant GFPmut3a optimized for Fluorescent Activated Cell Sorting (highlighted in grey) derived from EcoRI and HindIII restricted pFPV25. The multiple cloning site (highlighted in yellow) contains recognition sequences for the restriction enzymes EcoRI, SacI, KpnI, SmaI, BamHI, and XbaI.

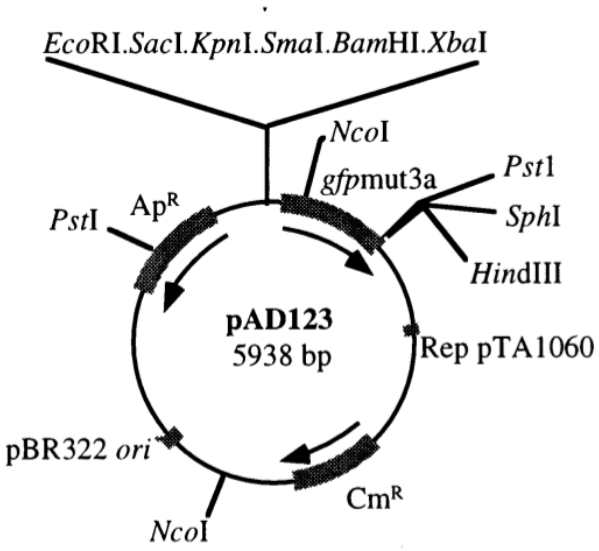

Figure 6.2. Schematic of the promoter-trap expression vector pAD123. Portrayed by Dunn and Handlesman (1997), constructed from pKK232-9, pHP13, and pFPV25. Key features include a multiple cloning site adjacent to a gfp mutant gene (gfpmut3a) optimized for Fluorescent Activated Cell Sorting (FACS), a chloramphenicol resistance gene (Cm^R), beta-lactamase ampicillin resistance gene (Ap^R) and pBR322 *Escherichia coli* origin of replication.

5’---tttttatagagctcATGCGATTACTACCGCGTGAaattgataagttaatgatcgttgttgctgcagacgttgccagaaga

cggagggaacgaggacttaaattgaatcaccctgaagcaatggctcttattacatatgaAgatggaaggtgccagaga

tgggaaaacagttgcggaacttatggcttatggtgcgacgattttaactcgtgaagatgtaatggatgggattcctgaaa

tgattgatgacattcaagtagaagcaacattccctgatgggacgaagttagtcacagtgcataacccgataagatagatt

gtttatgaaaagaagggagacgtaacgatgataccaggcgaatatattttaaaagatgaaccaatcatttgtaatgaagg

tgcagaaaatatacatgtacaagttattaatcatggggacagacccatccaaattggttcccattatcatttttatgaag

tgaatcttgcgttaaagtttgatcgggatgtgacgtatggtaaacgtttaaatattcctgcaggcgctgctgttcgtttt

gagccgggcgatgaaaaagaagtacagctaattgactatgctggagaaagagaagtgtacggttttcacaataaagtaga

cggagcattgggaggcgggaatacaaaatgagttttaaaatggatagagagcaatatgctcaaatgtacggaccgacaac

cggagactctgtccgactagcagatacagatttatttatccaaatcgaaaaagactacacaaaatatggagaagaagttg

tgttcggtggcgggaaagtcattcgcgatggaatgggccaacacccgtacataacgcgcgaagaagatgaacgcgtacct

gatacagtcattacaaatgttgtcgtgctggactatacaggaatatataaagcggatctagcaattcgagacggcaaaat

ttcgggtatcggcaaagcaggtaatccgcttgtgcaagacaaagtggatattattattggaacgtccactgaagttattt

cgggtgaaggtaaaatcattactgccggtgcaattgatacgcacgtgcactttattaatccggcacaagtagatgtcgca

cttactgcgggaacgacaacactaatcggtggtggagctggaccgggagatggttctagagctacgactgccacaccagg

tgcttggcatcttcattccatgctgaaggctttggatggacaaccgatcaatatcggtttaacagggaaagggcatgcag

cagcaggaggcccattagctgaacaaataattgccggtgcgattggtttgaaagttcatgaagattggggcgcaacaccg

tctgttctcgatcatgcattacgcattgctgatgaatatgacgtgcaagtcgcacttcacgcggatacattaaacgaatc

cggatttttgaagatacgatcaaagccattgatggtcgcggtatccatatgtaccatacagagggtgcaggaggcggac

atgctccggatttgattaaatctgcaggcatgatgaacgtgttgccggcttctaccaatccgacattgccgtatacaatt

aatacgattgatgagcatttggatatggtgatggtagcgcataacttaaatccttccgtgccagaagatatcgcatttgc

agattcacgtattcgcaatgaaacgattgcagcggaagatattttacaagacctaggtgtctttagtatgacaagctccg

attctcaggcgatgggccgtatcggagaagttgcacttcgcacatggcaagtagcccacaaaatgaaaaaccagcttgga

gttatggagggcgatagtgagtattcggataataatcgggtaaagcgctatgttgctaaatatacgattaatcctgctat

cgctcatggcgtatccgagtatatcggttcaattgaagtcgggaaaatggctgaccttgtcctatgggatccaaaattct

ttggcgttaaaccggaaatgatattgaagaatggaatggcagtctttagcttaatgggagatgctaatgcgacgatccca

acgccacaacccatgatttatcgtccgatgtatgcaacactcggtaaggcattgtcgcaaagttctattacgtttgtttc

ccaaattgcatatgatcaaggaataaaagagaagcttggacttgaaaaagtggtactgcctgttcgtaatatacgcagtc

tcacgaaaaaagatatgaaattaaatacagctacaccccatattgatgtagatccacaaacgtatgaagtgaaaattgac

ggaaaacttataacatgtgatccgattgacgtagtacctatgggtcaacgctatttcttattctgaggtgaagaaaatga

ttgtagaagaagtcttaatgaacgttagagatttagatccaagtaagtatgacagccttcataaagagaaagtgtactta

gaaagtgcacatttaatgaaaagaattcaacgtgtagaaaccgatcacgggcgtgaaattggaattcgattaaaaaaacc

ccgtgatttggaagcgggagacattctttttatggatgataagaatgttattttgattgacgtactttctgatgatttaa

ttattattagcccgcggacgatgcttgaaatgggaacgattgctcatcagctcggaaatcgtcatttacctgcgcagttt

gaggatgaggatatgctcgttcagtatgattatttagtcgaggaattgctacaagaaatgggtattccattcaagcgaga

agaacgaaaagttgcgaaggctttccgtcatatcggacatagccatgactaataacgcattgtccttgttacagctatgc

gattcaagttttccgatcggctcttttagccagtcatttggactggaaacgtatatccaaaacgacaaggtcaccgatgc

caatacgttttctgagtggttgaatgtctatctgcatgaacagcttgcttatgcagatggcttggccgtaagactcgttt

atgatgcacttgatgtggatgatcttaataagatttgggaattggatcgcatattgactgtacagaatcttgcccgtgaa

tcacgtgatggaacacaacgtatgggtgacagaatgttagacattgccgaatccatttacaaaataccagtgttatctat

ctacgcgcagaaaattcgtgacaaacaagctttcggacatccagctattgtttttacaatgatcggacatcaccttcaag

tagaaaagactacaacgattttatattatttatattcgacggttgttagtctcgtacaaaatgccgtgcgggccatcccg

cttggacagactgcgggacagaagattatttatacgtttcaacaacaacttcagcaaacaacagacaaaattatggaatt

agatcaagaagagtttggagtcgtatcgccaggactcgagctttcacaaatgcaacacgaacgtgttgggatacgtattt

ttagttcgtaacgaacacaatgaaattgagaataaggatgtgcttagaatgggagcaattaaaataggtgttggcggacc

agttggtgcaggaaaaactatgctggtcgaaaagattacacgcgctttagagggcgaagtaagtatggcagtcattacaa

atgatatatacacgaaagaagatgccaagtttttagttgcgaacggtattcttccagaagaccgcattgtcggggtggaa

acaggaggctgtccacatacagcaattcgagaagatgcatcgatgaactttgcggcgattaatgaattgcaggaaaagca

tcccgacgtagagttgatttttgtagagagtggcggcgataatctagcggctacattcagtccggaactcgtagacttttt

ccatttatataattgacgtagcgcagggtgaaaaaatcccgcgcaaaggcggacaaggaatgattaaatctgatttgttt

attataaacaaaacagatttggcgccatatgtcggggcaagtcttgaagtcatggagtctgacacaaaagtattccgagg

aaataagcctttctttttcactaatttgaaagacgatcaagggctagatgaagtagtagagtgggtcaggaaacatgctt

tgttaaaaggactaggacaagatgtctgaatggacaggcgttcttgaccttgtcatggaaaaccgcttaggacgctccgt

ggcaaaaagtgtctacttccagggtgcatttaaagtgatgcgccctgtctatttcaataagaatagttatccatgctact

atttattaaatcctggcggtggctatttagatggagatcggtatcaaatgaaagttacgcttggtgaacgagcgatgctg

acgttgacgacccagtcgtcgacgaaagtatatagaacgcccaccaagccagtgtaccaagagacgatctttcatatgaa

aaaagacagttatctagagtacttgccggatgcacttatcgcatacaaagatgccagttgttatcaaaaaaacagtatat

acatggaaaaaggcgcaacattgctatattccgatatactgactcccggctggtcgccggaaggagaaaagttcagctac

gatatgctccgtttgaaaacggagatttatatggaaaatcagcttgttgcctttgatcatattaaacttcatccagcgtc

tcagcatatgaatgagttaggttttatggaaggatacacacatttaggttccttgattgtcgttggagaaaagacaagcg

atgctttattggatcgattgtatgaaacaattcaacaagaggctggagaatttacatttggattatccaagcttgctgtt

cctggcttcaccatccgtatattagcaaactacacacaggtcatagaacgaattatttcagtgtgccatcacgtgattag

cgacgaatggtatcaaacgaagccaagtttttttaaggaagtactagacaggggcccgacaattctaaagagttgttgggct

tttcctgttaattttgctgcttatatataaattattatatgactagtagttcgcgcattggagtgtggtacctataaaaa—3’

Figure 6.3. Urease operon predicted PCR amplicon (serial cloner 2.0). The coding sequence for UreA-G was amplified from *S.ureae* genomic DNA, extracted from an overnight culture. The forward and reverse primer introduced SacI (yellow) and KpnI (green) restriction enzyme recognition sequences, respectively. Restriction recognition sequences for HaeIII (blue), BamHI (red), and EcoRI (grey) are also indicated.

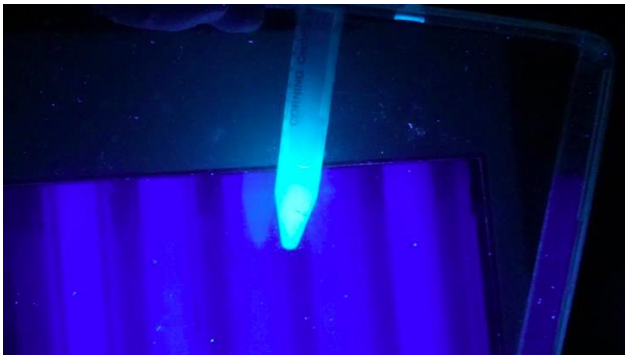

Figure 6.4. *E.coli* cells successfully transformed with pAD123-GroEl observed under UV light. *E.coli* cells were transformed with the recombinant pAD123-GroEl and plated on agar-ampicillin. Cells that successfully took up the recombinant glowed under UV light due to GFP (gfpmut3a) expression.

A)

5’GAAAAGAATGATGTAAGCGTGAAAAATTTTTTATCTTATCACTTGAAATTGGAAGGGAGATTCTTTAT
TATAAGAATTGTGGCCCAATTAAAGGAGGAA -3’

B)

5’GGGCTATAGAATTCGAAAAGAATGATGTAAGCGTGAAAAATTTTTTATCTTATCACTTGAAATTGGAA
GGGAGATTCTTTATTATAAGAATTGTGGCCCAATTAAAGGAGGAAGAGCTCTATAAAA-3’

Figure 6.5. A) GroEl promoter region derived from *Bacillus subtilis* (99bp) and **B) predicted GroEl promoter PCR amplicon (126 bp).** The PCR amplicon contains an EcoRI restriction enzyme recognition sequence (green) introduced by the forward primer and a SacI restriction enzyme recognition sequence introduced by the reverse primer.

6.2 Chapter 3

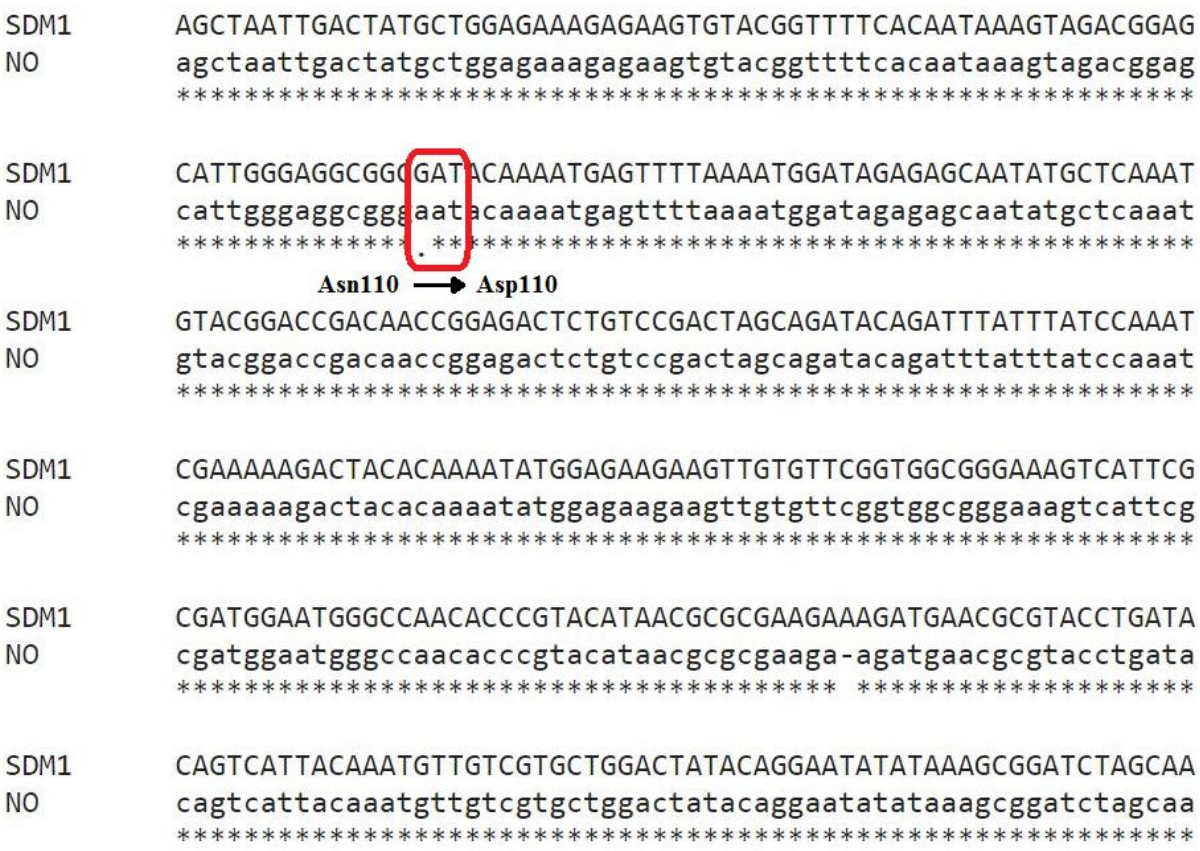

Figure 6.6: DNA sequencing data confirming first round of SDM. Proceeding site-directed mutagenesis of Asn110 to Asp110 using the Q5® Site-Directed Mutagenesis Kit, Sanger sequencing was conducted which confirmed the presence of the mutation in sequence from aat to gat (NO: native urease, SDM1: urease with Asp110).

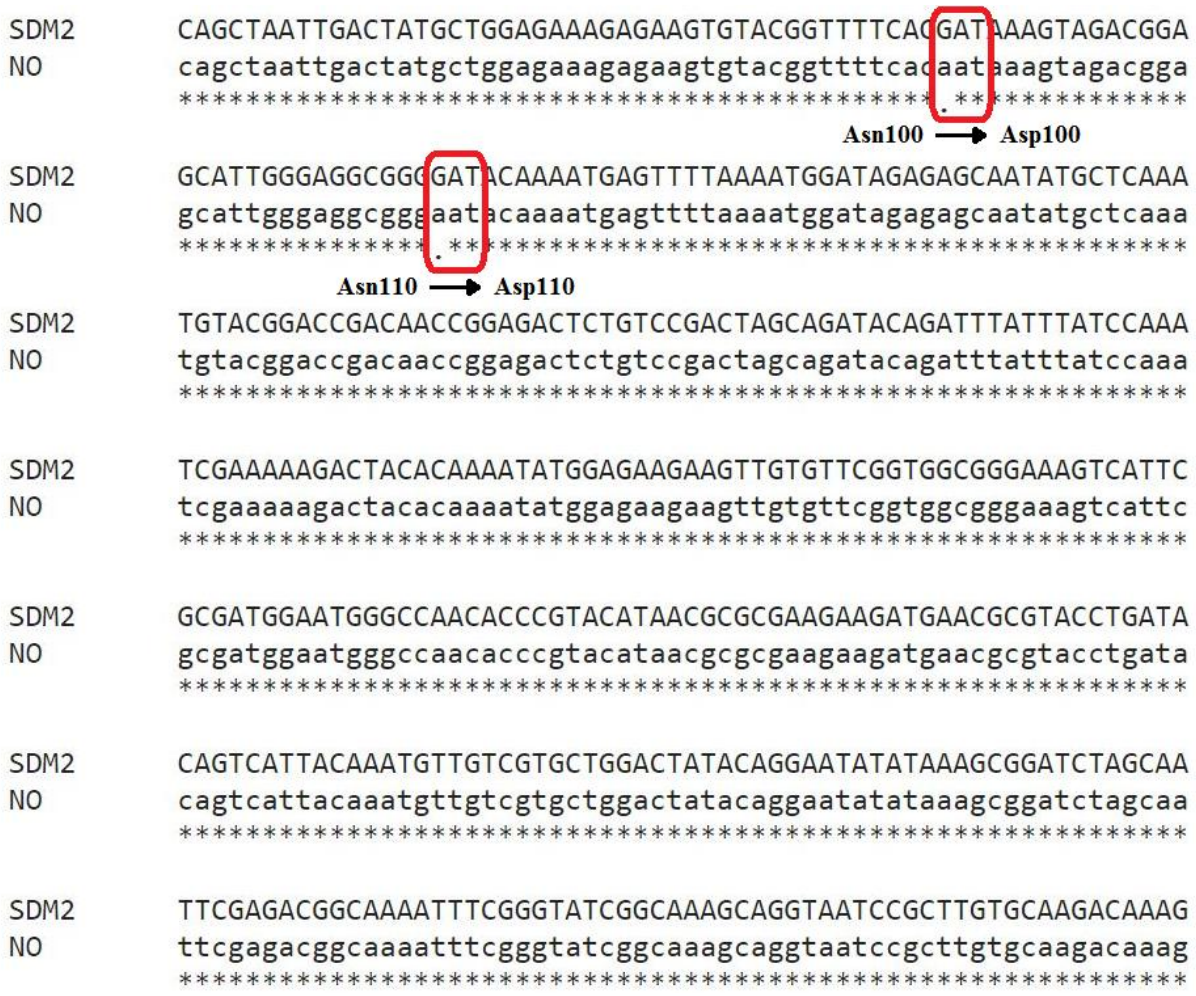

Figure 6.7: DNA sequencing data confirming second round of SDM. Proceeding site-directed mutagenesis of Asn100 to Asp100 using the Q5® Site-Directed Mutagenesis Kit, Sanger sequencing was conducted which confirmed the presence of both mutations present in urease subunit beta.